

# CONFORMAL GEOMETRY IN IDEAL MAGNETOHYDRODYNAMICS

vorgelegt von

M. Sc.

Oliver Karl Klaus Gross

von der Fakultät II – Mathematik und Naturwissenschaften  
der Technischen Universität Berlin  
zur Erlangung des akademischen Grades

Doktor der Naturwissenschaften

Dr. rer. nat.

genehmigte Dissertation

Promotionsausschuss:

Vorsitzender: Prof. Dr. Jörg Liesen

Gutachter: Prof. Dr. Ulrich Pinkall

Gutachter: Prof. Dr. Albert Chern

Gutachter: Prof. Dr. Alexander I. Bobenko

Gutachter: Prof. Dr. Boris Springborn

Tag der wissenschaftlichen Aussprache: 22. Mai 2024

Berlin 2024



© 2024

Oliver Gross

ORCID: 0000-0001-7970-5596

All rights reserved



## ZUSAMMENFASSUNG

In dieser Arbeit werden theoretische und praktische Aspekte konformer Geometrie in der idealen Magnetohydrodynamik untersucht. Die Hauptergebnisse setzen stationäre Punkte einer Hierarchie von  $L^2$  bzw.  $L^1$ -Optimierungsproblemen, welche sich hinsichtlich der ihnen auferlegten topologischen Zwangsbedingungen unterscheiden, durch eine konforme Änderung der Metrik miteinander in Beziehung. Insbesondere etablieren sie eine konforme Äquivalenz zwischen Feldern mit verschwindender Lorentzkraft und geodätischen Vektorfeldern sowie harmonischen Feldern und Eikonal Feldern.

Basierend auf einer geometrischen und strukturerhaltenden Diskretisierung von idealem Plasma wird die sogenannte *magnetische Relaxation* aus Sicht der konformen Geometrie interpretiert, was zu einem neuartigen Lagrange'schen Modell basierend auf diskreten Plasmafilamenten führt, welches geometrisch weniger starr ist als bisherige Ansätze. Die praktische Anwendbarkeit des vorgeschlagenen Modells wird anhand zweier Beispiele demonstriert: Zum einen werden stationäre Zustände von verknoteten oder vernüpften Plasmafilamenten approximiert. Zum anderen ist das vorgestellte Modell Teil einer prozeduralen Pipeline, die stellare Atmosphären für Computergrafikzwecke erzeugt.



## ABSTRACT

This thesis investigates theoretical and practical aspects of conformal geometry in ideal magnetohydrodynamics. The main results relate stationary points of a hierarchy of  $L^2$  *resp.*  $L^1$ -optimization problems, which are distinguished by the topological constraints they impose, by a conformal change of metric. In particular, they establish a conformal equivalence between force-free fields and geodesic vector fields as well as harmonic fields and eikonal fields.

Based on a geometric and structure preserving discretization of ideal plasma, so-called *magnetic relaxation* is interpreted from the viewpoint of conformal geometry, which gives rise to a novel Lagrangian model based on discrete plasma filaments which is less geometrically rigid than previous approaches. The practical applicability of the proposed model is demonstrated by two examples: First, we approximate stationary states of knotted or linked plasma filaments. Second, the presented model is part of a procedural pipeline that generates stellar atmospheres for computer graphics purposes.



## ACKNOWLEDGEMENTS

My greatest gratitude goes to my advisors: Ulrich, thank you for welcoming me into this unique group, for sharing your endless enthusiasm and creativity, and for allowing me so much freedom to explore during this time. I would also like to thank Peter for his guidance, support, encouragement and for inviting me to spend a wonderful time at Caltech. Much of this work was done in collaboration with others. Therefore, I would like to thank Albert for working with me on these topics and for always welcoming me at UC San Diego. I would also like to thank my colleagues Felix and Marcel for their collaboration, contributions, and numerous discussions.

Moreover, I would like to thank Jörg Liesen, Alexander Bobenko and Boris Springborn for serving as members of my committee.

*This work was funded by the Deutsche Forschungsgemeinschaft (DFG - German Research Foundation) - Project-ID 195170736 - TRR109 “Discretization in Geometry and Dynamics”. Additional support was provided by SideFX software.*



## PUBLISHED CONTENT AND CONTRIBUTIONS

[75] Marcel Padilla, Oliver Gross, Felix Knöppel, Albert Chern, Ulrich Pinkall, and Peter Schröder (2022). “*Filament Based Plasma*”. In: ACM Trans. Graph. 41, 4, Article 153 (2022), 14 pages.

DOI: [10.1145/3528223.3530102](https://doi.org/10.1145/3528223.3530102).

Oliver Gross contributed to the theoretical developments, the algorithm for the discrete ideal magnetic relaxation, implementation, preparation of the manuscript and contributed numerical examples and renderings.

[46] Oliver Gross, Ulrich Pinkall, and Peter Schröder (2023). “*Plasma Knots*”. In: Physics Letters A 480 (2023), p. 128986.

DOI: [10.1016/j.physleta.2023.128986](https://doi.org/10.1016/j.physleta.2023.128986).

Oliver Gross contributed to the topic selection, structuring of the content, the development and detailed elaboration of the theoretical results, developing and implementing the algorithm as well as the preparation of the manuscript and contributed the renderings.

[20] Albert Chern and Oliver Gross (2023). “*Force-Free Fields are Conformally Geodesic*”. Preprint (2023) arXiv: 2312.05252.

DOI: [10.48550/arXiv.2312.05252](https://doi.org/10.48550/arXiv.2312.05252).

Oliver Gross contributed to the topic selection, structuring of the content, the development and detailed elaboration of the theoretical results, as well as the preparation of the manuscript and contributed the renderings.



# CONTENTS

Zusammenfassung . . . . .	i
Abstract . . . . .	iii
Acknowledgements . . . . .	v
Published Content and Contributions . . . . .	vii
Table of Contents . . . . .	xi
List of Figures . . . . .	xiv
<b>1 Introduction</b>	<b>1</b>
1.1 Ideal Magnetohydrodynamics . . . . .	3
1.1.1 Magnetohydrostatics . . . . .	4
1.1.2 Variational Characterizations . . . . .	5
1.1.3 Magnetic Relaxation . . . . .	7
1.2 Geodesic Foliations . . . . .	9
1.3 Equivalence Theorems . . . . .	10
1.4 A Discrete Model for Ideal Plasma . . . . .	11
1.4.1 Stationary Plasma Knots . . . . .	11
1.4.2 Modeling the Solar Corona . . . . .	12
1.5 Contributions . . . . .	12
<b>2 Plasma in Riemannian Manifolds</b>	<b>14</b>
2.1 Riemannian Magnetohydrostatics . . . . .	14
2.1.1 Force-Free vs. Beltrami Fields . . . . .	18
2.1.2 Orthogonal Distributions . . . . .	21
2.1.3 Even-Dimensional Case . . . . .	22
2.2 Flux Form Representation . . . . .	23
2.2.1 Flux Forms in Riemannian Geometry . . . . .	23
2.2.2 Physical Flux Forms . . . . .	24
2.3 Structure Theorems on 3-Manifolds . . . . .	24

## CONTENTS

2.3.1	Arnold's Structure Theorem . . . . .	25
2.3.2	Constant Pressure Function . . . . .	26
<b>3</b>	<b>Geodesible and Conformally Geodesic Vector Fields</b>	<b>32</b>
3.1	Geodesic and Eikonal Fields . . . . .	32
3.2	Geodesible Vector Fields . . . . .	34
3.2.1	Reeb Vector Fields . . . . .	38
3.2.2	Stable Hamiltonian Structures . . . . .	41
3.3	Conformally Geodesic Vector Fields . . . . .	44
3.3.1	Killing Vector Fields are Conformally Geodesic . . . . .	45
3.3.2	Force-Free Fields are Conformally Geodesic . . . . .	47
<b>4</b>	<b>Equivalence Theorems for Variational Principles</b>	<b>53</b>
4.1	Boundary Conditions . . . . .	53
4.2	A Hierarchy of Variational Principles for the $L^2$ -Norm . . . . .	54
4.3	A Hierarchy of Variational Principles for the $L^1$ -Norm . . . . .	56
4.4	Conformal Change of Metric . . . . .	59
4.4.1	Conformal Transformations of Stationary Conditions . . . . .	60
4.4.2	Equivalence Theorem . . . . .	61
4.4.3	The Surface Case . . . . .	63
<b>5</b>	<b>Pressure Confined Plasma Domains</b>	<b>65</b>
5.1	Magnetohydrostatic Bubbles . . . . .	66
5.2	Variational Principles for Plasma Bubble Configurations . . . . .	69
5.3	Plasma Bubbles with Flux Boundaries . . . . .	71
<b>6</b>	<b>Discretization of Ideal Plasma</b>	<b>74</b>
6.1	Plasma Filaments . . . . .	74
6.1.1	Conformal Interpretation . . . . .	76
6.1.2	Unobstructed Plasma Filaments . . . . .	76
6.2	Discrete Ideal Plasma . . . . .	77
6.3	Twisted Plasma Filamentets . . . . .	79
6.3.1	Variational Principle for Twisted Plasma Filaments . . . . .	81
<b>7</b>	<b>Discrete Ideal Magnetic Relaxation</b>	<b>83</b>
7.1	Related Computational Methods . . . . .	83
7.2	A Geometric Relaxation Method . . . . .	84

## CONTENTS

7.2.1	Implementation . . . . .	85
7.3	Stationary Plasma Knots and Links . . . . .	86
7.3.1	Approximation of Steady Solutions to Ideal MHD . . . . .	88
7.4	The Solar Corona . . . . .	89
<b>8</b>	<b>Conclusion</b>	<b>92</b>
<b>References</b>		<b>96</b>

## LIST OF FIGURES

1.1	A free elastic curve, a minimal surface and a Willmore surface. . . . .	1
1.2	Illustration of the rope length of a knot. . . . .	2
1.3	A link of knotted plasma filaments relaxing to an equilibrium configuration. . . . .	3
1.4	Decomposition of a vector field on an annulus into an exact and a harmonic part. . . . .	5
1.5	Relaxation of a magnetic field supported on a Hopf link discretized in 100 plasma filaments per component. . . . .	8
1.6	A flux tube in the shape of a trefoil knot and a “ <i>relaxed state</i> ” of the same knot which is a stationary point of the magnetohydrostatic energy. . . . .	12
1.7	Coronal loops computed by the discrete ideal magnetic relaxation and a rendering of the resulting solar corona. . . . .	13
2.1	Hodge decomposition of a vector field on a 2-torus. . . . .	17
2.2	Visualizations of the orthogonal hyperplane distributions corresponding to an exact harmonic field and the ABC-flow. . . . .	22
2.3	Fundamental domains for the decomposition of an MHS equilibrium due to Arnold. . . . .	25
2.4	Force-free fields with non-constant proportionality factor. . . . .	27
2.5	ABC-flow for the parameters $A = B = C = 1$ . . . . .	28
2.6	Orthographic views on the ABC-flow for $A = B = C = 1$ and $A = 1, B = 1/2$ and $C = 0$ . . . . .	29
2.7	An exact harmonic field on the unit ball $\mathbb{B} = \{x \in \mathbb{R}^3 \mid  x  \leq 1\}$ and its potential. . . . .	30
2.8	Vector fields generating the homology of the 2-torus. . . . .	31
3.1	A Reeb annulus together with a higher dimensional analogue. . . . .	37

## LIST OF FIGURES

3.2	Reeb vector field and contact structure corresponding to the contact 1-form $\alpha = dz + y dx$ . . . . .	39
3.3	Killing vector fields on an Enneper surface and a piece of the hyperbolic plane in the upper half-plane model. . . . .	46
3.4	The Hopf fibration of $\mathbb{R}^3$ . . . . .	50
3.5	An overview of the results from this chapter for the case that $M$ is 3-dimensional. . . . .	51
3.6	An overview of the results from this chapter for the case that $M$ is $(2n + 1)$ -dimensional. . . . .	52
4.1	Eikonal geodesic foliation realizing a Beckmann optimal transport plan and a twisted geodesic foliation with constrained connectivity between source and sink endpoints. . . . .	58
4.2	An overview of the variation problems that are equivalent by a conformal change of metric according to Theorem 4.12. . . . .	62
4.3	Vector fields $B \in \Gamma(S^2)$ which are stationary points of the $L^1$ -, resp. $L^2$ -norm with boundary conditions given by a source and a sink. .	63
5.1	A plasma bubble configuration consisting of two interlinked components touching at a common boundary surface known as the <i>current sheet</i> . . . . .	65
5.2	An isolated flux tube as an example of a plasma bubble configuration.	66
6.1	The geometry of a plasma filament. . . . .	75
6.2	Relaxation of Borromean rings discretized by a single plasma filament per component. . . . .	78
6.3	A model for plasma filaments supporting a twisted magnetic field.	79
7.1	Examples for the evolution of different knots under the proposed model for magnetic relaxation. . . . .	86
7.2	Relaxed states of the Perko pair resulting from the proposed relaxation method. . . . .	87
7.3	Examples for the evolution of different links under the proposed model for magnetic relaxation. . . . .	88
7.4	Relaxation of a trefoil knot and Borromean rings discretized by a large collection of filaments. . . . .	89
7.5	Procedurally generated rendering of a solar corona. . . . .	90

## LIST OF FIGURES

7.6	Relaxation of an initial curve configuration in the solar corona as proposed by our method. . . . .	90
7.7	An untwisted and a twisted coronal loop discretized by a small number of filaments. . . . .	91
8.1	An untwisted and a twisted coronal loop. . . . .	93
8.2	Conceptual visualization of the helicity-preserving reconnection of the two components of a Hopf link to a single plasma filament supporting a twisted magnetic field. . . . .	94

# CHAPTER 1

## INTRODUCTION

The search for “*natural*” representatives for topological spaces is a fundamental task in mathematics. While the *round sphere* is arguably the undisputed representative for a topological sphere in any dimension, there are no such obvious candidates for most other cases—not even in lower dimensions such as for curves and surfaces.

A common remedy is to resort to energy functionals that promote desired properties and whose critical points are therefore good substitutes. Well known examples include *elastic curves*, the *Plateau problem*, *minimal surfaces* or *Willmore surfaces* (Fig. 1.1, [80]). The corresponding variational energies—the integrated squared curvature of plane curves, the area functional, the integrated mean or squared mean curvature—measure geometric quantities. Less common examples of such energies, which are used to find optimal geometric configurations of knots and links, or closed surfaces, are the *Möbius energy* [39, 61] and the *tangent-point energy* [44, 120, 119].

Many functionals are inspired by nature and assign physical properties to a mathematical object. One example is the bending energy that is used to model elastic space curves [80].

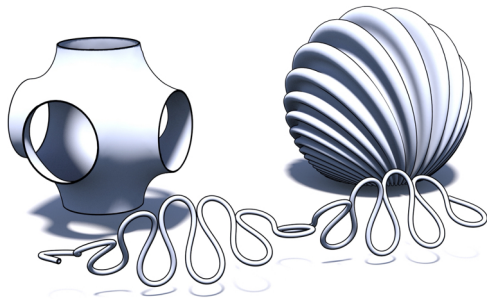


**Figure 1.1:** A free elastic curve (*front*), a minimal surface (*left*) or a Willmore surface (*right*), which are stationary points of geometric functionals [80].

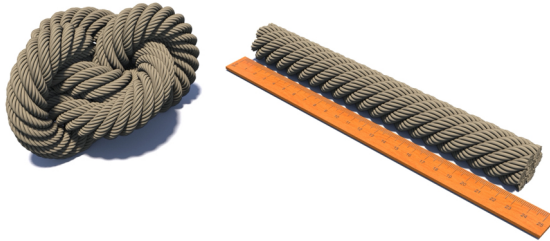


**Figure 1.2:** The rope length of tight knots is the minimum length of an idealized rope that is needed to tie a knot of a given isotopy class.

Another example is the *rope length* of *tight knots* [56], which is given by the minimum length of rope—perfectly hard, perfectly flexible and with circular cross section of fixed diameter—that is required to tie a knot of a given type. The center curve of such a rope can be thought of as

yet another “natural” representation of this knot type (Fig. 1.2). Thus, there are a number of meaningful motivations that lead to different “natural” representatives.

The present thesis studies geometric structures which are naturally formed by magnetic field lines in an ideal plasma. The key motivation for these analytical and numerical investigations is given by what is known as the *magnetic relaxation* problem [72, 115]:

“Imagine an electrically-conducting fluid (i.e., a plasma) initially at rest. If we allow the fluid to relax to some minimum-energy state subject to the magnetohydrodynamic (MHD) equations, can we understand the relaxation process, or predict the relaxed state?”

Moffatt [71] proposed the application of ideal magnetic relaxation in the field of knot theory. He considers equilibrium states of essentially knotted flux tubes resulting from the process and conjectured that the spectrum of (a normalized) relaxed state energies of an essentially knotted flux tube is a topological invariant capturing the complexity of the knot type. Relaxed states of knotted plasma filaments can be viewed as another “natural” representation of a given knot type.

More generally, steady states of the magnetic field in a plasma may be regarded as the “natural” representation of vector fields of a given topology: they represent the states obtained from a self-organization of the magnetic field lines into an equilibrium configuration by minimizing a variational energy.

The results presented in this thesis provide novel insights regarding the geometric structure of steady equilibria in ideal magnetohydrodynamics from a viewpoint of conformal geometry. More specifically, for strong magnetic fields, the field lines of such steady states are characterized as geodesics after a conformal change of metric [20]. This result establishes a more precise definition of an already known duality between special physical and geometric fields [34, 87, 20].

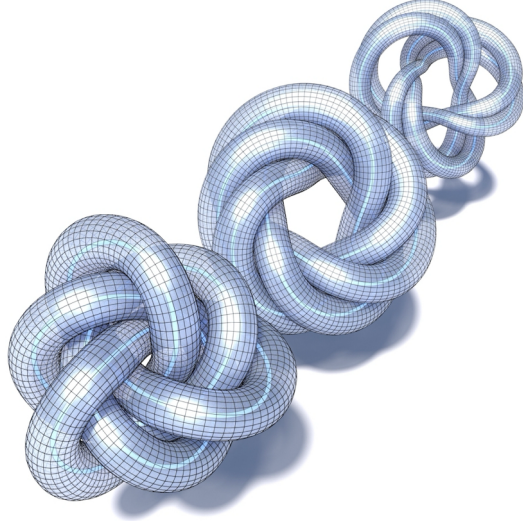


**Figure 1.3:** A link of knotted plasma filaments relaxing to an equilibrium configuration (from back to front).

Away from equilibrium states, the dynamics described in this work can also be interpreted in terms of geometry, which gives a novel interpretation of the originally physical motivation.

Using a discrete model for ideal plasma based on variational principles for pressure confined plasma regions with free boundary conditions, numerical investigations are carried out based on a novel algorithm [75, 46]. The practicability of this approach is demonstrated by two case studies. First, we consider the relaxation of knotted flux-ropes, so-called *plasma knots*. Second, the extrapolation of flux boundary conditions on the surface of a star to a magnetic field filling its atmosphere is studied.

## 1.1 IDEAL MAGNETOHYDRODYNAMICS

A plasma can be described as a state of matter in which there is a significant amount of charged particles such as ions or electrons [82]. According to Maxwell's equations, whenever an electric current flows, there is also a magnetic field [65, 38]. In their purest form the governing equations of *ideal magnetohydrodynamics* (*ideal MHD*) assume the surrounding fluid to be perfectly conducting, eliminating all effects of resistivity.

## CHAPTER 1. INTRODUCTION

The relevant time dependent variables for ideal MHD on a plasma domain  $M \subset \mathbb{R}^3$  are: a plasma density  $\rho : M \rightarrow \mathbb{R}$ , fluid velocity  $v : M \rightarrow \mathbb{R}^3$ , pressure  $p : M \rightarrow \mathbb{R}$ , a divergence-free magnetic field  $B : M \rightarrow \mathbb{R}^3$ ,  $\operatorname{div} B = 0$ , and an electric current  $J : M \rightarrow \mathbb{R}^3$ . Their time evolution is governed by

$$\begin{aligned}\frac{\partial}{\partial t} \rho + \operatorname{div}(\rho v) &= 0 \\ \frac{\partial}{\partial t} v + \nabla_v v &= -\frac{1}{\rho} \operatorname{grad} p + \mathbf{g} + \frac{1}{\rho} J \times B \\ \frac{\partial}{\partial t} B - \operatorname{curl}(v \times B) &= 0 \\ J &= \operatorname{curl} B \\ \rho &= \frac{m}{k_B T} p.\end{aligned}\tag{1.1}$$

Here,  $k_B$  is the Boltzmann constant,  $m$  the mass of a proton,  $T$  the temperature of the plasma, and  $\mathbf{g} : M \rightarrow \mathbb{R}^3$  the gravitational acceleration field.

### 1.1.1 MAGNETOHYDROSTATICS

The steady state solutions of Eqs. (1.1) are characterized by an equilibrium condition ( $\partial/\partial t = 0$ ,  $v = 0$ ), which reduces Eqs. (1.1) to the *magnetohydrostatic* (*MHS*) equation

$$(\operatorname{curl} B) \times B - \operatorname{grad} p + \frac{m}{k_B T} p \mathbf{g} = 0.\tag{1.2}$$

A divergence-free magnetic field  $B$  is said to be in *magnetohydrostatic equilibrium* if it satisfies Eq. (1.2), which in the absence of gravity reduces to

$$(\operatorname{curl} B) \times B = \operatorname{grad} p.\tag{1.3}$$

A variety of simplifications are commonly employed in physical models. When studying strong magnetic fields or fields in a vacuum, the *low-beta* limit can be employed [82], which neglects pressure effects and for which Eq. (1.3) reduces to the so called *force-free* condition

$$(\operatorname{curl} B) \times B = 0.\tag{1.4}$$

Divergence-free magnetic fields solving Eq. (1.4) are referred to as *force-free* fields. They can equivalently be characterized as the fields whose curl is co-linear to the original field, *i.e.*,

$$\operatorname{curl} B = f B$$

for some smooth function  $f \in C^\infty(M)$ , the *proportionality factor*. If the proportionality factor  $f$  is constant, the corresponding field is called *linear force-free*. Another important special case of (linear) force-free fields is given by *harmonic fields* for which  $f \equiv 0$ , *i.e.*, in addition to the divergence-free condition, satisfy

$$\operatorname{curl} B = 0. \quad (1.5)$$

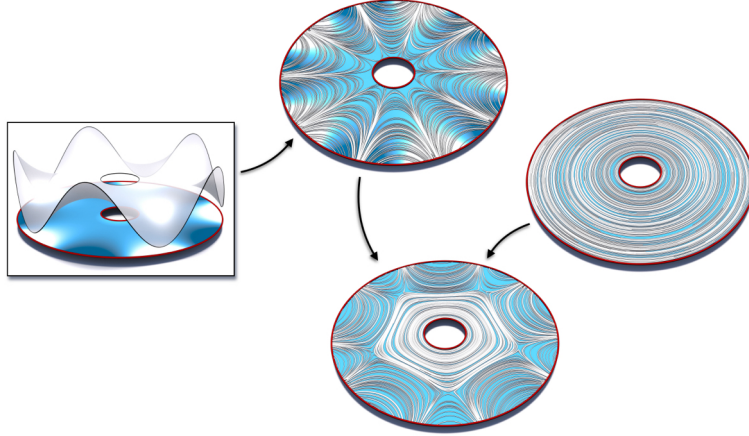


**Figure 1.4:** An exact harmonic field (top) is the gradient vector field of a harmonic function (left). Adding a harmonic field which is merely harmonic but not exact harmonic (right) gives a harmonic field which is not exact harmonic (bottom).

Divergence-free vector fields  $B = \operatorname{grad} \phi$  which are the gradient of some scalar function  $\phi$  are called *exact harmonic*. Since  $\Delta\phi = \operatorname{div} \circ \operatorname{grad} \phi = \operatorname{div} B = 0$ , they come as the gradients of a harmonic functions. However, not all harmonic fields are exact harmonic. This distinction becomes important on domains which are not simply connected (Figs. 1.4 and 2.1). Therefore, in the absence of gravity, the following inclusions hold:

$$\{B \in \operatorname{im}(\operatorname{grad})\} \subset \{\operatorname{curl} B = 0\} \subset \{(\operatorname{curl} B) \times B = 0\} \subset \{(\operatorname{curl} B) \times B = \operatorname{grad} p\}.$$

### 1.1.2 VARIATIONAL CHARACTERIZATIONS

Consider a magnetic field  $B$ , ( $\operatorname{div} B = 0$ ) which satisfies prescribed boundary conditions, *i.e.*,  $B \cdot N = \Phi$  for a given boundary flux condition  $\Phi \in C^\infty(M)$  and  $N$  being the unit normal of  $\partial M$ . The steady states being special cases of Eq. (1.3) emerge as the Euler-Lagrange equations of variational principles, which differ by the imposed constraints.

We obtain the MHS equation (1.3) by considering the total potential energy

$$\mathcal{E}(B, p) = \mathcal{B}(B) + \mathcal{P}(p),$$

which consists of the *magnetic energy* and the *internal energy* which are respectively given by

$$\mathcal{B}(B) = \frac{1}{2} \int_M |B|^2 dV, \quad \mathcal{P}(p) = \int_M p dV. \quad (1.6)$$

**Theorem 1.1** (Minimum Energy Theorem for MHS (Chapter 5)) When the magnetic flux and topological connections are given on a closed surface and the field within the surface possesses a minimum total potential energy under variations by flow fields (Eq. (1.7)), then it is in MHS equilibrium.

In the low-beta limit, *i.e.*, for negligible gas pressure  $p$  we have:

**Theorem 1.2** (Minimum Energy Theorem for Force-Free Fields [82, Sec. 2.8]) When the magnetic flux and topological connections are given on a closed surface and the field within the surface possesses a minimum magnetic energy, then it is force-free.

A famous result by Woltjer [113] does not impose a constraint on the exact topology of the field, but the degree of knottedness of the field lines, which is captured by the helicity [1].

**Definition 1.3** Let  $M$  be a finite plasma region and  $B$  be a magnetic field bounded by a flux surface. Moreover, let  $A$  be a vector potential, *i.e.*,  $\text{curl } A = B$ . Then the *helicity* is defined as

$$\mathcal{H}(B) := \int_M \langle A, B \rangle dV.$$

**Remark 1.4** As long as the magnetic field is bounded by a *flux surface*, that is,  $B \cdot N = 0$  where  $N$  is the outward pointing unit normal of  $\partial M$ , the helicity is independent of the choice of vector potential (*i.e.*, gauge invariant) [3, Ch. 3].

**Theorem 1.5** (Woltjer's Minimum Energy Theorem [82, Sec. 2.8]) When the normal component of the magnetic field on a closed surface and the total magnetic helicity within the surface are given, then the field with minimum magnetic energy is a linear force-free field.

The least restrictive version of these theorems does not constrain the field topology at all, but only asks for the field to satisfy given boundary conditions.

**Theorem 1.6** (Minimum Energy Theorem for Potential Fields [82, Sec. 2.8]) When the normal component of the magnetic field on a closed surface is given, the potential field in the volume enclosed by the surface has the minimum magnetic energy.

### 1.1.3 MAGNETIC RELAXATION

*Magnetic relaxation* describes the evolution of a magnetic field  $B$  with non-trivial topology that relaxes to a state with minimum energy. The *transport equation*

$$\frac{\partial B}{\partial t} = \operatorname{curl}(v \times B),$$

where  $v$  is the fluid velocity (Section 1.1), states that the field lines are “frozen into the fluid”. Hence, the *isotopy class* of the field  $B$ , that is the way the individual field lines are intertwined with each other, is preserved. Therefore, perturbations of the field  $B$  compatible with the model of ideal MHD are of the form

$$\dot{B} = \operatorname{curl}(v \times B), \quad (1.7)$$

where  $v$  is the fluid velocity of a corresponding plasma flow [40]. Ignoring boundary terms<sup>1</sup>, the variational gradient of Eq. (1.6) is then given by

$$dB(\dot{B}) = - \int_M ((\operatorname{curl} B) \times B) \cdot v \, dV.$$

By the Helmholtz decomposition [99, 38], the field  $B$  is a stationary point under all volume-preserving variations if and only if there is  $p \in C^\infty(M)$  such that Eq. (1.3) holds [38, Ch. 14].

Moffatt [68] gives an explicit construction for a volume preserving flow field which monotonically decreases the magnetic energy. We define

$$v := v((\operatorname{curl} B) \times B - \operatorname{grad} p), \quad (1.8)$$

where  $v > 0$  and the pressure field  $p$  is defined by the condition that  $\operatorname{div} v = 0$  at all times. The dynamics of such an energy decreasing flow is what we consider *magnetic relaxation*.

With the field lines frozen in the fluid, the way in which the individual field

---

<sup>1</sup>The general case will be discussed in Chapter 5.

lines are linked together is preserved throughout the process and topological obstructions (or a confining ambient pressure) eventually bring the relaxation process to a halt. More specifically, one can show that on a finite plasma region bounded by a flux surface. The magnetic energy in Eq. (1.6) is bounded from below as long as the topology of  $B$  is non-trivial [40, 3]. The notion of non-trivial topology can be formalized in terms of helicity, since it can be shown that

$$\mathcal{B}(B) \geq C |\mathcal{H}(B)|$$

for some constant  $C > 0$ , depending on the shape and size of  $M$  [3, Thm. 1.5].

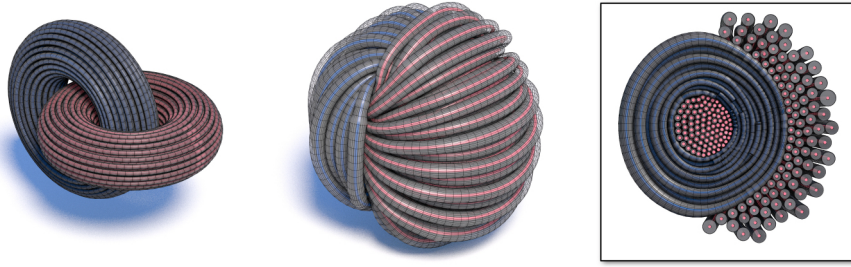


**Figure 1.5:** The initialized configuration (left) and the relaxed state (middle) of a Hopf link discretized by 100 plasma filaments per link component together with a cross-section of the relaxed state (right) resulting from the discrete ideal magnetic relaxation presented in this thesis.

Therefore, the magnetic energy has limit for  $t \rightarrow \infty$  under this magnetic relaxation and by construction we have  $v = 0$  in this limit, which holds if and only if Eq. (1.3). For more discussion on this argument we refer to Moffatt's original work, e.g., [70, 71, 68] or [3].

**Remark 1.7** Magnetic relaxation transports the initial field  $B_0$  by the flow map of Eq. (1.8), i.e., a family of diffeomorphisms  $t \mapsto \chi_t : M \rightarrow M$  such that  $B_t = d\chi_t(B_0)$ . Although this is an isotopy for finite time, in the limit  $t \rightarrow \infty$  discontinuities are likely to form. Fig. 1.5 shows a typical example of this instance: the two components of the Hopf link are initially separated, but in the limit they share a common boundary—a so-called *current sheet*—where the magnetic field is discontinuous. For these instances, Moffatt [70] coined the notion of *topological accessibility*.

With pioneering work by Moffatt [70, 71], research questions derived from the magnetic relaxation problem were established as an active area of research in the

realm of *Geometric Fluid Mechanics* with influence ranging from plasma physics and classical fluid dynamics to purely mathematical disciplines such as differential geometry, differential topology and knot theory [69, 14, 97, 96, 3, 87, 72, 117, 24, 33, 78, 17].

**Remark 1.8** Magnetic relaxation as proposed by Moffatt [70] assumes volume preservation ( $\operatorname{div} v = 0$ ) in order to account for the gas pressure. Considering the gaseous nature of, *e.g.*, stellar plasma, this assumption may be deemed unnatural. With Theorem 1.1 (more precisely Theorem 5.6) we have an alternative variational principle which circumvents this shortcoming, yet exhibits the same stationary points. For an algorithmic treatment, dropping the incompressibility assumption turns out to be favorable, as no additional pressure projection steps are needed (Chapter 7).

## 1.2 GEODESIC FOLIATIONS

In addition to steady plasma states, another important class of vector fields are those whose field lines foliate a space by geodesics [42, 103, 43, 87, 24, 29, 17]. These vector fields play an important role in physics, where they are found, *e.g.*, as optical paths according to Fermat's principle [49].

A special subclass of geodesic vector fields consists of gradients of distance functions, termed *eikonal fields*. These fields correspond to solutions to Beckmann optimal transport problems [94, 13, 28], minimizing the integral

$$\int |B| dV$$

subject to boundary conditions and are untwisted light fields with applications in caustic designs [98] and calibrated forms in calibrated geometry [50, 121, 109].

Now a natural question to ask is:

*“Given a vector field on a manifold, does there exist a Riemannian metric such that the field lines form a geodesic foliation?”*

It is clear that the vector field must be non-vanishing, which at first might seem very restrictive. By the Poincaré-Hopf index theorem [38, Ch. 16], on closed 2-manifolds this only leaves non-trivial cases on tori. However, we will see that restricting our attention to the support of a given vector field yields a variety of interesting cases, in fact we do so for most of the cases we consider.

Necessary and sufficient conditions for an affirmative answer have been given by, e.g., Gluck [42, 43] and Sullivan [103]. So-called *geodesible* vector fields have been studied in numerous contexts. For example, they are of interest in the context of adaptions of the *Seifert conjecture*<sup>2</sup> or *Weinstein conjecture*<sup>3</sup> and relate to Reeb vector fields on contact manifolds, stable Hamiltonian structures or Beltrami fields [34, 87, 24, 17].

A generalized concept of geodesic fields is the notion of *conformally geodesic fields* [36, 37, 32], which are fields that become geodesic after some conformal change of metric. Conformal geodesic fields can depict optical paths in a medium with a non-uniform index of refraction [98].

### 1.3 EQUIVALENCE THEOREMS

On 3-dimensional manifolds there is a remarkable equivalence between force-free fields and geodesible fields [87, 24], connecting the seemingly unrelated topics we introduced in Section 1.1 and Section 1.2.

We demonstrate that for the stationary fields of the  $L^2$ -norm (including force-free and harmonic fields) and the stationary fields of the  $L^1$ -norm (including geodesic foliations and eikonal fields) this relationship holds in an even stronger sense within the framework of conformal geometry. To this end we will establish the following equivalence theorems:

**Theorem 1.9** Force-free fields are conformally geodesic.

**Theorem 1.10** Harmonic fields are conformally eikonal.

Theorems 1.9 and 1.10 assert that a flux form admits a metric with respect to which the corresponding vector field representation is force-free (*resp.* harmonic) if and only if it admits a metric (possibly different, but conformally equivalent) with respect to which the corresponding vector field representation is geodesic (*resp.* eikonal). They can be expressed as statements about field lines on conformal manifolds of arbitrary dimension and there are several significant implications thereof.

---

<sup>2</sup>The Seifert conjecture states that every nonsingular, continuous vector field on the 3-sphere has a closed orbit.

<sup>3</sup>The Weinstein conjecture claims that on a compact contact manifold, its Reeb vector field should carry at least one periodic orbit.

## 1.4 A DISCRETE MODEL FOR IDEAL PLASMA

For our practical considerations, we first develop a rigorous decomposition of Riemannian manifolds representing pressure bounded plasma regions in general magnetohydrostatic equilibrium (Chapter 5). We provide corresponding variational principles allowing for free boundary surfaces in the sense of Dixon et al. [30].

On the basis of these decompositions, we then derive a discretization of ideal plasma domains in terms of so-called *plasma filaments* in Chapter 6. Plasma filaments are curves with thickness, which represent bundles of magnetic field lines in an ideal plasma of a fixed cross-sectional flux and interior pressure. There is a one-to-one correspondence between physical quantities of the discretized magnetic field and the geometry of the curve with thickness.

The motivation for our model goes back as early as the 1850's, when Faraday envisioned electromagnetic fields as "lines of force" [35]. For our investigations we assign material properties to these lines of force, so that the self-organization of the field lines which is studied in plasma physics is described by interactions of these material curves. This approach allows us to describe the dynamics of field lines, which is governed by electromagnetic laws, in terms of mechanical interactions instead.

In Chapter 6, we relate the observed interaction and self-organization to geometry optimization from the vantage point of conformal geometry. More specifically, in view of Theorems 1.9 and 1.10 we reduce the gradient flow of magnetic energy to a curve-shortening flow of the individual filaments in a conformally changed metric. Here, the subtlety is that the metric itself depends on the state of the magnetic field. This approach does not only provide a mathematically elegant description, but also builds the foundation of our numerical relaxation algorithm, which performs relaxations of a plasma region discretized into plasma filaments in an unconstrained and purely geometric fashion (Section 7.2).

We demonstrate the efficacy of the approach on two applications, the computation of stationary plasma knots (Section 7.3) and extrapolations of the magnetic field in the solar atmosphere from prescribed boundary flux data (Section 7.4).

### 1.4.1 STATIONARY PLASMA KNOTS

The structure preserving discretization of ideal plasma into plasma filaments we introduce in Chapter 6 establishes a corresponding energy on the space of curves

with thickness and thus can also be used for knots and links (Figs. 1.3, 1.5 and 1.6). In particular, the geometric optimization we derive in Section 7.2 will provide us with a computational method to determine equilibrium configurations which may be regarded as a “natural” representative of a given type of knot or link.

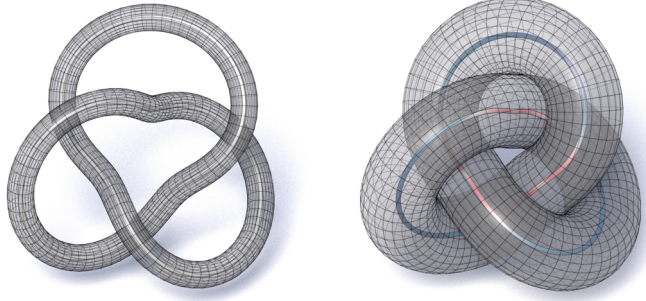


**Figure 1.6:** A flux tube in the shape of a trefoil knot (left) and a “relaxed state” of the same knot (right) which is a stationary point of the magnetohydrostatic energy.

By choosing to represent a plasma region in the shape of a knot or link not only by a single, but many plasma filaments per connected component (Figs. 1.5 and 7.5), we approximate pressure confined steady solutions to ideal MHD.

#### 1.4.2 MODELING THE SOLAR CORONA

The solar atmosphere (or *solar corona*) consists of plasma and the study of the structure of its magnetic field is an active field of research [7, 6, 22, 82, 84, 85, 118, 117]. Based on the presented model of ideal plasma and the corresponding geometric method for magnetic relaxation, in [75] a fully procedural pipeline to extrapolate arbitrary prescribed flux boundary conditions into the solar atmosphere is presented. It includes a physically inspired rendering pipeline, which generates images as seen in Figs. 1.7 and 7.5.

### 1.5 CONTRIBUTIONS

This thesis examines the rich geometric structures exhibited by special steady solutions to the ideal magnetohydrodynamics equations as well as geometric aspects of the related magnetic relaxation problem. The main results extend equivalence theorems between force-free and geodesible fields in the context of conformal geometry. Extending on Arnold’s seminal structure theorems, albeit with the loss of

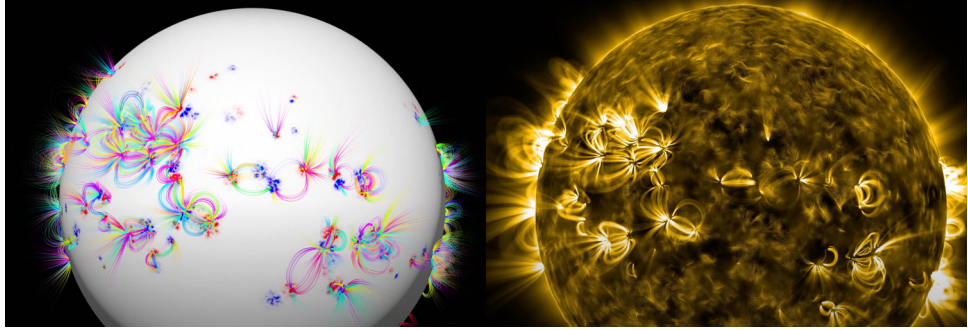


**Figure 1.7:** Coronal loops computed by the discrete ideal magnetic relaxation (left). Rendering of the resulting solar corona (right) as proposed in [75].

invariant surfaces, these results find geometric order even in flows that are known to be chaotic by stating that: “*the field lines are conformal geodesics.*”

Moreover, the results relate stationary points of a hierarchy of  $L^2$  resp.  $L^1$ -optimization problems, which are distinguished by the topological constraints they impose, by a conformal change of metric.

From a practical point of view, variational principles for stable equilibria of an ideal plasma in the case of a free boundary subjected to external magnetic or pressure forces are derived, from which a structure-preserving discretization of the ideal plasma is developed.

This model for ideal plasma in terms of so-called *plasma filaments* is geometrically less rigid than previous Lagrangian models, as it allows for filaments of variable thickness which interact with one another. Our model allows us to numerically perform the ideal magnetic relaxation by geometry optimization and thus finding approximate solutions to the variational problems introduced above. In light of the equivalence theorems, the purely geometric nature of energy minimization offers a new perspective, and a geometric reinterpretation of the relaxation process, which was physically motivated in its original formulation.

We apply our discrete magnetic relaxation to two problems drawn from applications: First, we demonstrate the practicability of our method to approximate stationary plasma knots—a case when the magnetic field is bounded by a flux surface (pressure confined, free-boundary condition). Second, we allow for fixed flux-boundary components of our plasma domain, which we use to extrapolate the magnetic field in the solar corona from prescribed flux boundary conditions.

## CHAPTER 2

# PLASMA IN RIEMANNIAN MANIFOLDS

In this chapter we develop a mathematical description of ideal plasma in a Riemannian manifold  $M$ . To this end we generalize the notions and equations introduced in Section 1.1. It will be convenient to express the governing equations in the formalism of exterior calculus. For a general introduction to differential forms in plasma physics we refer the reader to [63] and [38].

### 2.1 RIEMANNIAN MAGNETOHYDROSTATICS

Let  $M$  be an orientable  $n$ -dimensional Riemannian manifold with Riemannian metric  $g$ . Then we denote the corresponding induced volume form, *Hodge star*, norm and Levi-Civita connection by  $\mu_g$ ,  $\star$ ,  $|\cdot|$  and  $\nabla$  respectively.

We want to consider magnetic fields in a plasma, *i.e.*, a volume preserving vector field  $B \in \Gamma TM$  on  $M$ . Typical other examples of such fields are velocity fields of an ideal incompressible fluid.

**Definition 2.1** A *magnetic field*  $B$  on a Riemannian manifold  $M$  is a divergence-free vector field  $B \in \Gamma TM$ ,  $\mathcal{L}_B \mu_g = 0$ .

Whenever we loosely speak of a magnetic field, we refer to Definition 2.1, or respective reformulations of it in terms of exterior calculus as introduced in the forthcoming sections.

In this section we derive the defining equations for steady solutions to the MHD equations Eq. (1.1) on a Riemannian manifold, *i.e.*, Riemannian versions of Eqs. (1.3), (1.4) and (1.5).

To generalize the defining equations we need to overcome two obstacles. First, the cross product which is present in Eq. (1.3) and Eq. (1.4) is only defined for 3-

manifolds and second, the curl-operator. Both constraints can be overcome with help of a classical vector-calculus identity.

**Lemma 2.2** ([12, Ch. 6]) A vector field  $X \in \Gamma T\mathbb{R}^3$  satisfies

$$(\operatorname{curl} X) \times X = \nabla_X X - \frac{1}{2} \operatorname{grad} |X|^2.$$

In view of Lemma 2.2, Eq. (1.3) can be rewritten as

$$\nabla_B B = \operatorname{grad}\left(\frac{|B|^2}{2} + p\right), \quad (2.1)$$

which involves neither a cross-product, nor the curl operator. The MHS Eq. (1.3) essentially states a force balance between the Lorentz force  $((\operatorname{curl} B) \times B)$  and a pressure force  $(\operatorname{grad} p)$ . However, this is not reflected in Eq. (2.1). Moreover, as pointed out by MacKay [63]:

“[...] it is natural to consider forces as covectors rather than vectors, because the work done by a force  $F$  moving through a displacement  $\xi$  is  $F^\flat(\xi)$ <sup>1</sup>.”

Therefore, we rather aim for a generalization of Eq. (1.3) to manifolds, which reflects this force balance in terms of 1-forms. Moreover, the special cases of force-free fields and harmonic fields should naturally emerge from it when gas pressure is negligible or the corresponding field is (exact) harmonic.

**Lemma 2.3** For  $X \in \Gamma TM$  we have

$$\iota_X dX^\flat = (\nabla_X X)^\flat - \frac{1}{2} d|X|^2.$$

*Proof.* By denoting the identity vector-valued 1-form  $I \in \Omega^1(M; TM)$ ,  $I(X) := X$ , and the torsion-freeness  $d^\nabla I = 0$  of the Levi-Civita connection  $\nabla$ , a straightforward computations shows that

$$g(\nabla_X X, I) = \iota_X g(\nabla X \wedge I) + g(\nabla X, X) = \iota_X dg(X, I) + \frac{1}{2} d|X|^2,$$

which yields the claim after re-arranging the terms by the non-degeneracy of the metric.  $\square$

---

<sup>1</sup>Here,  $(\cdot)^\flat$  denotes the *musical isomorphism* which turns a vector field  $X \in \Gamma TM$  into a 1-form  $X^\flat(\cdot) = g(X, \cdot) \in \Omega^1(M)$ .

In view of Lemma 2.2 and by turning vectors into 1-forms, the MHS Eq. (1.3) can be expressed as

$$(\nabla_B B)^b - \frac{1}{2}d|B|^2 = dp,$$

which by virtue of Lemma 2.3 yields the desired force-balance

$$\iota_B dB^b = dp. \quad (2.2)$$

The derivation shows that Eq. (2.2) generalizes Eq. (1.3) in terms of a force-balance between the *Lorentz force* ( $\iota_B dB^b$ ) and a pressure force ( $dp$ ). Notably, this generalization matches the physical equation<sup>2</sup> as it indeed handles forces as 1-forms  $dp, \iota_B dB^b \in \Omega^1(M)$  and has no constraints on the dimension of  $M$ . Moreover, with negligible (or constant) pressure, Eq. (2.2) reduces to

$$\iota_B dB^b = 0 \quad (2.3)$$

which defines force-free fields as fields with vanishing Lorentz force.

**Definition 2.4** A k-form  $\alpha \in \Omega^k(M)$  is said to be *harmonic* if it is closed and co-closed, i.e.,  $d\alpha = d \star \alpha = 0$ .

**Remark 2.5** For vector field  $X : \mathbb{R}^3 \rightarrow \mathbb{R}^3$ , we have

$$\operatorname{div} X = \star d \star (X^b) \quad \text{and} \quad \operatorname{curl} X = (\star d X^b)^\#.$$

Therefore, the vector field  $X$  is harmonic ( $\operatorname{div} X = 0$  and  $\operatorname{curl} X = 0$ ) if and only if  $X^b$  (or equivalently  $\star X^b$ ) are harmonic forms.

From

$$0 = \mathcal{L}_B \mu_g = d\iota_B \mu_g = d \star B^b$$

we conclude that  $\mathcal{L}_B \mu_g = 0$  implies that the 1-form  $B^b$  is co-closed. Therefore,  $B^b$  is harmonic if and only if

$$dB^b = 0. \quad (2.4)$$

A special case of harmonic fields are so-called *exact harmonic* fields, for which  $B^b$  is exact, i.e.,

$$B^b \in \operatorname{im}(d). \quad (2.5)$$

---

<sup>2</sup> Although in higher dimensions, the field lines do not correspond to a magnetic field anymore.

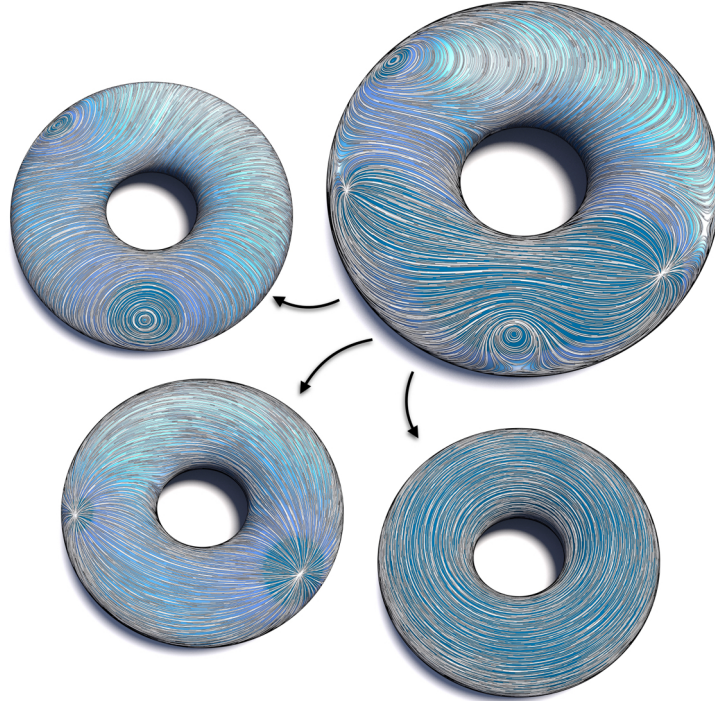


**Figure 2.1:** By the Hodge Decomposition, every vector field  $B$  (top right) can be decomposed into a divergence-free field (top left), a curl-free field (bottom left) and a harmonic (bottom right), which is neither the exact, nor co-exact, i.e., it cannot be written as the derivatives of scalar potentials and vector potentials [99].

That is,  $B^\flat = d\phi$  for some function  $\phi \in C^\infty(M)$  and therefore, since  $d^2 = 0$ ,  $B^\flat$  is closed. Again, the converse does not hold, because a merely harmonic field may have components corresponding to the non-trivial generators of the de Rham cohomology of the domain (Figs. 1.4 and 2.1). Therefore, the following inclusions hold:

$$\{B^\flat \in \text{im}(d)\} \subset \{dB^\flat = 0\} \subset \{\iota_B dB^\flat = 0\} \subset \{\iota_B dB^\flat = dp\}.$$

**Definition 2.6** Let  $M$  be a Riemannian manifold and  $B \in \Gamma TM$  a divergence-free vector field ( $\text{div } B = 0$ ). Then  $B$  is said to be

- (i) *in MHS equilibrium* if there is a smooth function  $p \in C^\infty(M)$  such that Eq. (2.2) holds, i.e.,  $\iota_B dB^\flat = dp$ .
- (ii) *force-free* if it satisfies Eq. (2.3), i.e.,  $\iota_B dB^\flat = 0$ .
- (iii) *harmonic* if it satisfies Eq. (2.4), i.e.,  $dB^\flat = 0$ .
- (iv) *exact harmonic* if it satisfies Eq. (2.5), i.e.,  $B^\flat \in \text{im}(d)$ .

As an immediate consequence of (ii), (iii) and (iv) of definition 2.6 we conclude

**Proposition 2.7** (Exact) harmonic fields  $B \in \Gamma TM$  are force-free.

**Remark 2.8** In Section 4.2 we will derive the defining equations of Definition 2.6 as the Euler-Lagrange equations of a hierarchy of variational principles distinguished by the topological constraints they impose. This is consistent with the 3-dimensional Euclidean case (Section 1.1.2).

### 2.1.1 FORCE-FREE VS. BELTRAMI FIELDS

In plasma physics divergence-free vector fields  $B \in \Gamma TM$  on a 3-dimensional Riemannian manifold  $M$  which satisfy  $(\operatorname{curl} B) \times B = 0$  are known as *force-free* fields. In the realm of fluid dynamics these vector fields are commonly referred to as *Beltrami fields* and the equivalent characterization as those vector fields whose curl is co-linear to the original field, *i.e.*,  $\operatorname{curl} B = fB$  for some smooth function  $f : M \rightarrow \mathbb{R}$  is commonly used. As pointed out in Section 1.1.1, force-free *resp.* Beltrami fields include special cases such as fields with constant  $f$  (linear force-free fields) or  $f \equiv 0$  (harmonic fields).

In the literature, a common approach when generalizing these fields to odd-dimensions ( $2n + 1 > 3$ ) is to use the co-linearity of  $B$  and  $\operatorname{curl} B$  as the defining property [3, 17].

**Definition 2.9** Let  $M$  be a Riemannian manifold of odd dimension  $2n + 1$ . Then a divergence-free vector field  $B \in \Gamma TM$  is Beltrami if there is a smooth function  $f \in C^\infty(M)$ —the *proportionality factor*—such that

$$\operatorname{curl} B = fB, \quad (2.6)$$

where the vector field  $\operatorname{curl} B \in \Gamma TM$  is defined by

$$\iota_{\operatorname{curl} B} \mu_g = (dB^\flat)^n \in \Omega^{2n}(M). \quad (2.7)$$

Clearly, this approach is conceptually very different from the “force-balance” stated in Eq. (2.3). Since the  $n$ -th power<sup>3</sup> of the 2-form  $dB^\flat$  is a  $2n$ -form and the left-hand side of Eq. (2.7) is an  $(\dim(M) - 1)$ -form, this generalization of Beltrami fields can only be well defined on manifolds of odd-dimension.

---

<sup>3</sup>The  $n$ -th power  $\omega^n$  of  $\omega \in \Omega^k(M)$  denotes the  $n$ -fold wedge product  $\omega \wedge \dots \wedge \omega$  of  $\omega$  with itself.

The two definitions coincide on a 3-dimensional Riemannian manifold [63], since by contracting Eq. (2.7) with  $B$  and for  $n = 1$  we have

$$\iota_B dB^\flat = \iota_B \iota_{\text{curl } B} \mu_g.$$

On a 3-dimensional manifold, the *Beltrami equation* ( $\text{curl } B = fB$ ) can be expressed in terms of exterior calculus by  $\star dB^\flat = fB^\flat$ . However, for odd-dimensions dimensions  $n > 3$  there is a subtle difference, which is why in this thesis we carefully distinguish between those two notions of force-free and Beltrami fields.

We make this distinction more precise by first showing that all force-free fields are Beltrami.

**Proposition 2.10** Let  $B \in \Gamma TM$  be a force-free vector field on a Riemannian manifold  $M$  of odd dimension  $2n + 1$ . Then  $B$  is Beltrami.

*Proof.* By assumption  $B$  is force-free, i.e.,  $\iota_B dB^\flat = 0$ . Thus,

$$\iota_B \iota_{\text{curl } B} \mu_g = \iota_B (dB^\flat)^n = 0,$$

which implies the existence of a function  $f \in C^\infty(M)$  such that  $\text{curl } B = fB$ .  $\square$

However, the converse statement only holds with an additional assumption.

**Definition 2.11** The *rank* of a 2-form  $\omega \in \Omega^2(M)$  is the largest power  $r \in \mathbb{Z}_{\geq 1}$  such that

$$\omega^r \neq 0 \quad \text{and} \quad \omega^{r+1} = 0.$$

The rank is said to be *maximal* if  $r = n$  on a manifold of even dimension  $2n$ , resp. odd dimension  $2n + 1$ .

**Lemma 2.12** Let  $M$  be a manifold of odd dimension  $2n + 1$  and  $\omega \in \Omega^2(M)$  of maximal rank. Then for every vector field  $X \in \Gamma TM$  we have that  $\iota_X \omega^n = 0$  if and only if  $\iota_X \omega = 0$ .

*Proof.* From  $\iota_X \omega^n = n(\iota_X \omega) \wedge \omega^{n-1}$  it is clear that  $\iota_X \omega = 0$  implies  $\iota_X \omega^n = 0$ .

For the converse statement, locally pick a basis  $\xi, \eta_1, \dots, \eta_{2n} \in \Omega^1(M)$  such that  $\omega^n = \eta_1 \wedge \dots \wedge \eta_{2n}$  and  $\xi(X) > 0$ . Now, for the sake of contradiction, suppose  $\iota_X \omega \neq 0$ , i.e.,  $\omega$  is of the form

$$\omega = \xi \wedge \alpha + \beta$$

for  $\alpha \in \text{span}\{\eta_1, \dots, \eta_{2n}\}$  and  $\beta \in \text{span}\{\eta_1 \wedge \eta_2, \dots, \eta_{2n-1} \wedge \eta_{2n}\}$ . Then

$$\omega^n = n \xi \wedge \alpha \wedge \beta + \beta^n,$$

which by contracting with  $X$  gives

$$0 = \iota_X \omega^n = n \alpha \wedge \beta.$$

Since  $\alpha \wedge \beta \neq 0$  we have reached the desired contradiction, hence  $\iota_X \omega = 0$ .  $\square$

**Remark 2.13** Following Cardona Aguilar [17] we will refer to the vector field  $B \in \Gamma TM$  (*resp.*  $B^\flat$ ) on a Riemannian manifold  $M$  as *generic* if  $dB^\flat$  has maximal rank almost everywhere.

**Proposition 2.14** Let  $B \in \Gamma TM$  be a nowhere vanishing and generic Beltrami field on a Riemannian manifold  $M$  of odd dimension  $2n + 1$ . Then  $B$  is force-free.

*Proof.* Let  $f \in C^\infty(M)$  such that  $\text{curl } B = fB$ , then

$$f\iota_B \mu_g = \iota_{\text{curl } B} \mu_g = (dB^\flat)^n$$

and therefore

$$0 = f\iota_B \iota_B \mu_g = \iota_B (dB^\flat)^n.$$

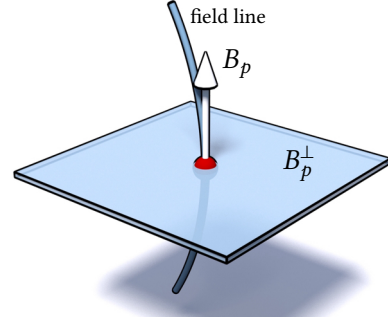
By the genericity assumption,  $f$  is non-vanishing almost everywhere, hence from Lemma 2.12 and  $B \in \ker(dB^\flat)^n$  we conclude that  $B \in \ker dB^\flat$  almost everywhere, which yields the claim by continuity.  $\square$

Unfortunately, the equivalence between geodesic vector fields and Beltrami fields on 3-manifolds (Section 3.2) cannot be generalized to dimensions  $2n + 1 > 3$  [87, 17]. However, in Section 3.2 we show that in return for our additional genericity assumption, our Definition 2.6 preserves an even stronger version of this equivalence, not only in odd but arbitrary dimensions. Moreover, our definition preserves the property that the defining equations for force-free forms contain (exact) harmonic forms as special cases. Lastly, again in agreement with the 3-dimensional theory, our defining equations emerge as the Euler-Lagrange equations of corresponding variational principles (Sections 4.2 and 4.3).

### 2.1.2 ORTHOGONAL DISTRIBUTIONS

**Definition 2.15** A *distribution* is a section  $\Xi \in \Gamma G_k(TM)$  in the Grassmannian bundle of  $k$ -planes.

Consequently, a *hyperplane distribution* is a section  $\Xi \in \Gamma G_{n-1}(TM)$  in the Grassmannian bundle of hyperplanes. A vector field  $B \in \Gamma TM$  is said to be *in the distribution* if for every  $p \in M$  we have that  $B_p \in \Xi_p \subseteq T_p M$ . We denote this instance by  $B \in \Xi$ . Moreover, a distribution  $\Xi \in \Gamma G_k(TM)$  is said to be *involutive* if  $[X, Y] \in \Xi$  for any two vector fields  $X, Y \in \Xi \subset TM$ . For each point  $p \in M$ , the *orthogonal distribution* to a vector field  $B$  is given by



$$B_p^\perp := \{Y \in T_p M \mid g(B_p, Y) = 0\}.$$

**Lemma 2.16**  $B^\perp \in \Gamma G_{n-1}(TM)$  is involutive if and only if  $B^\flat$  is closed.

*Proof.* Let  $X, Y \in \Gamma TM$ , then

$$\begin{aligned} dB^\flat(X, Y) &= g(\nabla B \wedge I)(X, Y) \\ &= g(\nabla_X B, Y) - g(\nabla_Y B, X) \\ &= Xg(B, Y) - g(B, \nabla_X Y) - Yg(B, X) + g(B, \nabla_Y X) \\ &= g(B, [X, Y]) + Xg(B, Y) - Yg(B, X). \end{aligned}$$

Now let  $dB^\flat = 0$ . Then for  $X, Y \in \Gamma B^\perp$  the above computation implies  $[X, Y] \perp B$ , i.e.,  $B^\perp$  is involutive.

Conversely, let  $B^\perp$  be involutive. Then for  $X, Y \in B^\perp$ , we have  $dB^\flat(X, Y) = 0$ . Moreover, by assumption  $0 = \iota_B dB^\flat$ , so that  $B \in \ker dB^\flat$  and thus  $dB^\flat = 0$ .  $\square$

By Frobenius' theorem, a distribution is involutive if and only if it is integrable [38, Ch. 6], from which we conclude a condition for the converse statement of Proposition 2.7 to be true (Fig. 2.2).

**Corollary 2.17**  $B \in \Gamma TM$  is harmonic if and only if  $B^\perp \in \Gamma G_{n-1}(TM)$  is integrable.

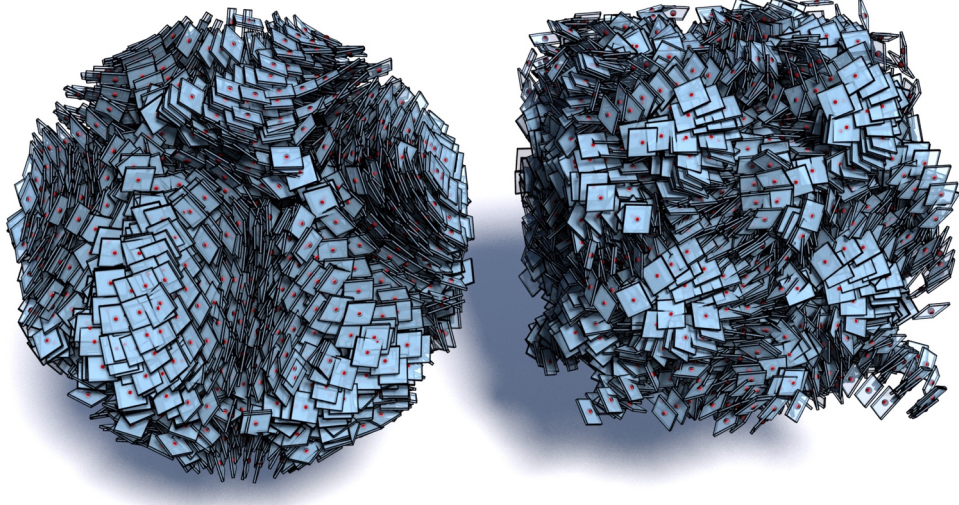


**Figure 2.2:** Visualization of the orthogonal distribution  $B^\perp$  for a harmonic field (left; Fig. 2.7) and a force-free field (right; Fig. 2.5). By Lemma 2.16 the planes of the harmonic are tangent planes to surfaces, whereas for the ones from the force-free case such surfaces cannot exist.

### 2.1.3 EVEN-DIMENSIONAL CASE

In Section 2.1.1 we pointed out that in odd dimensions an alternative definition is common for the fields we consider and worked out the conceptual differences. In even dimensions we instead consider the equation

$$f\mu_g = (dB^\flat)^n, \quad (2.8)$$

which defines the so-called *vorticity function*  $f \in C^\infty(M)$  [41, 3]. Eq. (2.8) is well defined for generic  $B$ , in the sense that  $dB^\flat$  is symplectic 2-form on  $M$ .

**Lemma 2.18** If  $B$  is in MHS equilibrium, the vorticity function is a first integral of the flow of  $B$ , i.e.,  $df(B) = 0$ .

*Proof.* Taking the exterior derivative on both sides of  $\iota_B dB^\flat = dp$  gives  $\mathcal{L}_B dB^\flat = 0$ . Since  $\mathcal{L}_B \mu_g = 0$ , we have

$$0 = \mathcal{L}_B(dB^\flat)^n = \mathcal{L}_B(f\mu_g) = df(B)\mu_g,$$

which concludes the proof as  $\mu_g$  is a volume form. □

The existence of this first integral  $f$  in addition to the first integral  $p$  allows

a generalization of Arnold's structure theorem (Section 2.3.1) in four dimensions for generic  $B$  (in the sense that neither  $f$  nor  $p$  vanish) [41]. However, our main interest focuses on force-free fields. By contracting Eq. (2.8) with  $B$  we find

$$f\iota_B\mu_g = \iota_B(dB^\flat)^n = 0$$

from which we conclude that  $f = 0$  whenever  $B \neq 0$ . Consequently, similar to the 3-dimensional setup, a lot of the structure is lost in the force-free case.

In order to better place this finding in our previous observations, let us consider the case  $n = 1$ . Consider a non-vanishing and force-free  $B \in \Gamma TM$ . Then  $f \equiv 0$  together with Eq. (2.8) implies that  $0 = dB^\flat$ . Hence, by Corollary 2.17,  $B^\perp$  is integrable.

## 2.2 FLUX FORM REPRESENTATION

In the absence of a specific reference metric, we can chose to represent field lines of a divergence-free vector field by merely a closed  $(n - 1)$ -form  $\beta$  to which we refer to as a *flux form*. Then, the field lines are curves in  $M$  tangent to  $\ker \beta$  at every point  $p \in M$ . The representation of geometry in terms of co-dimensional forms has become a popular tool in, e.g., geometry processing [109, 110, 93].

### 2.2.1 FLUX FORMS IN RIEMANNIAN GEOMETRY

On a Riemannian manifold  $M$ , a flux form  $\beta \in \Omega^{n-1}(M)$  together with the metric define the *vector field*  $B \in \Gamma TM$  associated to the flux form by

$$\beta = \iota_B\mu_g = \star B^\flat.$$

The divergence-free condition ( $\operatorname{div} B = 0$ ) of the magnetic vector field translates to a closedness condition ( $d\beta = 0$ ) on the level of the flux form, since

$$d\beta = d\iota_B\mu_g = \mathcal{L}_B\mu_g = \operatorname{div}(B)\mu_g.$$

**Definition 2.19** The *flux form* of a magnetic field  $B \in \Gamma TM$  is given by

$$\beta = \iota_B\mu \in \Omega^{n-1}(M),$$

and satisfies  $d\beta = 0$ .

## CHAPTER 2. PLASMA IN RIEMANNIAN MANIFOLDS

The Riemannian structure induces a norm on  $k$ -forms which, for  $\omega \in \Lambda^k T_p^*(M)$ , is defined by

$$|\omega|^2 := \star(\omega \wedge (\star\omega)).$$

Moreover, from the non-degenerate pairing

$$\langle \cdot | \cdot \rangle : \Lambda^k T_p^*(M) \times \Lambda^{(n-k)} T_p^*(M) \mapsto \mathbb{R}, (\eta, \omega) \mapsto \star(\eta \wedge \omega)$$

we have an isomorphism  $\Lambda^k T_p^*(M) \cong \Lambda^{(n-k)} T_p^*(M)$ .

### 2.2.2 PHYSICAL FLUX FORMS

To characterize special flow fields from our physically motivated applications, such as steady solutions to the ideal MHD equations, force-free fields and harmonic fields, we can use the Hodge star we can convert the 1-form  $B^\flat$  into a flux form  $\beta$  by

$$\beta = \star B^\flat \quad \text{and} \quad \star \beta = (-1)^{n-1} B^\flat,$$

where we used that for  $\alpha \in \Omega^k(M)$  it holds that  $\star(\star\alpha) = (-1)^{k(n-k)}\alpha$ . The definitions stated in Definition 2.6 can be directly carried over.

**Definition 2.20** A closed flux form  $\beta \in \Omega^{n-1}(M)$  with the associated vector field  $B \in \Gamma TM$  is said to be

- (i) *in magnetohydrostatic equilibrium* if it satisfies  $\iota_B d \star \beta = (-1)^{n-1} dp$  for some  $p \in C^\infty(M)$ .
- (ii) *force-free* if it satisfies  $\iota_B d \star \beta = 0$ .
- (iii) *harmonic* if it is co-closed, i.e.,  $d \star \beta = 0$ .
- (iv) *exact harmonic* if it is co-exact, i.e.,  $\beta \in \text{im}(\star d)$ .

In the course of this thesis, we will always use the most convenient representation for the flow fields depending on the context and will not distinguish between the representations as a 1-form, a vector field or a flux form.

## 2.3 STRUCTURE THEOREMS ON 3-MANIFOLDS

In this section we review some of the remarkable (geometric) structures steady solutions to Eq. (1.1) (Definition 2.6) exhibit in Riemannian 3-manifolds. Moreover,

steady Euler flows are known to be formally equivalent to these steady solutions and thus exhibit the same structures [3, Ch. 2]. For their classification the pressure function  $p$  (Definition 2.6) as well as the proportionality factor  $f$  (Definition 2.9) play an important role.

### 2.3.1 ARNOLD'S STRUCTURE THEOREM

In 1965, V.I. Arnold [2] gave a seminal classification of flows in MHS equilibrium for non-constant pressure function (Fig. 2.3).

**Theorem 2.21 (Arnold's structure theorem)** Let  $M$  be a compact analytic 3-manifold,  $B \in \Gamma TM$  be analytic and in MHS equilibrium for a non-constant pressure function  $p \in C^\infty(M)$ . If  $\partial M \neq \emptyset$ , let  $B$  be tangent to the boundary. Then  $M$  can be partitioned by an analytic submanifold into finitely many domains  $M_i$  such that either

- (i)  $M_i$  is trivially fibered by invariant tori of  $B$  and on each torus the flow lines are either all closed or all dense.
- (ii)  $M_i$  is trivially fibered by invariant cylinders of  $B$  whose boundaries lie on the boundary of  $M$  and all flow lines are closed.

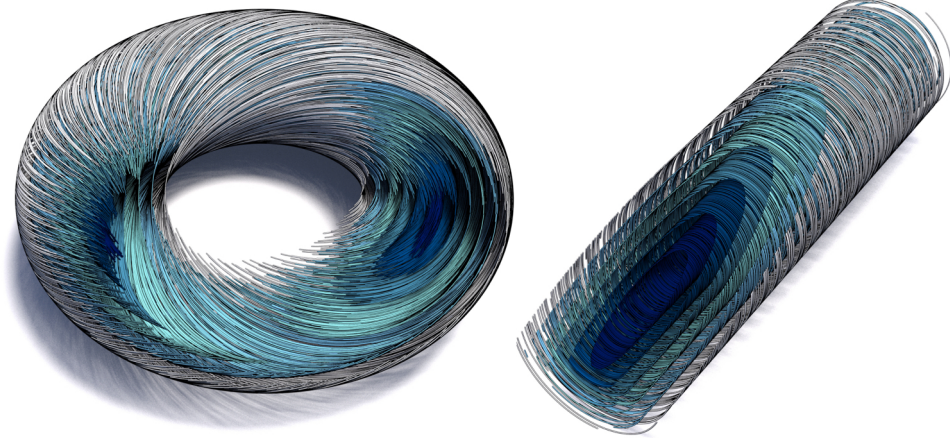


**Figure 2.3:** According to Arnold's structure Theorem 2.21, the domains of solutions to Eq. (1.3) can be decomposed into finitely many subdomains each of the form of one of the depicted template geometries.

Arnold's result has since been generalized to, e.g., four-dimensional [41] or relativistic settings [47]. For a thorough discussion of Theorem 2.21, we refer the

reader to [3, Thm 1.2] or [17, Thm 2.1.1]. Notably, a lot of the structure is lost for a constant pressure function  $p$ , *i.e.*, when the right-hand side of Eq. (1.3) vanishes.

### 2.3.2 CONSTANT PRESSURE FUNCTION

For the case of a constant pressure function  $p \in C^\infty(M)$  Eq. (2.2) reduces to Eq. (2.3). Therefore, we investigate the structure of force-free fields (Definition 2.6 (ii)). By Proposition 2.10, a force-free field is everywhere proportional to its curl. We consider two cases: first fields with non-vanishing proportionality factor  $f \in C^\infty(M)$  and second the case when  $f$  is vanishing.

#### NON-VANISHING PROPORTIONALITY FACTOR

The flow of a force-free (*resp.* Beltrami) field  $B$  with non-vanishing proportionality factor can still admit invariant surfaces given by the level sets of  $f$ , provided that  $\text{grad } f \neq 0$ . By taking the divergence of  $\text{curl } B = fB$  we see that

$$\text{grad } f \perp B,$$

hence the proportionality factor is a first integral of  $B$ . Before starting to explore some examples, let us prove the following Lemma 2.22 which will be useful at a later point.

**Lemma 2.22** Let  $M$  be a Riemannian manifold of dimension  $2n + 1$ ,  $B \in \Gamma TM$  and the proportionality factor  $f \in C^\infty(M)$  defined by  $\text{curl } B = fB$  non-vanishing. Then  $B$  is divergence-free if and only if either of the two conditions is satisfied:

(i)  $f$  is constant.

(ii)  $\text{grad } f \perp B$ .

*Proof.* With  $(dB^\flat)^n = \iota_{\text{curl } B} \mu_g = f \iota_B \mu_g = f \star B^\flat$  the claim follows from

$$\text{div}(B)\mu_g = d(\star B^\flat) = -\frac{1}{f^2} df \wedge (dB^\flat)^n = -\frac{1}{f} df \wedge \star B^\flat = -\frac{1}{f} g(\text{grad } f, B)$$

□

Clelland and Klotz [25, Sec. 5] provide constructions for force-free fields with the non-constant proportionality factor. For example, define a vector field  $B \in$

$\Gamma\text{TR}^3$  by  $B \perp \frac{\partial}{\partial z}$  and

$$g(B, \frac{\partial}{\partial x}) = v(x, y) \cos(\Phi(z)) + w(x, y) \sin(\Phi(z)),$$

$$g(B, \frac{\partial}{\partial y}) = -v(x, y) \sin(\Phi(z)) + w(x, y) \cos(\Phi(z)),$$

where  $u$  and  $v$  are such that  $F(x, y) := v(x, y) + i w(x, y)$  is a holomorphic function on the  $xy$ -plane.

**Lemma 2.23** A vector field  $B$  as defined above is force-free with proportionality factor  $f(x, y, z) = \Phi'(z) =: \phi(z)$ .

*Proof.* Evidently  $B$  is divergence-free by Lemma 2.22. By straightforward calculations we convince ourselves that  $g(\operatorname{curl} B, \frac{\partial}{\partial x}) = \Phi'(z) g(B, \frac{\partial}{\partial x})$ ,  $g(\operatorname{curl} B, \frac{\partial}{\partial y}) = \Phi'(z) g(B, \frac{\partial}{\partial y})$  and, since  $v$  and  $w$  satisfy the Cauchy-Riemann equations,

$$g(\operatorname{curl} B, \frac{\partial}{\partial z}) = -\frac{\partial v}{\partial x} \sin(\Phi) + \frac{\partial w}{\partial x} \cos(\Phi) - \frac{\partial v}{\partial y} \cos(\Phi) - \frac{\partial w}{\partial y} \sin(\Phi) = 0.$$

Therefore,  $\operatorname{curl} B = \phi B$  as claimed. □

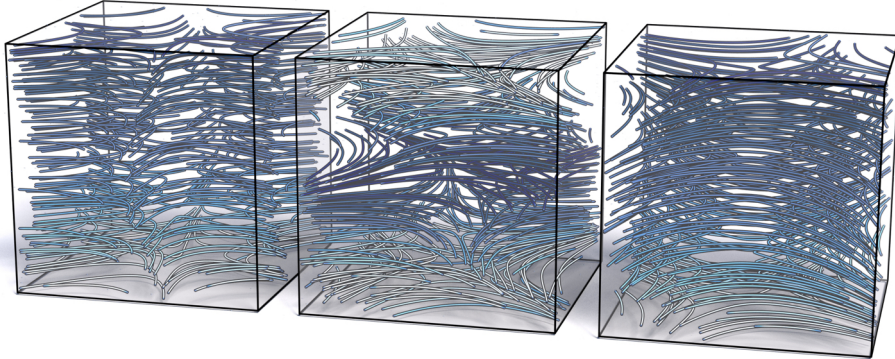


**Figure 2.4:** The force-free fields with non-constant proportionality factor  $f$  (colored) from Example 2.24 (from left to right).

**Example 2.24** In Fig. 2.4 we visualize three examples of force-free fields with non-constant proportionality factor  $f(x, y, z) = \phi(z)$  for the following choices of functions:

- (i) For  $\zeta = x + i y$ , the holomorphic function  $F(\zeta) = \zeta^2$  with real part  $v(x, y) =$

$2xy$ , imaginary part  $w(x, y) = x^2 - y^2$  and  $\Phi(z) = \frac{1}{2}z^2$  gives rise to a force-free field with proportionality factor  $\phi(z) = z$ .

- (ii) For  $\zeta = x + iy$ , the holomorphic function  $F(\zeta) = \sin(\zeta)$  with real part  $v(x, y) = \sin(x)\cosh(y)$ , imaginary part  $w(x, y) = \cos(x)\sinh(y)$  and  $\Phi(z) = \sin(\pi z)$  gives rise to a force-free field with proportionality factor  $\phi(z) = \pi \cos(\pi z)$ .
- (iii) For  $\zeta = x + iy$ , the holomorphic function  $F(\zeta) = \sin(\zeta)$  with real part  $v(x, y) = \sin(x)\cosh(y)$ , imaginary part  $w(x, y) = \cos(x)\sinh(y)$  and  $\Phi(z) = \frac{1}{2}z^2$  gives rise to a force-free field with proportionality factor  $\phi(z) = z$ .

**Remark 2.25** Enciso and Peralta-Salas [33] show that most non-constant functions  $f$  cannot occur as the proportionality factor for any non-vanishing Beltrami field, even locally [25]. However, a more recent result of Clelland and Klotz [25] shows that a generic Beltrami field has non-constant proportionality factor in the sense that Beltrami fields are locally parametrized by 3 functions of 2 variables, while for those with constant proportionality factor only 2 functions of 2 variables suffice.

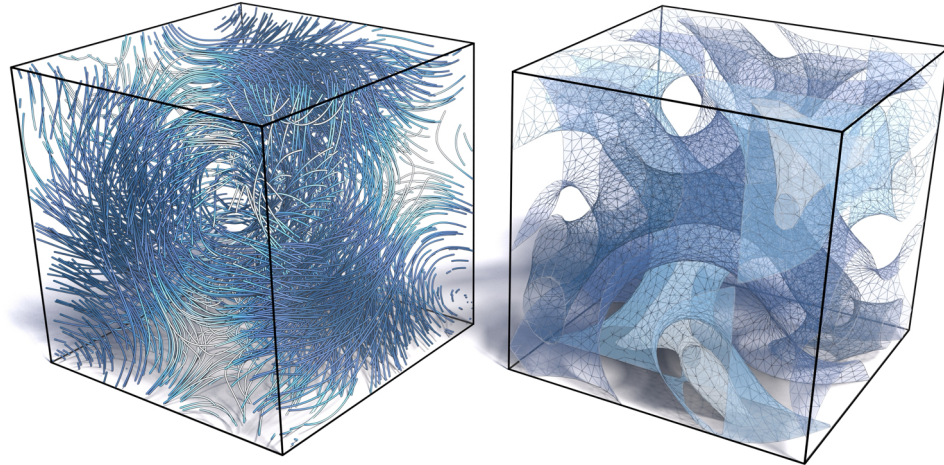


**Figure 2.5:** Left: Field lines of the ABC-flow Eq. (2.9) for  $A = B = C = 1$ . Right: Levelsets of the squared magnitude of the flow field which, taken as a conformal factor, make the field lines geodesics (Corollary 3.47).

The Arnold–Beltrami–Childress flow (ABC-flow) (Figs. 2.5 and 2.6) is a popular example for a Beltrami field with constant  $f$ . It is defined on the three dimensional

flat torus  $(\mathbb{R}/2\pi)^3$  and generated by

$$X_{ABC} = \begin{bmatrix} A \sin(z) + C \cos(y) \\ B \sin(x) + A \cos(z) \\ C \sin(y) + B \cos(x) \end{bmatrix} \quad (2.9)$$

for parameters  $A, B, C \in \mathbb{R}$ . By a straightforward computation one can check that

$$\operatorname{curl} X_{ABC} = 1 \cdot X_{ABC}. \quad (2.10)$$

Dombre et al. [31] investigate the topology of the ABC-flow both analytically and numerically finding that the flow is non-vanishing whenever  $B^2 + C^2 < 1$ , where we assume  $1 = A \geq B \geq C \geq 0$ . Moreover, whenever one of the parameters  $A, B, C$  vanishes, the flow is integrable (Fig. 2.6). For generic choices of parameters  $ABC \neq 0$ , integrability is typically lost and the ABC-flow typically exhibits complicated topologies, including chaotic streamlines. For more information on the ABC-flow we refer the reader to [3, Ch. 2.1] and [31, 33, 10].

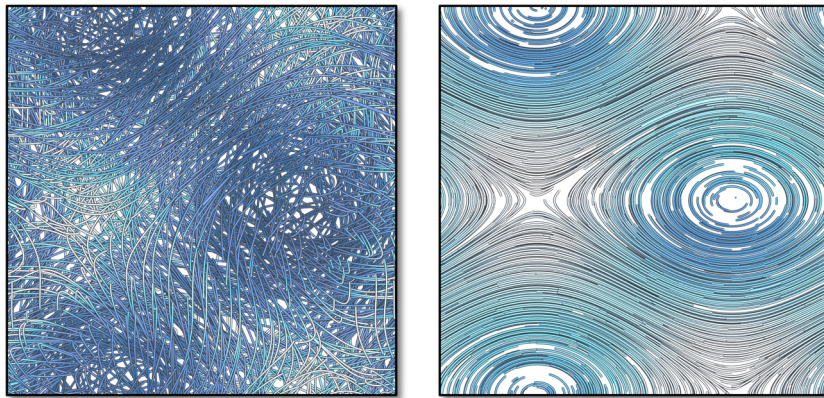


**Figure 2.6:** Orthographic views on the ABC-flow for  $A = B = C = 1$  (left; see Fig. 2.5) and  $A = 1, B = 1/2$  and  $C = 0$  (right).

### VANISHING PROPORTIONALITY FACTOR

If the proportionality factor vanishes, the field is harmonic. In that case, by Corollary 2.17, the conditions (iii) and (iv) of Definition 2.6 can be related to the integrability of the hyperplane distribution orthogonal to  $B$ . That is,

$$dB^\flat = 0 \iff B^\perp \text{ is integrable.}$$

Fig. 2.7 shows an example of an exact harmonic field on the unit ball  $\mathbb{B} = \{x \in \mathbb{R}^3 \mid |x| \leq 1\}$ . The distribution  $B^\perp$  orthogonal to  $B$  is tangent to the levelsets of the potential function. Merely harmonic, but not exact harmonic examples are shown in Fig. 2.8. In particular, since the co-dimension of the foliation is too small, it does not allow for a “twistedness” of the flow lines of  $B$  which distinguishes merely force-free from harmonic fields. The following statement asserts that this is true in general as long as the field does not vanish.

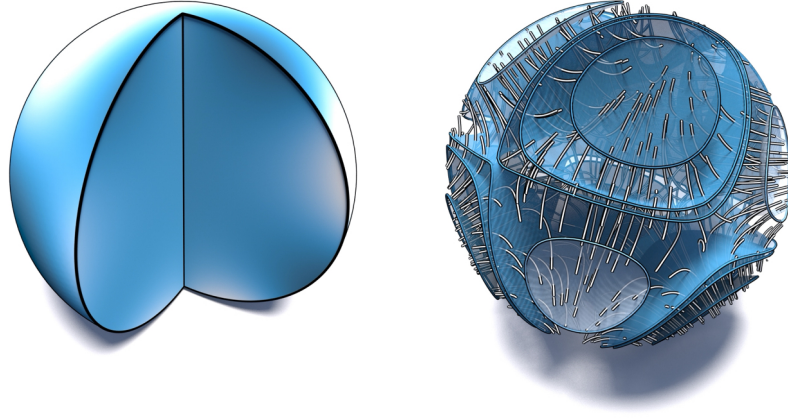


**Figure 2.7:** The field lines of an exact harmonic vector field  $X = \text{grad } \phi$  (right) on the unit ball  $\mathbb{B} = \{x \in \mathbb{R}^3 \mid |x| \leq 1\}$  intersect levelsets (right) of  $\phi$  (left) orthogonally. Although the statement also holds for harmonic fields which are not exact (cf. Fig. 2.8), for non-harmonic fields, such level surfaces cannot exist by Lemma 2.16.

**Corollary 2.26** Let  $B \in \Gamma M$  be a non-vanishing vector field on a 2-dimensional Riemannian manifold. Then,  $B$  is force-free if and only if  $B$  is harmonic.

*Proof.* Since  $M$  is 2-dimensional and  $B \neq 0$  we have  $\dim(B_p^\perp) = 1$  for all  $p \in M$ . Hence, for two vector fields  $X, Y \in \Gamma B^\perp$ , there is  $f \in C^\infty(M)$  such that  $X = fY$ . Then,

$$[X, Y] = df(X)X \in B^\perp$$

is a scalar multiple of  $X$  so that with Corollary 2.17 we conclude that  $dB^\circ$  and hence  $B$  is harmonic.  $\square$

**Definition 2.27** A *global cross section* to a flow on a closed  $n$ -dimensional manifold  $M$  is a closed  $(n-1)$ -dimensional submanifold  $S$ , transverse to  $X$  and meeting every orbit in at least one point.



**Figure 2.8:** Two vector fields on a torus generating the homology, hence they are harmonic, but not exact. Moreover, they mutually constitute the integrable orthogonal distribution in the sense of Lemma 2.16.

**Example 2.28** The flows generated by vector fields corresponding to non-trivial generators of the de Rham cohomology of, e.g., an  $n$ -torus admit a global cross section (Fig. 2.8).

Harmonic vector fields are characterized by a vanishing proportionality factor. In particular, for those foliations the 1-form  $B^\flat$  is closed, i.e.,  $dB^\flat = 0$ , and the orthogonal hyperplane distribution  $B^\perp$  is integrable in the Frobenius' sense. Hence, if the manifold  $M$  is closed,  $B^\perp$  is tangent to a family of global cross-sections  $S$ . This observation matches a result by Tischler [106].

**Theorem 2.29 ([106, Thm. 1])** Let  $M$  be a closed  $n$ -dimensional manifold. Suppose  $M$  admits a non-vanishing closed 1-form. Then  $M$  is a fiber bundle over  $S^1$ .

# CHAPTER 3

## GEODESIBLE AND CONFORMALLY GEODESIC VECTOR FIELDS

In the course of this thesis, we investigate geometric structures of the physical fields that we introduced in Chapter 2. We start this chapter with an overview of some known results and examples on the *geodesibility* of vector fields. The problem describes the question whether there is a metric for a given vector field with respect to which the flow lines are geodesic. The goal is to contextualize the results presented in this thesis and provide a basis for new insights.

We do not necessarily need to have knowledge of a reference metric to speak about the geodesibility of a vector field. Consequently, in Section 3.2 we will consider a general differentiable manifold  $M$ , assuming for Sections 3.2.1 and 3.2.2 that  $M$  is orientable and of odd dimension. In Section 3.3 we then relate the vector fields that are geodesible to fields that are physical (*i.e.*, plasma fields) or Killing fields in a conformal manifold. Ultimately, the goal of this chapter is to establish a conformal equivalence between the metrics that make a given field geodesic and the metrics that make it, *e.g.*, force-free.

### 3.1 GEODESIC AND EIKONAL FIELDS

**Definition 3.1** A vector field  $X \in \Gamma TM$  on a Riemannian manifold  $M$  is called *pre-geodesic* if its acceleration is always proportional to itself, *i.e.*, there is a  $\rho \in C^\infty(M)$  such that

$$\nabla_X X = \rho X.$$

If  $\rho = 0$ , then  $|X|$  is constant along flow lines and  $X$  is called *geodesic*.

The flow lines associated to a (pre-)geodesic vector field trace out geodesics (possibly up to reparametrization) in the Riemannian manifold. Therefore, we will say the flow lines of a field are *geodesic* if the field is (pre-)geodesic. Whenever  $X$  is non-vanishing we may consider the *directional vector field*  $H := |X|^{-1}X \in \Gamma TM$  without changing the geometry of the field lines. The corresponding *directional covector field* is given by  $H^\flat(\cdot) = g(H, \cdot)$ .

Consider a flux form  $\beta \in \Omega^{n-1}(M)$  with associated vector field  $B \in \Gamma TM$ .

**Definition 3.2** A flux form  $\beta \in \Omega^{n-1}(M)$  is *geodesic* if the associated vector field  $B$  is (pre-)geodesic in the sense of Definition 3.1.

Normalization of the field  $B$  amounts to a reparametrization of the field lines and therefore does not change their specific geometry. In particular, the flux form  $\beta$  determines the flow lines it represents only up to reparametrization, hence the flux forms  $\beta$  and  $\frac{\beta}{|\beta|} = \star H^\flat$  describe the same field line geometries. Since  $|B| = |\beta| = |\star \beta|$  (Section 2.2.1), Lemma 2.3 implies that

$$(\nabla_H H)^\flat = \iota_H dH^\flat = (-1)^{n-1} \iota_H d\left(\frac{\star \beta}{|\star \beta|}\right),$$

from which we conclude:

**Lemma 3.3** A vector  $B \in \Gamma TM$  is (pre-)geodesic resp. the corresponding flux form  $\beta \in \Omega^{n-1}(M)$  is geodesic if and only if on its support

$$0 = \iota_B d\left(\frac{B^\flat}{|B|}\right) = \iota_B d\left(\frac{\star \beta}{|\star \beta|}\right). \quad (3.1)$$

Note that Eq. (3.1) implies that a vector field  $B$  is geodesic if and only if its directional vector field is force-free.

## NORMALIZATIONS

The statement of Lemma 3.3 can be reformulated to eliminate the restriction to the support of  $\beta$ . To this end, we address the ill-posedness of normalization when the flux form  $\beta$  vanishes on open sets.

**Definition 3.4** Let  $\alpha \in \Omega^k(M)$ . Then a  $k$ -form  $\eta \in \Omega^k(M)$  is called a normalization of  $\alpha \in \Omega^k(M)$  if

$$|\alpha|\eta = \alpha \quad \text{and} \quad |\eta| \leq 1.$$

At every point  $p \in M$ , a normalization can be seen as an element of the subdifferential  $\partial|\beta|$  (Section 4.3). Thus, whenever the flux form  $\beta$  is non-vanishing, it is

uniquely determined. In particular, on the support of a flux form, a normalization coincides with the directional covector field. Therefore, we may more adequately state Lemma 3.3 as follows:

**Lemma 3.5** A flux form  $\beta \in \Omega^{n-1}(M)$  is geodesic if and only if there exists a normalization  $\eta \in \Omega^1(M)$  of  $\star\beta$  such that

$$0 = \iota_B d\eta. \quad (3.2)$$

**Definition 3.6** A closed flux form  $\beta \in \Omega^{n-1}(M)$  is called *eikonal* (*resp. exact eikonal*) if there exists a closed (*resp. exact*) normalization  $\eta \in \Omega^1(M)$  of  $\star\beta$ .

**Proposition 3.7** (Exact) eikonal flux forms are geodesic.

## 3.2 GEODESIBLE VECTOR FIELDS

Foliations of a space with geodesics do not only play an important role in physics (Section 1.2), but also show up in theoretical investigations of, *e.g.*, adaptions of the Seifert conjecture, minimal foliations or stable Hamiltonian structures [87, 121, 17]. The importance of these vector fields in a multitude of both, theoretical and practical applications, naturally leads to the question if there is always some Riemannian metric for which a given vector field is geodesic?

**Definition 3.8** A vector field  $X \in \Gamma TM$  on a manifold  $M$  is *geodesible* if there is a Riemannian metric  $g$  such that  $X$  is geodesic with respect to  $g$ .

There is a multitude of results on the geodesibility of vector fields. Let us recall the perhaps most well-known characterizations due to Gluck [42, 43] and Sullivan [103].

**Theorem 3.9 ([43, Sec. 10])** Let  $M$  be a smooth manifold and  $X \in \Gamma TM$  a smooth non-vanishing vector field on  $M$ . Then the following conditions are equivalent:

- (i) There exists a 1-form  $\alpha \in \Omega^1(M)$  such that  $\alpha(X) = 1$  and  $\mathcal{L}_X \alpha = 0$ , *i.e.*,  $\alpha$  is *invariant under the flow of  $X$* .
- (ii) There exists a 1-form  $\alpha \in \Omega^1(M)$  such that  $\alpha(X) = 1$  and  $\iota_X d\alpha = 0$ .
- (iii) There exists a Riemannian metric on  $M$  making the field lines of  $X$  geodesic and  $X$  of unit length.

*Proof.* For the equivalence between (i) and (ii) we note that for  $\alpha \in \Omega^1(M)$  with  $\alpha(X) = 1$  we have

$$\mathcal{L}_X \alpha = d\iota_X \alpha + \iota_X d\alpha = \iota_X d\alpha.$$

For the equivalence between (i) and (iii) we note that by Lemma 2.3, for any Riemannian metric

$$\mathcal{L}_X \alpha = d\iota_X \alpha + (\nabla_X X)^b + \frac{1}{2}d|X|^2.$$

If the Riemannian metric  $g$  is such that  $|X| = 1$  and  $\nabla_X X = 0$ , we set  $\alpha := X^b$  and all terms on the right-hand side of the equation vanish, hence  $\mathcal{L}_X \alpha = 0$ . Conversely, we can define a Riemannian metric  $g$  on  $M$  by asking that for  $X \in (\ker \alpha)^\perp$ ,  $g(X, X) = 1$  and  $g$  arbitrary on  $\ker \alpha$ . Then  $0 = \mathcal{L}_X \alpha = (\nabla_X X)^b$  implies that the flow lines of  $X$  are geodesic.  $\square$

**Theorem 3.10** Let  $X$  be a non-vanishing vector field on  $M$ . Then there is a Riemannian metric on  $M$  making the integral curves of  $X$  geodesic if and only if there exists a 1-form  $\alpha \in \Omega^1(M)$  on  $M$  satisfying

$$\alpha(X) > 0 \quad \text{and} \quad X \in \ker(d\alpha).$$

*Proof.* Let  $g$  be a Riemannian metric on  $M$  such that the orbits of  $X$  are geodesics. Then, since  $X$  is non-vanishing, the directional vector field  $H := |X|^{-1}X$  is well defined and satisfies the assumptions of (iii) in Theorem 3.9, which is equivalent to (ii) and thus the claim follows.

Let conversely be  $\alpha \in \Omega^1(M)$  be the proposed 1-form. Then the vector field  $\bar{X} := \alpha(X)^{-1}X$  satisfies the assumptions of (ii) in Theorem 3.9, which is equivalent to (iii) and thus the claim follows.  $\square$

Theorem 3.10 is often attributed to an open letter by Gluck [42] titled “Can space be filled by geodesics, and if so, how?”. Note that the statement only refers to the direction of  $X$ , not to its specific length. Therefore, an equivalent characterization of geodesible vector fields can be given in terms of transverse hyperplane distributions.

**Definition 3.11** A hyperplane distribution  $\Xi \in \Gamma G_{n-1}(TM)$  is said to be *transverse* to a vector field  $X \in \Gamma TM$  if  $X_p \notin \Xi_p$  for all  $p \in M$ .

A hyperplane distribution transverse to a vector field  $X$  can be described by a 1-form  $\xi \in \Omega^1(M)$  which satisfies  $\ker \xi = \Xi$  and  $\xi(X) > 0$ . This 1-form is not

uniquely determined. In view of Theorems 3.9 and 3.10, the admissible  $\xi$  come from a rescaling by a non-vanishing function. Consequently we say that the distribution  $\Xi$  is *preserved by*  $X$  if  $\mathcal{L}_X \xi = 0$  for  $\xi$  scaled such that  $\xi(X) = 1$ .

**Corollary 3.12** A vector field  $X \in \Gamma TM$  is geodesible of unit length if and only if it preserves a transverse hyperplane distribution  $\Xi \in \Gamma G_{n-1}(TM)$ .

*Proof.* This follows from the equivalence between (ii) and (iii) in Theorem 3.9 where the hyperplane distribution is given by  $\Xi := \ker \alpha$ .  $\square$

By rewriting the second condition  $X \in \ker(d\alpha)$  as  $\iota_X d\alpha = 0$  we immediately see that our Definition 2.6 (ii) in Section 2.1 satisfies the assumptions of Theorem 3.10. The converse statement is also true even if the vector field is not necessarily divergence-free, which gives rise to:

**Theorem 3.13** A vector field  $X \in \Gamma TM$  on a Riemannian manifold and  $M$  satisfies the force-free condition ( $\iota_X dX^\flat = 0$ ) if and only if it is geodesible.

In view of Theorem 3.13 it is now clear why geodesible vector fields are of interest for our purposes.

Notably, Theorems 3.9 and 3.10 resp. Theorem 3.13 only guarantee that the field is geodesic resp. the 1-form representing the Lorentz force vanishes, but not that the field preserves the induced (or any) volume form. With Lemma 2.22 we have conditions on the proportionality factor  $f$  which, if fulfilled, ensure that the volume form induced by the metric is preserved. Alternatively, it is sufficient if the field preserves any volume form  $\mu$ . In that case we can use the degrees of freedom in the choice of metric and choose  $g$  accordingly so that the induced volume form and  $\mu$  match. The following Lemma 3.14 will be useful for the proof.

**Lemma 3.14** ([16, Lem. 3.2]) Let  $X \in \Gamma TM$  be a non-vanishing vector field and  $\alpha \in \Omega^1(M)$  such that  $\alpha(X) > 0$ . Further, let  $\mu$  be a volume form on  $M$ . Then there exists a Riemannian metric  $g$  such that  $\iota_X g = \alpha$  and  $\mu$  is the induced volume form, i.e.,  $\mu = \mu_g$ .

**Corollary 3.15** Let  $X \in \Gamma TM$  be a non-vanishing vector field. Then there exists a metric  $g$  on  $M$  such that  $X$  is force-free if and only if there exists a 1-form  $\alpha \in \Omega^1(M)$  on  $M$  satisfying  $\alpha(X) > 0$  and  $X \in \ker(d\alpha)$  and  $\mathcal{L}_X \mu_g = 0$ , i.e.,  $\mu_g = \mu$ .

*Proof.* Let  $\alpha$  be the 1-form existing according to the assumption. By Lemma 3.14 there is a metric  $g$  on  $M$  such that  $\alpha = \iota_X g$  and  $\mu = \mu_g$ . Therefore,  $0 = \iota_X d\alpha = \iota_X dX^\flat$  and  $0 = \mathcal{L}_X \mu = \mathcal{L}_X \mu_g$ , i.e.,  $X$  is force-free.

Conversely, let  $g$  be such that  $X$  is force-free. Then by definition it preserves the volume form  $\mu_g$ . Moreover, with  $\alpha := X^\flat$  we find that  $\alpha(X) = g(X, X) > 0$ , since  $X \neq 0$ , and  $0 = \iota_X dX^\flat = \iota_X d\alpha$ , i.e.,  $X \in \ker d\alpha$ .  $\square$

### EXAMPLES OF NON-GEODESIBLE VECTOR FIELDS

In this section we give some examples of vector field which are not geodesible. The most common examples are fields which contain a *Reeb annulus*. That is an oriented annulus  $A$  consisting of leaves of a foliation such that the boundary orientation of  $\partial A$  coincides with the orientation of the foliation (Fig. 3.1).

**Lemma 3.16** A vector field  $X \in \Gamma A$  generating the foliation of a Reeb annulus  $A$  is not geodesible.

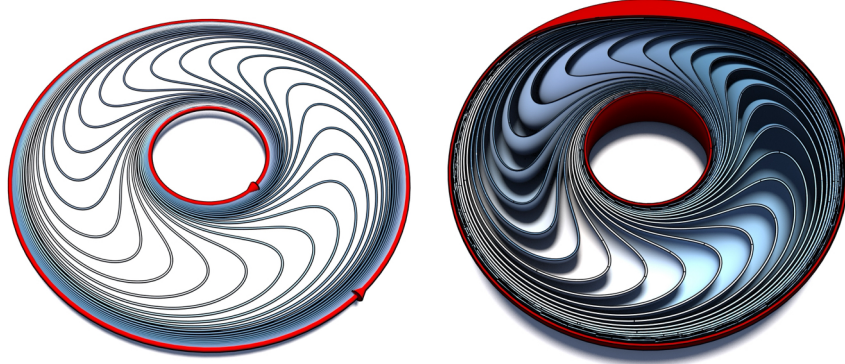


**Figure 3.1:** A foliation of an annulus known as Reeb annulus (left) and a higher dimensional analogue (right). There is no Riemannian metric on the annulus resp. the full torus such that the leaves of the foliations become minimal submanifolds.

*Proof.* For the sake of contradiction let us assume that a vector field  $X$  generating the foliation is geodesible and let  $\alpha \in \Omega^1(A)$  be the 1-form whose existence is assured by Theorem 3.10. Then, by Stokes' theorem,

$$0 = \int_A d\alpha = \int_{\partial A} \alpha,$$

which contradicts  $\alpha(X) > 0$ .  $\square$

**Remark 3.17** In [43] Gluck proves that on a closed surface a *Reeb component*<sup>1</sup> is in fact the only obstruction from geodesibility for a non-vanishing vector field.

In Section 2.1.1 we discussed that force-free fields are Beltrami fields which satisfy an additional genericity condition. For our purposes, this condition cannot be dropped, since without it the equivalence of Theorem 3.13 would no longer be true in dimensions  $2n + 1 > 3$ , since Beltrami fields admit *plugs*. Plugs are 3-manifolds with boundary endowed with a non-vanishing vector field that is either transverse or parallel to the boundary and which can be used to modify a vector field on a compact domain by suitably gluing them in. Their crucial property is that some integral curves enter the plug, but cannot leave it again. For our purposes, the important observation is that by a characterization of geodesible vector fields given by Sullivan [103], plugs are not geodesible in any dimension.

Plugs can be constructed smoothly, which was used by Kuperberg [60] to disprove the Seifert conjecture, or even volume preserving as done by Cardona [16] to construct volume preserving Beltrami fields which are not geodesible:

**Theorem 3.18 ([16, Thm. 4.3])** There are divergence-free Beltrami fields in any manifold of dimension  $2n+1 > 3$  and any homotopy class of non-vanishing vector fields which are not geodesible.

Since we restrict our attention to the generic case of force-free fields which by Theorem 3.13 do not admit plugs, a precise definition is beyond the scope of this thesis and we refer to [87, 17] for more details.

Next, we turn to the classes of vector fields that are geodesible and place them in the context of our earlier discussion of physical vector fields and their structures.

### 3.2.1 REEB VECTOR FIELDS

One example for geodesible vector fields are so-called *Reeb vector fields* on a contact manifold.

**Definition 3.19** On an orientable manifold of odd dimension  $2n + 1$ ,  $\alpha \in \Omega^1(M)$  is said to be *contact 1-form* if

$$\alpha \wedge (d\alpha)^n \neq 0.$$

---

<sup>1</sup>A component in the vector field which is obtained by suitably gluing in a Reeb annulus.

Any contact 1-form describes a hyperplane distribution  $\Xi := \ker \alpha$  and vice versa. The hyperplane distribution  $\Xi$  is referred to as a *contact structure* on  $M$  and the pair  $(M, \Xi)$  is a *contact manifold*. It should be noted that this relationship is not unique and that any other form of contact 1-form that determines  $\Xi$  is a rescaling of  $\alpha$  by a non-vanishing function.

**Example 3.20** The standard example for a contact 1-form on  $\mathbb{R}^3$  is given by  $\alpha = dz + y dx$  (Fig. 3.2).

**Definition 3.21** On an orientable manifold of odd dimension  $2n + 1$  with contact 1-form  $\alpha \in \Omega^1(M)$ , the *Reeb vector field*  $R \in \Gamma TM$  is uniquely defined by

$$\alpha(R) = 1, \quad R \in \ker(d\alpha). \quad (3.3)$$

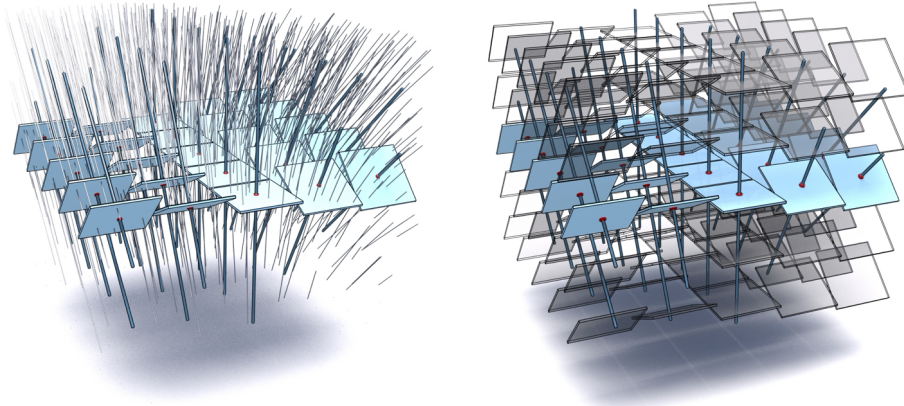


**Figure 3.2:** Left: Field lines of the Reeb vector field corresponding to the contact 1-form  $\alpha = dz + y dx$ . Right: the corresponding contact structure of the contact manifold  $(\mathbb{R}^3, \ker \alpha)$ .

The latter condition of Eq. (3.3) can equivalently be expressed as  $\iota_R d\alpha = 0$ , so that clearly the conditions of Theorem 3.9 are met and we conclude

**Theorem 3.22** Reeb vector fields are geodesible.

However, the converse is not true, *i.e.*, not all geodesible vector fields are Reeb vector fields. For example, on 3-dimensional manifolds we may consider harmonic fields, for which the 1-form  $X^\flat$  is closed. Then  $X^\flat \wedge dX^\flat = 0$  is not a volume form. Therefore, although harmonic fields are geodesible they are not Reeb vector fields of a contact structure [87, Sec. 1.2].

Therefore,  $dX^b \neq 0$  is a necessary condition for a vector field to be a Reeb vector field. Moreover, we know that Reeb vector fields are geodesible, hence force-free with respect to some other metric. As we will show now, if  $X$  is a Reeb vector field for a contact 1-form  $\alpha \in \Omega^1(M)$ , the condition  $d\alpha \neq 0$  is sufficient to conclude that the proportionality factor  $f$  of  $X$  as a force-free field is non-vanishing.

**Theorem 3.23** Let  $M$  be an orientable manifold of odd dimension  $2n + 1$  and  $X \in \Gamma TM$  non-vanishing. Then  $X$  is the reparametrization of a Reeb vector field of a contact 1-form  $\alpha \in \Omega^1(M)$  if and only if there is a Riemannian metric  $g$  on  $M$  such that  $X$  satisfies the force-free condition  $\iota_X dX^b = 0$  and has non-vanishing proportionality factor.

*Proof.* Let  $g$  be a Riemannian metric on  $M$  such that  $X$  satisfies the force-free condition and the proportionality factor  $f$  given by  $(dX^b)^n = f \star X^b$  is non-vanishing. Define  $\alpha := X^b$ , then  $\alpha(X) = |X|^2 > 0$ , since  $X$  does not vanish. Therefore,  $R \in \Gamma TM$  defined by  $|X|^2 R = X$  satisfies  $\alpha(R) = 1$  as well as  $\iota_R dR^b = 0$ . Lastly we check that

$$\alpha \wedge (d\alpha)^n = X^b \wedge \iota_{\text{curl } X} \mu_g = f X^b \wedge \iota_X \mu_g = f X^b \wedge \star X^b = f |X|^2 \mu_g \neq 0,$$

hence  $X$  is the reparametrization of the Reeb vector field  $R$  of  $\alpha$ .

Conversely let  $X = \lambda R$ ,  $\lambda > 0$  for the Reeb vector field  $R$  of  $\alpha \in \Omega^1(M)$ . By Lemma 3.14 there exists a Riemannian metric  $g$  such that  $\alpha = \iota_X g$ . Then with  $R \in \ker d\alpha$  also  $X \in \ker d\alpha$ , which gives the force-free condition. Moreover,

$$0 \neq \alpha \wedge (d\alpha)^n = f X^b \wedge \star X^b = f |X|^2 \mu_g$$

implies that  $f \neq 0$ , which concludes the proof.  $\square$

Again, the proof reveals that the property of being a reparametrization of a Reeb vector field is sufficient for the force-free property, but the vector field  $X$  is not necessarily divergence-free. However, for the converse statement,  $g$  can be chosen such that  $X$  will preserve the volume form  $\mu_g = \frac{1}{\alpha(X)} \alpha \wedge (d\alpha)^n$ , which describes a *barotropic fluid*. Alternatively, we derived additional conditions to ensure divergence-freeness in Lemma 2.22.

**Corollary 3.24** In the situation of Theorem 3.23, the vector field  $X$  is divergence-free and hence force-free with respect to  $g$  if and only if the proportionality factor

$f \neq 0$  is either constant, or  $\text{grad } f \perp X$ .

The ABC-flow (Section 3.3.2) also provides an example for Theorem 3.23 (and since it is divergence-free also Corollary 3.24). Note that the divergence-freeness and the fact that  $f \equiv 1$  (Eq. (2.10)) matches Lemma 2.22. Cardona Aguilar [17, Exp. 1.1.16] shows that with

$$\alpha := X_{\text{ABC}}^b$$

where  $(\cdot)^b$  is taken with respect to the flat metric on  $(\mathbb{R}/2\pi)^3$  induced by  $\mathbb{R}^3$ ,

$$\alpha \wedge d\alpha = (A^2 + B^2 + C^2) dx \wedge dy \wedge dz,$$

which is non-vanishing whenever  $A^2 + B^2 + C^2 > 0$ .

We may summarize our findings by stating that

$$\{\text{curl } X = fX, f \neq 0\} \cong \{\text{Reeb vector fields}\} \subset \{\text{geodesible vector fields}\}.$$

Note that the result of Theorem 3.23 nicely complements the result of Corollary 2.17 and Theorem 2.29 which states that the hyperplane distribution perpendicular to  $B$  is integrable if and only if  $B^b$  is closed (Fig. 2.7). In contrast to that, contact 1-forms are associated to hyperplane distributions which are *maximally non-integrable* [1, App. 4] (Fig. 3.2).

### 3.2.2 STABLE HAMILTONIAN STRUCTURES

Following Cieliebak and Volkov [24] let us briefly introduce the notion of a *stable Hamiltonian structure*, which generalize *contact structures*. Similar to the Reeb vector fields of contact structures, stable Hamiltonian structures provide us with examples for geodesible vector fields and we will show that the existence of a stable Hamiltonian structure is equivalent to the geodesibility of an associated 1-dimensional foliation. In Section 3.3.2, we will then build on this result and deduce a novel connection to force-free fields from our main theorem.

**Definition 3.25** A *Hamiltonian structure* on an oriented manifold of odd dimension  $2n + 1$  is a closed 2-form  $\omega \in \Omega^2(M)$  of maximal rank, *i.e.*, such that  $\omega^n \neq 0$ .

To every Hamiltonian structure we associate a foliation which is tangent to the kernel distribution  $\ker \omega$  and can be equipped with a natural orientation [24].

**Definition 3.26** A Hamiltonian structure is called *stabilizable* if it admits a *stabilizing* 1-form, i.e.,  $\eta \in \Omega^1(M)$  such that

$$\eta \wedge \omega^n > 0 \quad \text{and} \quad \ker \omega \subset \ker d\eta.$$

The pair  $(\omega, \eta)$  is called a *stable Hamiltonian structure*.

We note that if  $(\omega, \eta)$  is a stable Hamiltonian structure, then also  $(\omega, -\eta)$  is a stable Hamiltonian structure with the opposite orientation. Moreover, a stable Hamiltonian structure induces a canonical *Reeb vector field*  $R \in \Gamma TM$  which satisfies  $R \in \ker \omega$  and is normalized by  $\eta(R) = 1$ . In particular, the property to be stabilizable depends only on the kernel distribution of  $\omega$ .

**Example 3.27** Let  $(M, \Xi)$  be a contact manifold with contact 1-form  $\alpha \in \Omega^1(M)$ . Then  $(\pm d\alpha, \alpha)$  is a stable Hamiltonian structure on  $M$ , hence stable Hamiltonian structures indeed generalize the notion of contact structures.

**Definition 3.28** An oriented 1-dimensional foliation is *stabilizable* if there exists a vector field  $X$  tangent to the foliation and a 1-form  $\eta \in \Omega^1(M)$  such that  $\eta(X) > 0$  and  $\iota_X d\eta = 0$ .

We note that the conditions in Definition 3.28 match the conditions in Theorem 3.10 and consequently:

**Theorem 3.29** ([108]) An orientable 1-dimensional foliation is stabilizable if and only if it is geodesible.

**Corollary 3.30** Let  $X \in \Gamma TM$  be vector field on an oriented 3-manifold  $M$ . Then,

- (i) given a metric  $g$  such that  $X$  is divergence-free with respect to  $\mu_g$ , geodesic and of unit length,  $(\omega, \eta) = (\iota_X \mu_g, X^\flat)$  is a stable Hamiltonian structure.
- (ii) given a stable Hamiltonian structure  $(\omega, \eta)$  with Reeb vector field  $X \in \Gamma TM$ , there is a metric  $g$  on  $M$  such that  $\mu_g = \eta \wedge \omega$  and  $X$  is divergence-free with respect to  $\mu_g$ , geodesic and of unit length.

*Proof.* Given  $g$  such that  $X$  is geodesic of unit length and preserves the induced volume form, we define  $(\omega, \eta) := (\iota_X \mu_g, X^\flat)$ . Since  $X$  is divergence-free,  $d\omega = d\iota_X \mu = \mathcal{L}_X \mu_g = 0$ , which shows that  $\omega$  is closed. Moreover,

$$\eta \wedge \omega = |X|^2 \mu_g \neq 0.$$

Then,  $X$  is a Reeb vector field, because  $\eta(X) = |X|^2 = 1$  and  $\text{span } X = \ker \omega$ . By Lemma 2.3

$$\iota_X d\eta = \iota_X dX^\flat = (\nabla_X X)^\flat = 0,$$

we see that  $\ker \omega \subset \ker d\eta$ , hence  $(\omega, \eta)$  is a stable Hamiltonian structure with Reeb vector field  $X$ .

Conversely, let  $(\omega, \lambda)$  be a stable Hamiltonian structure with Reeb vector field  $X$ . Then by Lemma 3.14 there is a metric  $g$  on  $M$  such that  $\eta = \iota_X g$  and  $\mu_g = \eta \wedge \omega$ . Since  $X$  is a Reeb vector field we have  $1 = \eta(X) = g(X, X)$ , hence  $|X| = 1$ . Moreover, by Lemma 2.3 and  $X \in \ker \omega \subset \ker d\eta$  we have

$$0 = \iota_X d\eta = \iota_X dX^\flat = (\nabla_X X)^\flat.$$

Lastly,

$$\mathcal{L}_X \mu_g = d\iota_X(\eta \wedge \omega) = d(\omega - \iota_X \omega) = 0,$$

hence  $X$  is divergence-free. □

**Corollary 3.31** Let  $X \in \Gamma TM$  be a non-vanishing vector field on an oriented 3-manifold  $M$ . Then,

- (i) given a metric  $g$  such that  $X$  is force-free,  $(\omega, \eta) = (\iota_X \mu_g, X^\flat)$  is a stable Hamiltonian structure.
- (ii) given a stable Hamiltonian structure  $(\omega, \eta)$  so that  $X$  is tangent to the associated foliation, there is a metric  $g$  on  $M$  such that  $\mu_g = \frac{1}{\eta(X)} \eta \wedge \omega$  and  $X$  is force-free.

*Proof.* Given a metric  $g$  such that  $X$  is force-free, we define  $(\omega, \eta) := (\iota_X \mu_g, X^\flat)$ . Since  $X$  is divergence-free,  $d\omega = d\iota_X \mu = \mathcal{L}_X \mu_g = 0$ , which shows that  $\omega$  is closed. Moreover,

$$\frac{1}{\eta(X)} \eta \wedge \omega = \frac{1}{\eta(X)} X^\flat \wedge \star X^\flat = \mu_g.$$

Then,  $X$  is tangent to the associated foliation since  $\eta(X) = |X|^2 > 0$  and  $\iota_X \omega = \iota_X \iota_X \mu_g = 0$ , i.e.,  $X \in \ker \omega$  the field  $X$  is tangent to the foliation associated to  $(\omega, \eta)$ . By the force-free condition we have  $0 = \iota_X dX^\flat = \iota_X d\eta$ , hence  $\ker \omega \subset \ker d\eta$  which makes  $(\omega, \eta)$  a stable Hamiltonian structure.

Conversely, let  $(\omega, \eta)$  be a stable Hamiltonian structure, then by Lemma 3.14 there is a metric  $g$  on  $M$  such that  $\eta = \iota_X g$  and  $\mu_g = \frac{1}{\eta(X)} \eta \wedge \omega$ . Therefore, since

$X \in \ker \omega \subset \ker d\eta$ , we have  $0 = \iota_X d\eta = \iota_X dX^\flat$ . Moreover,

$$\mathcal{L}_X \mu_g = d\iota_X(\eta \wedge \omega) = d(\omega - \iota_X \omega) = 0,$$

hence  $X$  is force-free.

□

**Remark 3.32** Cieliebak and Volkov [24, Cor. 2.3, Cor. 2.4] show that the statement of Corollaries 3.30 and 3.31 also hold for barotropic fluids, *i.e.*, the case that the volume form is not necessarily the one induced by  $g$ .

### 3.3 CONFORMALLY GEODESIC VECTOR FIELDS

In Section 3.2 we collected some results and examples for geodesible vector fields on a manifold  $M$ . In particular, by Theorem 3.13, a vector field  $X$  satisfies the force-free condition if and only if it is geodesible. However, the two metrics with respect to which the vector field is force-free *resp.* geodesic have no relation to each other.

In this section, we will establish such a relationship in terms of conformal geometry and build upon some of the earlier results. More concretely, we deal with the question of “conformal geodesibility”. In special cases where a reference metric already exists, such as for harmonic, force-free or Killing vector fields, we can restrict admissible Riemannian metrics with respect to which the field lines are geodesic to the same conformal class as the reference metric.

**Definition 3.33** A *conformal class* on an  $n$ -dimensional smooth manifold  $M$  is an equivalence class of Riemannian metrics, where two metrics  $g$  and  $h$  are considered *conformally equivalent* if there exists a smooth function  $u \in C^\infty(M)$  such that

$$e^{2u} g = h.$$

A manifold  $M$  together with a conformal class (denoted by  $[g]$ ) is a *conformal manifold*.

There is a useful explicit formula for the Levi-Civita connection after a conformal change of metric.

**Theorem 3.34 ([59, Lemma 8.27])** Let  $M$  be a conformal manifold and  $g, h \in [g]$  such that  $h = e^{2u}g$  and denote the Levi-Civita connections of the respective metrics by  $\nabla^g$  and  $\nabla^h$ . Then

$$\nabla_Y^h X = \nabla_Y^g X + du(Y)X + du(X)Y - g(X, Y) \operatorname{grad} u.$$

### FLUX FORMS IN CONFORMAL MANIFOLDS

There is no particular reference metric in a conformal manifold. Nonetheless, it is possible to define the types of flux forms as in Sections 2.2.2 and 3.1 on a conformal manifold by requiring the existence of a representative metric within the equivalence class that satisfies the defining equations.

**Definition 3.35** A closed flux form  $\beta \in \Omega^{n-1}(M)$  on a conformal manifold  $M$  is

- (i) *conformally force-free* if there exists a metric in the conformal class of  $M$  such that  $\beta$  is force-free.
- (ii) *conformally geodesic* if there exists a metric in the conformal class of  $M$  such that  $\beta$  is geodesic.
- (iii) *conformally harmonic (resp. conformally exact harmonic)* if there exists a metric in the conformal class of  $M$  such that  $\beta$  is harmonic (resp. exact harmonic).
- (iv) *conformally eikonal (resp. conformally exact eikonal)* if there exists a metric in the conformal class of  $M$  such that  $\beta$  is eikonal (resp. exact eikonal).

#### 3.3.1 KILLING VECTOR FIELDS ARE CONFORMALLY GEODESIC

Let  $M$  be an  $n$ -dimensional Riemannian manifold with Riemannian metric  $g$ . Then an infinitesimal isometry of  $M$ , *i.e.*, a vector field which generates an isometric flow, is called a *Killing vector field* (Fig. 3.3).

**Definition 3.36** A vector field  $X \in \Gamma TM$  on a Riemannian manifold  $M$  is called a *Killing vector field* if

$$\mathcal{L}_X g = 0.$$

**Proposition 3.37** A vector field  $X \in \Gamma TM$  on a Riemannian manifold  $M$  is a Killing vector field if and only if for  $Y, Z \in \Gamma TM$ ,

$$g(\nabla_Y X, Z) = -g(Y, \nabla_Z X).$$

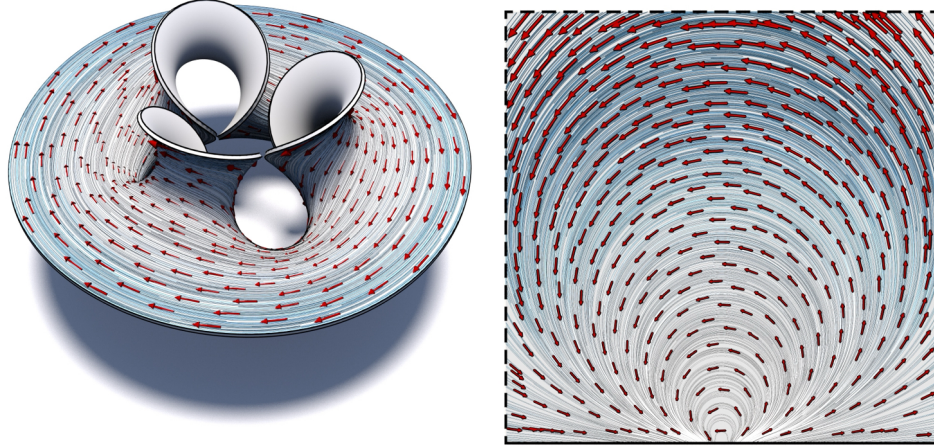


**Figure 3.3:** A Killing vector field and the associated flow lines on an Enneper surface (left) and on a piece of the hyperbolic plane in the upper half-plane model (right).

On Riemannian manifolds, Killing vector fields of constant length are known to be related to geodesic foliations.

**Lemma 3.38** ([8, Prop. 1]) A Killing vector field  $X \in \Gamma TM$  on a Riemannian manifold  $M$  has constant length if and only if  $X$  is geodesic.

**Remark 3.39** Conditions on the curvature of the manifold  $M$  must be fulfilled for the inverse statement of Lemma 3.38 to be true, i.e., for the case that a geodesic vector field of constant length is Killing, are given in [28].

*Proof.* By Proposition 3.37,

$$dg(X, X) = 2g(\nabla X, X) = -2(\nabla_X X)^b,$$

from which the claim immediately follows.  $\square$

We can use Lemma 3.38 to show that Killing vector fields are an example for conformally geodesic vector fields.

**Theorem 3.40** Let  $M$  be an  $n$ -dimensional manifold with Riemannian metric  $g$  and  $X \in \Gamma TM$  a Killing vector field. Then there exists a Riemannian metric  $h$  in the same conformal class such that  $X$  is geodesic.

*Proof.* From Proposition 3.37 we conclude that  $g(\nabla_X X, X) = 0$ . Define  $h := e^{-2u} g$

for  $e^{2u} := g(X, X)$ , then

$$d_X e^{-2u} = -2g(X, X)^{-2}g(\nabla_X X, X) = 0.$$

Therefore,

$$\mathcal{L}_X h = \mathcal{L}_X(e^{-2u}g) = d_X e^{-2u}g + e^{-2u} \mathcal{L}_X g = 0,$$

i.e.,  $X$  is also a Killing vector field with respect to  $h$ . In particular,  $h(X, X) = \frac{1}{g(X, X)}g(X, X) = 1$ . The claim now follows from Lemma 3.3.  $\square$

### 3.3.2 FORCE-FREE FIELDS ARE CONFORMALLY GEODESIC

In this section we now turn to proving a stronger version of Theorem 3.13, stating that the field lines of force-free fields are in fact *conformal geodesics*. In doing so, we establish the novel insight that these problems actually belong to the realm of conformal geometry.

**Theorem 3.41** Let  $M$  be an  $n$ -dimensional manifold with Riemannian metric  $g$  and  $X \in \Gamma TM$  a non-vanishing vector field. Then  $X$  satisfies the force-free condition ( $\iota_X dX^\flat = 0$ ) with respect to  $g$  if and only if its field lines are geodesic with respect to  $h := e^{2u} g$ , where  $e^{2u} := g(X, X)$ .

*Proof.* Unless otherwise stated, all operators or functions are to be read in relation to  $g$ . Writing  $e^{2u} := |X|^2$  we have  $u = \ln(|X|)$ , hence

$$\text{grad } u = \frac{\text{grad}|X|}{|X|}.$$

Moreover, by Theorem 3.34 and denoting the Levi-Civita connection of a conformally changed metric  $h$  by  $\nabla^h$ , we have

$$\begin{aligned} \nabla_X^h X &= \nabla_X X + 2g(\text{grad } u, X)X - |X|^2 \text{grad } u \\ &= \nabla_X X + 2g(\text{grad } u, X)X - |X| \text{grad } |X| \\ &= \nabla_X X + 2g(\text{grad } u, X)X - \text{grad } \frac{|X|^2}{2}. \end{aligned}$$

The vector  $\nabla_X X - \text{grad } \frac{|X|^2}{2}$  corresponding to the Lorentz force is normal to  $X$ , hence by Lemma 2.3

$$(\nabla_X^h X)^\perp = \nabla_X X - \text{grad } \frac{|X|^2}{2} = (\iota_X dX^\flat)^\sharp,$$

where  $(\cdot)^\perp$  denotes the component normal to  $X$ .  $\square$

Notably the proof is straightforward and the theorem statement even precisely determines the conformal factor.

**Corollary 3.42** Force-free vector fields are conformally geodesic.

**Corollary 3.43** Harmonic vector fields are conformally geodesic.

**Remark 3.44** We point out that the conformally changed metric in Theorem 3.41 itself depends on the field. A similar situation is known in the theory of general relativity, where a mass point in motion travels on geodesics in space, while at the same time warping it.

In particular, we find that we do not need a specific reference metric for this result to hold: On a merely conformal 3-dimensional manifold  $M$ , that force-free and geodesic flux forms are related by an involution in a metric associated to 2-form at hand.

**Theorem 3.45** Let  $M$  be a conformal 3-manifold and  $\beta \in \Omega^2(M)$  be nowhere vanishing. Then there is a conformal metric  $g$  such that  $|\beta| = 1$ . Furthermore, if  $g_{\pm} := e^{\pm 2u} g$  for  $u \in C^\infty M$ , then  $\beta$  satisfies the force-free condition with respect to  $g_-$  if and only if  $\beta$  is geodesic with respect to  $g_+$ .

*Proof.* That the metric  $g$  exists is trivial. Then the volume forms and the vector fields associated to the respective conformally changed metrics  $g_{2\pm} = e^{\pm u} g$  can be expressed in terms of the associated vector field  $X$  and volume form  $\mu$  with respect to  $g$  by  $\mu_{\pm} = e^{\pm 3u} \mu$  and  $X_{\pm} = e^{\mp u} X$ . Then,

$$\begin{aligned}\iota_{X_-} dg(X_-, I) &= e^{3u} \iota_B d(e^u g(X, I)) \\ &= e^{4u} \iota_B (du \wedge g(X, I) + g(\nabla X \wedge I)) \\ &= e^{4u} g(\nabla_X X - (\text{grad } u - du(X)X), I) \\ &= e^{4u} (\nabla_X X - (\text{grad } u)^\perp),\end{aligned}$$

where  $(\cdot)^\perp$  denotes the component orthogonal to  $X$ . We conclude that  $\beta$  satisfies the force-free condition with respect to  $g_-$  if and only if  $\nabla_X X - (\text{grad } u)^\perp = 0$ .

On the other hand, by Theorem 3.34,

$$\begin{aligned}
 \nabla_{X_+}^+ X_+ &= \nabla_{X_+} X_+ + 2du(X_+)X_+ - \text{grad } u \\
 &= e^{-3u}(\nabla_X(e^{-3u}X) + 2e^{-6u}du(X)X - \text{grad } u) \\
 &= e^{-3u}(-3e^{-3u}du(X)X + e^{-3u}\nabla_X X) + 2e^{-6u}du(X)X - \text{grad } u \\
 &= e^{-6u}(\nabla_X X - du(X)X - \text{grad } u) \\
 &= e^{-6u}(\nabla_X X - (\text{grad } u)^\perp - 2du(X)X).
 \end{aligned}$$

Since  $|X| = 1$  implies that  $\nabla X \perp X$  we conclude that  $\beta$  is geodesic with respect to  $g_+$  if and only if  $\nabla_X X - (\text{grad } u)^\perp = 0$ .  $\square$

**Corollary 3.46** If  $|\beta| = 1$ , then  $\beta$  satisfies the force-free condition if and only if  $\beta$  is geodesic.

#### EXAMPLES AND IMPLICATIONS

Despite the increasing topological complexity in the loss of invariant surfaces, Theorem 3.41 finds geometric order in force-free fields, finding that their field lines are conformal geodesics. Considering the potentially chaotic behavior field lines of force-free fields may exhibit (Section 2.3), it is astonishing to find that their field lines foliate the space with geodesics after suitable rescaling of the metric. Notably, this insight is true in arbitrary dimensions and does not require knowledge of a proportionality factor (Section 2.1.1) or vorticity function (Section 2.1.3).

**Corollary 3.47** ABC-flows are conformally geodesic.

A non-trivial example for Corollary 3.46 is given by  $\beta = \iota_X \mu$  for the Hopf field

$$X_{\text{Hopf}} = (-x_2, x_1, -x_4, x_3) \in \Gamma TS^3$$

on the round 3-sphere  $S^3 = \{x \in \mathbb{R}^4 \mid x_1^2 + x_2^2 + x_3^2 + x_4^2 = 1\} \subset \mathbb{R}^4$  (Fig. 3.4). It is divergence-free, has unit length and great circles as its integral curves [38]. Therefore, by the previous corollary,  $\beta$  is force-free (see also [100]).

Finally, we will infer stronger versions of the results of Corollaries 3.30 and 3.31 from our newly gained insights. As a consequence of Corollary 3.46 we obtain:

**Corollary 3.48** With the assumptions of Corollary 3.30, the vector field  $X$  is force-free with respect to the Riemannian metric  $g$ .

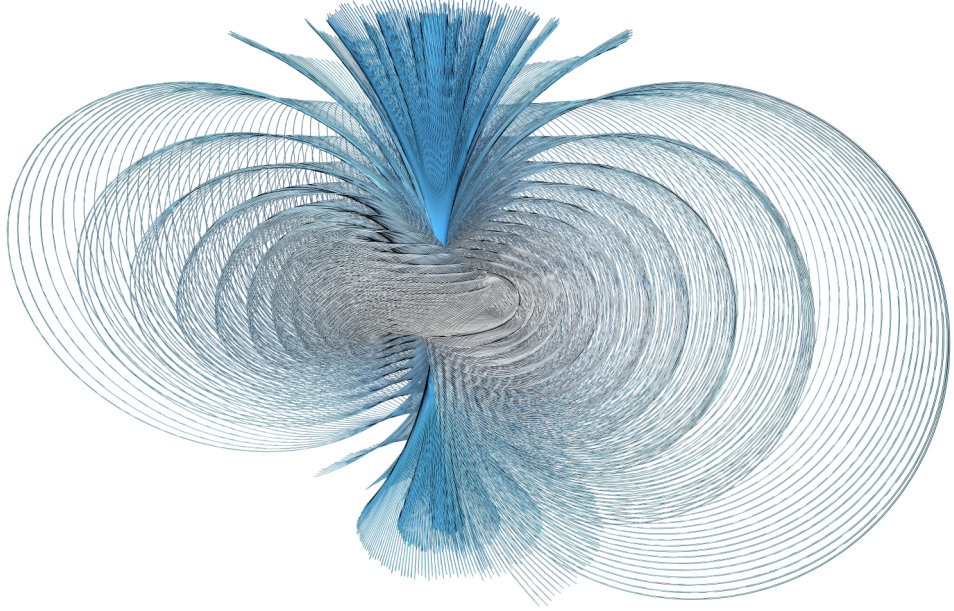


**Figure 3.4:** The Hopf fibration of  $\mathbb{R}^3$ , i.e., the stereographic projection of the field lines of the Hopf field in  $S^3$  onto  $\mathbb{R}^3$  [51]. It is a geodesic and Killing vector field of unit length in  $S^3$  and therefore force-free, by Theorem 3.38 and Theorem 3.46.

**Theorem 3.49** Let  $M$  be an oriented 3-manifold with stable Hamiltonian structure  $(\omega, \eta)$  and non-vanishing vector field  $X \in \Gamma TM$  tangent to the associated foliation. Then,

- (i) there exists a metric  $g$  such that  $\mu_g = \frac{1}{\eta(X)}\eta \wedge \omega$  is the induced volume form and  $X$  is force-free with respect to  $g$ .
- (ii) there exists a metric  $h$  such that  $\mu_h = \frac{1}{\eta(\bar{X})}\eta \wedge \omega$  is the volume form induced by  $h$  and  $X$  is the reparametrization of a geodesic vector field  $\bar{X}$  which is divergence-free with respect to  $\mu_h$ .

For  $e^u := |X|_g$ , the metrics  $g$  and  $h$  are conformally related by  $h = e^{2u}g$  and the corresponding volume forms by  $\mu_h = e^{3u}\mu_g$ .

*Proof.* Statement (i) is the same as in Theorem 3.31. For (ii), let  $(\omega, \eta)$  be a stable Hamiltonian structure and  $X \in \Gamma TM$  generate the kernel foliation. We first choose  $g$  as in (i) and define  $e^u := |X|_g$  as well as  $h = e^{2u}g$  and  $\bar{X} = e^{-3u}X$ . Then  $\mu_h = e^{3u}\mu_g$  and with  $X$ , also  $\bar{X}$  generates kernel foliation of  $(\omega, \eta)$ . In particular,

by Theorem 3.41, the field lines are geodesic with respect to  $h$ . Moreover,

$$\mathcal{L}_{\tilde{X}} \mu_h = d\iota_{\tilde{X}}(\frac{1}{\eta(\tilde{X})}\eta \wedge \omega) = d\omega - d(\frac{1}{\eta(\tilde{X})}\eta \wedge \iota_{\tilde{X}}\omega) = 0,$$

where we use that  $d\omega = 0$  and  $\tilde{X} \in \ker \omega \subset \ker d\eta$ . By construction,  $g$  and  $h$  are conformally equivalent and the claimed relations hold.  $\square$

**Remark 3.50** For the special case of  $h(X, X) = 1$  in Theorem 3.49 (ii) we recover the statement of Corollary 3.30 (ii).

**Corollary 3.51** Let  $M$  be a 3-dimensional Riemannian manifold with metric  $h$  and induced volume form  $\mu_h$ . If a vector field  $X \in \Gamma TM$  on  $M$  is geodesic and divergence-free, then the pair  $(\omega, \eta) := (\iota_X \mu_h, \iota_X h)$  is a stable Hamiltonian structure.

*Proof.* This is an analogous statement as in Theorem 3.31 (i), only that we use the conformally changed metric. Since the stable Hamiltonian structure does not depend on the specific metric, the claim remains true.  $\square$

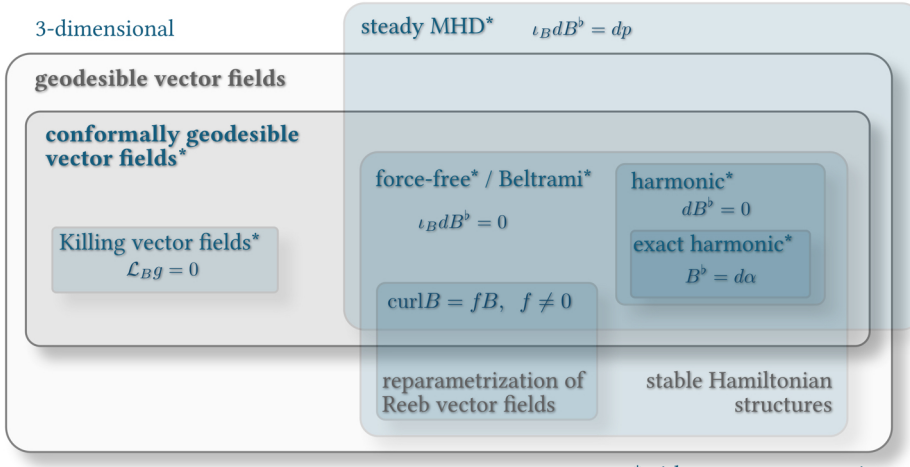


**Figure 3.5:** An overview of the results from this chapter for the case that  $M$  is 3-dimensional.

In Figs. 3.5 and 3.6 we summarize the insights obtained in this chapter for 3 dimensions resp.  $(2n + 1)$  dimensions. The main result shows that force-free fields belong to the class of conformally geodesic vector fields—a class previously only

### CHAPTER 3. GEODESIBLE AND CONFORMALLY GEODESIC VECTOR FIELDS

considered for Killing vector fields. In particular, we note that due to this equivalence we obtain a form of mirror principle: from every result about geodesibility of a vector field, for instance about Reeb vector fields, follows directly another result which says that a metric exists in the same conformal class with respect to which the vector field satisfies the force-free property. For Reeb vector fields of a contact structure, these two metrics even coincide, which is consistent with the result of Corollary 3.46. Furthermore, we emphasize once again that the equivalence between geodesic and force-free fields as we have defined them in this thesis is preserved. This contrasts the case of the possible generalization of these fields via the definition as Beltrami fields (Section 2.1.1), which according to a result of Cardona [16] are not even necessarily steady MHD equilibria anymore (Fig. 3.6).

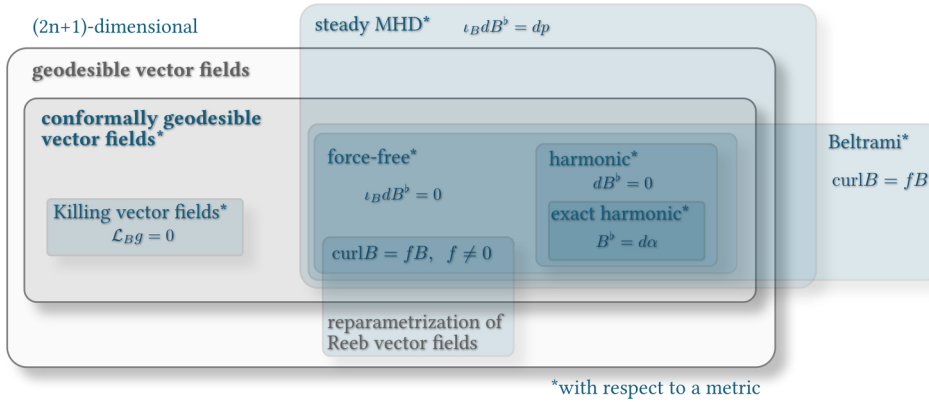


**Figure 3.6:** An overview of the results from this chapter for the case that  $M$  is  $(2n + 1)$ -dimensional.

Lastly, in the following Chapter 4 we will show that—again matching the 3-dimensional case—our defining equations emerge as the Euler-Lagrange equations from a suitable hierarchy of variational principles.

## CHAPTER 4

# EQUIVALENCE THEOREMS FOR VARIATIONAL PRINCIPLES

In the preceding sections we have established a conformal equivalence between force-free fields and geodesic fields. In this section we establish a conformal equivalence between the corresponding variational problems. This result is later used to derive an algorithm and to address the problem of minimizing the  $L^2$  norm of a magnetic field in  $\mathbb{R}^3$  by introducing a conformal change of metric [75, 46].

Let us consider a closed flux form  $\beta \in \Omega^{n-1}(M)$  on an oriented Riemannian manifold  $M$ , then the  $L^1$ -norm *resp.*  $L^2$ -norm of the flux form, is given by

$$\|\beta\|_{L^1} := \int_M |B| \mu_g = \int_M \sqrt{\star(\beta \wedge \star\beta)} \mu_g \quad (4.1)$$

and

$$\|\beta\|_{L^2}^2 := \int_M |B|^2 \mu_g = \int_M \beta \wedge \star\beta. \quad (4.2)$$

Although up to this point we have restricted ourselves to manifolds without boundary, in this chapter we allow our flow fields to be defined on manifolds with boundary. The equivalence of variational principles holds as long as the constraints and boundary conditions are expressed independently of the metric.

### 4.1 BOUNDARY CONDITIONS

Let  $M$  be an oriented Riemannian manifold with boundary and outward pointing unit normal  $N \in \Gamma TM$  of  $\partial M$ . To handle boundaries we assume that the magnetic field is either tangent to the boundary, *i.e.*,  $g(B, N) = 0$ , or satisfies given boundary

conditions, i.e.,  $g(B, N) = \Phi$  for a given boundary flux condition  $\Phi \in C^\infty(M)$ .

The flux boundary condition  $\Phi \in C^\infty(M)$  corresponds to an  $(n-1)$ -form  $\beta_{\partial M} \in \Omega^{n-1}(\partial M)$  such that

$$\Phi \lrcorner_N \mu_g = \beta_{\partial M}.$$

Therefore, a flux form  $\beta \in \Omega^{n-1}(M)$  satisfies a given boundary condition  $\beta_{\partial M} \in \Omega^{n-1}(\partial M)$  if  $j_{\partial M}^* \beta = \beta_{\partial M}$ , where  $j : \partial M \hookrightarrow M$  denotes the inclusion of  $\partial M$  into  $M$ .

All our definitions up to now can be carried over to the case of manifolds with boundary, as long as we require that the boundary conditions are met.

## 4.2 A HIERARCHY OF VARIATIONAL PRINCIPLES FOR THE $L^2$ -NORM

In this section we establish the variational principles which give us the defining equations for force-free fields and the more specialized cases of (exact) harmonic fields as their Euler-Lagrange equations. The different variational principles emerge from considering the  $L^2$ -norm under different classes of admissible variations with suitable boundary conditions.

**Theorem 4.1** A closed flux form  $\beta \in \Omega^{n-1}(M)$  with  $j_{\partial M}^* \beta = \beta_{\partial M}$  for a given boundary condition  $\beta_{\partial M} \in \Omega^{n-1}(\partial M)$  is a stationary point of the  $L^2$ -norm under variations in the space of closed flux forms which respect the boundary condition ( $d\dot{\beta} = 0$  and  $j_{\partial M}^* \dot{\beta} = 0$ ) if and only if  $\beta$  is exact harmonic.

*Proof.* The stationary condition of the  $L^2$ -norm (Eq. (4.2)) is given by

$$0 = \int_M \dot{\beta} \wedge \star \beta$$

for all  $\dot{\beta}$  satisfying  $d\dot{\beta} = 0$  and  $j_{\partial M}^* \dot{\beta} = 0$ . That is, the stationary condition is equivalent to

$$\beta \in \{\dot{\beta} \in \Omega^{n-1}(M) \mid d\dot{\beta} = 0, j_{\partial M}^* \dot{\beta} = 0\}^\perp = \text{im}(\star d)$$

where the last equality is given by the Hodge–Morrey–Friedrichs decomposition [99].  $\square$

**Theorem 4.2** A closed flux form  $\beta \in \Omega^{n-1}(M)$  with  $j_{\partial M}^* \beta = \beta_{\partial M}$  for a given boundary condition  $\beta_{\partial M} \in \Omega^{n-1}(\partial M)$  is a stationary point of the  $L^2$ -norm under *homolog-*

## 4.2. A HIERARCHY OF VARIATIONAL PRINCIPLES FOR THE $L^2$ -NORM

*ically constrained variations, i.e.,  $\dot{\beta} = d\alpha$  for some  $\alpha \in \Omega^{n-2}(M)$  with  $j_{\partial M}^* \alpha = 0$ , if and only if  $\beta$  is harmonic.*

*Proof.* The stationary condition of the  $L^2$ -norm (Eq. (4.2)) under variations  $\dot{\beta} = d\alpha$ ,  $j_{\partial M}^* \alpha = 0$ , is given by

$$0 = \int_M d\alpha \wedge \star \beta = (-1)^{n-1} \int_M \alpha \wedge d \star \beta$$

for all  $\alpha \in \Omega^{n-2}(M)$  with  $j_{\partial M}^* \alpha = 0$ . This condition holds if and only if  $d \star \beta = 0$ .  $\square$

**Lemma 4.3** For  $\xi \in \Gamma TM$  and  $\beta \in \Omega^{n-1}(M)$  we have

$$\iota_\xi \beta \wedge d \star \beta = \xi^\flat \wedge \star(\iota_B d \star \beta).$$

*Proof.* First, we recall that the duality between interior and the wedge product [19, App. A] states that for any  $\alpha \in \Omega^k(M)$  and  $X \in \Gamma TM$  we have

$$(-1)^k \iota_X \star \alpha = \star(X^\flat \wedge \alpha).$$

Therefore

$$\star(B^\flat \wedge \star d \star \beta) = (-1)^{n-2} \iota_B \star \star d \star \beta = (-1)^{n-2} \iota_B d \star \beta,$$

hence by applying another Hodge star on both sides leads to

$$B^\flat \wedge \star d \star \beta = (-1)^{n-1} (-1)^{n-2} \star (\iota_B d \star \beta) = -\star(\iota_B d \star \beta).$$

Now, with  $\beta = \star B^\flat$  and again using the duality between the interior and the wedge product, we have

$$\iota_\xi \beta \wedge d \star \beta = -(\star(\xi^\flat \wedge B^\flat)) \wedge d \star \beta = -\xi^\flat \wedge B^\flat \wedge \star d \star \beta = \xi^\flat \wedge \star(\iota_B d \star \beta)$$

which concludes the proof.  $\square$

**Theorem 4.4** A closed flux form  $\beta \in \Omega^{n-1}(M)$  with  $j_{\partial M}^* \beta = \beta_{\partial M}$  for a given boundary condition  $\beta_{\partial M} \in \Omega^{n-1}(M)$  is a stationary point of the  $L^2$ -norm under *isotopy constraint variations*, i.e.,  $\dot{\beta} = -\mathcal{L}_\xi \beta$  for some  $\xi \in \Gamma TM$  which is compactly supported in the interior of  $M$ , if and only if  $\beta$  is force-free.

*Proof.* By Cartan's formula and  $d\beta = 0$ , the isotopic variations take the form  $\dot{\beta} = -\mathcal{L}_\xi \beta = -d\iota_\xi \beta$  for compactly supported vector fields  $\xi \in \Gamma TM$ . The variation of Eq. (4.2) under such variation is given by

$$\frac{1}{2}(\|\beta\|_{L^2}^2)^\circ = \int_M -d\iota_\xi \beta \wedge \star \beta = (-1)^n \int_M \iota_\xi \beta \wedge d \star \beta = (-1)^n \int_M \xi^\flat \wedge \star(\iota_B d \star \beta),$$

where we use Lemma 4.3 for the last equality. Therefore, the vanishing variation condition for all compactly supported  $\xi \in \Gamma TM$  is equivalent to  $\iota_B d \star \beta = 0$ , i.e.  $\beta$  is force-free.  $\square$

### 4.3 A HIERARCHY OF VARIATIONAL PRINCIPLES FOR THE $L^1$ -NORM

In this section we derive the variational principles which give us the defining equations for geodesic fields and the more specialized cases of (exact) eikonal fields as their Euler-Lagrange equations. Analogous to Section 4.2, the different variational principles emerge from considering the  $L^1$ -norm under different classes of variations with suitable boundary conditions.

First, we note that the integrand  $|\beta|$  of the  $L^1$ -norm (Eq. (4.1)) fails to be smooth at zeros of  $\beta$ . Therefore, when considering variations of the  $L^1$ -norm

$$\left( \int_M |B| \mu_g \right)^\circ = \int_M \left( \sqrt{\star(\beta \wedge \star \beta)} \right)^\circ \mu_g = \int_M \dot{\beta} \wedge \partial |\beta|, \quad (4.3)$$

we need to resort to the subdifferential

$$\partial |\beta| = \begin{cases} \frac{\star \beta}{|\star \beta|} & \text{if } \beta \neq 0 \\ \{\alpha \in \Omega^1(M) \mid |\alpha| \leq 1\} & \text{if } \beta = 0 \end{cases}$$

of  $\beta$  in order to state the stationary conditions. As pointed out in Section 3.1, the subdifferential  $\partial |\beta|$  consists of the normalizations  $\eta$  of  $\star \beta$ .

**Lemma 4.5**  $\partial |\beta| = \{\eta \in \Omega^1(M) \mid |\eta| \leq 1, |\star \beta| \eta = \star \beta\}$

*Proof.* Let  $\eta \in \partial |\beta|$ . When  $\beta \neq 0$ , then  $\eta = \frac{\star \beta}{|\star \beta|}$  and therefore  $|\eta| = 1$ . Moreover, when  $\beta = 0$ , then  $\eta \in \Omega^1(M)$  which (by definition) satisfies  $|\eta| \leq 1$ . Clearly, also  $0 \cdot \eta = 0$  and therefore  $\eta$  is a normalization.

### 4.3. A HIERARCHY OF VARIATIONAL PRINCIPLES FOR THE $L^1$ -NORM

Let conversely  $\eta \in \Omega^1(M)$  be a normalization of  $\star\beta$ , i.e.  $|\star\beta| \eta = \star\beta$  and  $|\eta| \leq 1$ . By definition, the subdifferential of  $|\beta|$  is given by

$$\partial|\beta| = \{\alpha \in \Omega^1(M) \mid |\tilde{\beta}| \geq |\beta| + \langle \alpha | \tilde{\beta} - \beta \rangle \quad \forall \tilde{\beta} \in \Omega^{n-1}(M)\}.$$

Now if  $\beta = 0$ , then

$$|\eta| \leq 1 \Leftrightarrow \sup_{\tilde{\beta} \in \Omega^{n-k}(M), |\tilde{\beta}|=1} \langle \eta | \tilde{\beta} \rangle \leq 1 \Leftrightarrow \langle \eta | \tilde{\beta} \rangle \leq |\tilde{\beta}| \quad \forall \tilde{\beta} \in \Omega^{n-1}(M).$$

Moreover, if  $\beta \neq 0$  we have that  $\langle \eta | \beta \rangle = |\star\beta| = |\beta|$  and hence

$$|\tilde{\beta}| \geq |\beta| + \langle \eta | \tilde{\beta} - \beta \rangle = \langle \eta | \tilde{\beta} \rangle \quad \forall \tilde{\beta} \in \Omega^{n-1}(M)$$

holds if and only if  $|\eta| \leq 1$ , which is true by assumption.  $\square$

**Theorem 4.6** A closed flux form  $\beta \in \Omega^{n-1}(M)$  with  $j_{\partial M}^* \beta = \beta_{\partial M}$  for a given boundary condition  $\beta_{\partial M} \in \Omega^{n-1}(M)$  is a stationary point of the  $L^1$ -norm ( $d\dot{\beta} = 0$  and  $j_{\partial M}^* \dot{\beta} = 0$ ) if and only if  $\beta$  is exact eikonal.

*Proof.* Analogous to the proof of Theorem 4.1 we conclude from Eq. (4.3) that the stationary condition

$$0 \in \int_M \dot{\beta} \wedge \partial|\beta| \quad \text{for all } \dot{\beta} \text{ with } d\dot{\beta} = 0 \text{ and } j_{\partial M}^* \dot{\beta} = 0$$

is equivalent to the existence of an exact normalization  $\eta \in \partial|\beta|$  of  $\star\beta$ , i.e.  $\beta$  is exact eikonal (Definition 3.6).  $\square$

**Theorem 4.7** A closed flux form  $\beta \in \Omega^{n-1}(M)$  with  $j_{\partial M}^* \beta = \beta_{\partial M}$  for a given boundary condition  $\beta_{\partial M} \in \Omega^{n-1}(M)$  is a stationary point of the  $L^1$ -norm under *homologically constraint variations*, i.e.,  $\dot{\beta} = d\alpha$  for some  $\alpha \in \Omega^{n-2}(M)$  with  $j_{\partial M}^* \alpha = 0$ , if and only if  $\beta$  is eikonal.

*Proof.* The stationary condition for the variation of the  $L^1$ -norm under variations  $\dot{\beta} = d\alpha$ ,  $j_{\partial M}^* \alpha = 0$  is given by

$$0 \in \int_M \dot{\beta} \wedge \partial|\beta| = (-1)^{n-1} \int_M \alpha \wedge d(\partial|\beta|)$$

for all  $\alpha \in \Omega^{n-2}(M)$  with  $j_{\partial M}^* \alpha = 0$ , which is equivalent to the existence of a closed normalization  $\eta \in \partial|\beta|$  of  $\star\beta$ , i.e.  $\beta$  is eikonal (Definition 3.6).  $\square$

**Theorem 4.8** A closed flux form  $\beta \in \Omega^{n-1}(M)$  with  $j_{\partial M}^* \beta = \beta_{\partial M}$  for a given boundary condition  $\beta_{\partial M} \in \Omega^{n-1}(M)$  is a stationary point of the  $L^1$ -norm under *isotopy constraint variations*, i.e.,  $\dot{\beta} = -\mathcal{L}_{\xi} \beta$  for some  $\xi \in \Gamma TM$  which is compactly supported in the interior of  $M$ , if and only if there exists a normalization  $\eta \in \partial|\beta|$  of  $\star\beta$  such that  $\iota_B d\eta = 0$ .

*Proof.* With analogous arguments as for Theorem 4.4 the vanishing condition for all compact-support  $\xi \in \Gamma TM$  is given by

$$0 \in - \int_M d\iota_{\xi} \beta \wedge \partial|\beta| = (-1)^n \int_M \xi^b \wedge \star \iota_B d(\partial|\beta|),$$

where for the last equality we use an analogous computation as for the proof of Lemma 4.3. The stationary condition is equivalent to  $0 \in \star \iota_B d(\partial|\beta|)$ , i.e. the existence of a normalization  $\eta \in \partial|\beta|$  of  $\star\beta$  which satisfies  $0 = \star \iota_B d\eta$ .  $\square$

On the support of  $\beta$ , the stationary condition is given by  $0 = \iota_B d\eta$  and the normalization agrees with the directional covector field (Section 3.1). Therefore, the stationary condition coincides with Eq. (3.2) and the associated field lines form a geodesic foliation. We refer to these fields as *twisted geodesic foliations* as they do not necessarily solve an optimal transport problem (Fig. 4.1). The corresponding *untwisted* cases solve a Beckmann optimal transport problem and correspond to (exact) eikonal fields.

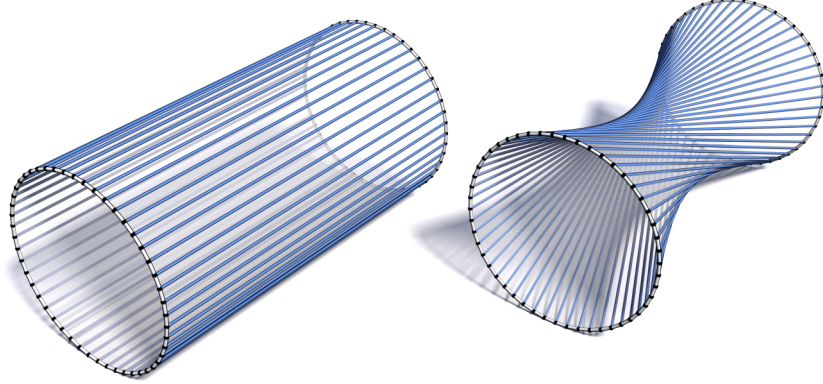


**Figure 4.1:** Left: Eikonal geodesic foliation realizing a Beckmann optimal transport plan. Right: Twisted geodesic foliation with constrained connectivity between source and sink endpoints.

**Remark 4.9 (Twisted Minimal Foliations)** In the field of calibrated geometry [50, 121], the directional covector field  $\eta$  is referred to as a *calibration*. In more gen-

erality, a calibration is a closed form  $\alpha \in \Omega^k(M)$  which for every oriented  $k$ -dimensional subspace  $V \subset T_p M$  satisfies  $\alpha|_V \leq \mu_V$ , where  $\mu_V$  is the volume form on  $V$  induced by the Riemannian metric. The existence of a calibration gives rise to a foliation of minimal  $k$ -dimensional submanifolds—in our setup a geodesic foliation by field lines. On the basis of the hierarchy of stationary conditions

$$\{\eta = d\alpha\} \subset \{d\eta = 0\} \subset \{\iota_B d\eta = 0\}$$

we have introduced in this section, it would be interesting to investigate *twisted minimal foliations*, generalizations of twisted geodesic foliations for calibrations with  $k \geq 2$  in future work.

## 4.4 CONFORMAL CHANGE OF METRIC

It turns out that the stationary conditions for the  $L^1$ -optimization problems can equivalently be derived from the Euler-Lagrange equations for the  $L^2$ -optimization problems by applying a conformal change of metric. Our results suggest that for practical applications the problem of minimizing the  $L^2$ -norm of a magnetic field in  $\mathbb{R}^3$  can be approached by introducing a conformal change of the form  $|B|^2 g$  for a non-vanishing magnetic field  $B$ . This approach has been applied in, e.g., [121, 75, 46].

Consider a closed flux form  $\beta$  and a representative of the conformal class  $\widehat{g} \in [\bar{g}]$ . From these given objects, we may construct a conformally changed metric  $\bar{g} \in [\widehat{g}]$  on the support of  $\beta$  by defining

$$\bar{g} := |\beta|_{\widehat{g}}^2 \widehat{g}. \quad (4.4)$$

This conformal change determines transformation rules for all metric dependent objects. Denoting the volume forms induced by the respective metrics by  $\widehat{\mu}$  resp.  $\bar{\mu}$ , the vector fields  $\widehat{B}, \bar{B}$  associated to a  $\beta$  are defined by

$$\beta = \iota_{\widehat{B}} \widehat{\mu} = \iota_{\bar{B}} \bar{\mu}.$$

**Lemma 4.10** For  $n \geq 3$  we have for the conformal change of metric given in Eq. (4.4) that

$$|\beta|_{\widehat{g}} = |\widehat{B}|_{\widehat{g}} = |\bar{B}|_{\bar{g}}^{-\frac{1}{n-2}}, \quad |\beta|_{\bar{g}} = |\bar{B}|_{\bar{g}} = |\widehat{B}|_{\widehat{g}}^{-(n-2)}.$$

The vector fields can be expressed in terms of one another as

$$\widehat{B} = |\overline{B}|_{\overline{g}}^{-\frac{n}{n-2}} \overline{B}, \quad \overline{B} = |\widehat{B}|_{\widehat{g}}^{-n} \widehat{B},$$

whereas the corresponding volume forms and Hodge stars satisfy

$$\begin{aligned} \widehat{\mu} &= |\overline{B}|_{\overline{g}}^{\frac{n}{n-2}} \overline{\mu}, \quad \overline{\mu} = |\widehat{B}|_{\widehat{g}}^n \widehat{\mu}, \\ \widehat{\star}\beta &= |\overline{B}|_{\overline{g}}^{-1} \overline{\star}\beta, \quad \overline{\star}\beta = |\widehat{B}|_{\widehat{g}}^{-(n-2)} \widehat{\star}\beta. \end{aligned} \quad (4.5)$$

*Proof.* Let us express the objects with respect to  $\overline{g}$  in terms of  $\widehat{g}$  and write  $e^u = |\beta|_{\widehat{g}} = |\widehat{B}|_{\widehat{g}}$ . Under a conformal change of metric  $\overline{g} = e^{2u} \widehat{g}$  the induced volume form transforms<sup>1</sup> as  $\overline{\mu} = e^{nu} \widehat{\mu}$ , hence  $\overline{\mu} = |\widehat{B}|_{\widehat{g}}^n \widehat{\mu}$ . In particular this implies that the corresponding vector fields transform as  $\overline{B} = e^{-nu} \widehat{B} = |\widehat{B}|_{\widehat{g}}^{-n} \widehat{B}$ .

Using this transformation, we can check that

$$|\widehat{B}|_{\widehat{g}}^{2-n} = \frac{|\widehat{B}|_{\widehat{g}} |\widehat{B}|_{\widehat{g}}}{|\widehat{B}|_{\widehat{g}}^n} = \frac{|\widehat{B}|_{\widehat{g}}}{|\widehat{B}|_{\widehat{g}}^n} = |\overline{B}|_{\overline{g}},$$

hence  $e^u = |\widehat{B}|_{\widehat{g}} = |\overline{B}|_{\overline{g}}^{-\frac{1}{n-2}}$ . Using the last identity we express the objects with respect to  $\widehat{g}$  in terms of  $\overline{g}$ . From  $\overline{B} = e^{-nu} \widehat{B} = |\overline{B}|_{\overline{g}}^{\frac{n}{n-2}} \widehat{B}$  we conclude that  $\widehat{B} = |\overline{B}|_{\overline{g}}^{-\frac{n}{n-2}} \overline{B}$  and similarly we find that  $\overline{\mu} = e^{nu} \widehat{\mu} = |\overline{B}|_{\overline{g}}^{-\frac{n}{n-2}} \widehat{\mu}$ , hence  $\widehat{\mu} = |\overline{B}|_{\overline{g}}^{\frac{n}{n-2}} \overline{\mu}$ . Moreover, under the conformal transformation in Eq. (4.4) the Hodge star on  $k$ -forms transforms as

$$\overline{\star} = e^{(n-2k)u} \widehat{\star} = |\widehat{B}|_{\widehat{g}}^{n-2k} \widehat{\star}, \quad (4.6)$$

hence  $\overline{\star}\beta = |\widehat{B}|_{\widehat{g}}^{-(n-2)} \widehat{\star}\beta$  and similarly we conclude  $\widehat{\star}\beta = |\overline{B}|_{\overline{g}}^{-1} \overline{\star}\beta$ .  $\square$

#### 4.4.1 CONFORMAL TRANSFORMATIONS OF STATIONARY CONDITIONS

Having established the transformation rules for the individual objects in the Euler-Lagrange equations for  $n \geq 3$ , we may derive the corresponding stationary conditions with respect to the conformally changed metric.

Let  $\beta$  be a closed flux form and exact harmonic with respect to  $\widehat{g}$ . Then there

---

<sup>1</sup>For review on how the objects derived from the Riemannian metric transform under a conformal change of metric see [11, Ch. 1J].

is a  $\phi \in C^\infty(M)$  such that  $\widehat{\star}\beta = d\phi$  and by Eq. (4.5), whenever  $\beta$  is non-zero,

$$d\phi = \widehat{\star}\beta = |\bar{B}|_{\bar{g}}^{-1} \bar{\star} \beta.$$

This can be stated by saying that there exists  $\phi \in C^\infty(M)$  such that  $d\phi$  is a normalization of  $\bar{\star}\beta$ , i.e.,  $\beta$  is exact eikonal with respect to  $\bar{g}$ .

Similarly, let  $\beta$  be a closed flux form and harmonic with respect to  $\widehat{g}$ . Then  $d\widehat{\star}\beta = 0$  and by Eq. (4.5), whenever  $\beta$  is non-zero, we have

$$0 = d\widehat{\star}\beta = d(|\bar{B}|_{\bar{g}}^{-1} \bar{\star} \beta),$$

which can be stated by asking for the existence of a closed normalization  $\bar{\eta} \in \Omega^1(M)$  of  $\bar{\star}\beta$ , i.e.,  $\beta$  is eikonal with respect to  $\bar{g}$ .

Finally, let  $\beta$  be a closed flux form which is force-free with respect to  $\widehat{g}$ . Then  $\iota_{\bar{B}} d\widehat{\star}\beta = 0$  and by Eq. (4.5), whenever  $\beta$  is non-zero, we have

$$0 = \iota_{\bar{B}} d\widehat{\star}\beta = |\bar{B}|_{\bar{g}}^{-\frac{n}{n-2}} \iota_{\bar{B}} d(|\bar{B}|_{\bar{g}}^{-1} \bar{\star} \beta).$$

This can be stated by asking for the existence of a normalization of  $\bar{\eta} \in \Omega^1(M)$  of  $\bar{\star}\beta$  which satisfies  $0 = \iota_{\bar{B}} d\bar{\eta}$ , i.e., the vector field  $\bar{B}$  associated with  $\beta$  forms—up to reparametrization—a geodesic foliation.

#### 4.4.2 EQUIVALENCE THEOREM

Considering the squared  $L^2$ -norm of a flux form and applying the conformal change of metric we have

$$\|\beta\|_{L^2, \widehat{g}}^2 = \int_M |\widehat{B}|_{\widehat{g}}^2 \widehat{\mu} = \int_M |\bar{B}|_{\bar{g}} \bar{\mu} = \|\beta\|_{L^1, \bar{g}}. \quad (4.7)$$

Moreover, we note that the constraints and boundary conditions in Theorems 4.1, 4.2 and 4.4 were expressed independent of a metric. Therefore, after fixing the respective metrics, we conclude:

**Theorem 4.11** For  $n \geq 3$ , after the conformal change of metric  $\bar{g} = |\beta|_{\widehat{g}}^2 \widehat{g}$ , stationary points of the squared  $L^2$ -norm with respect to  $\widehat{g}$  become stationary points of the  $L^1$ -norm with respect to  $\bar{g}$  with the same constraints and boundary conditions and vice versa.

By considering the different constraints on the admissible variations we thus obtain (Fig. 4.2):

**Theorem 4.12** Let  $M$  be an  $n$ -dimensional conformal manifold,  $n \geq 3$ ,  $\beta \in \Omega^{n-1}(M)$  be a closed flux form with  $j_{\partial M}^* \beta = \beta_{\partial M}$  for given boundary conditions  $\beta_{\partial M} \in \Omega^{n-1}(M)$  and  $\widehat{g}, \overline{g} \in [\widehat{g}]$  be related by  $\overline{g} = |\beta|_{\widehat{g}}^2 \widehat{g}$ . Then,

- (i)  $\beta$  is force-free with respect to  $\widehat{g}$  if and only if it is geodesic with respect to  $\overline{g}$ .
- (ii)  $\beta$  is harmonic with respect to  $\widehat{g}$  if and only if it is eikonal with respect to  $\overline{g}$ .
- (iii)  $\beta$  is exact harmonic with respect to  $\widehat{g}$  if and only if it is exact eikonal with respect to  $\overline{g}$ .

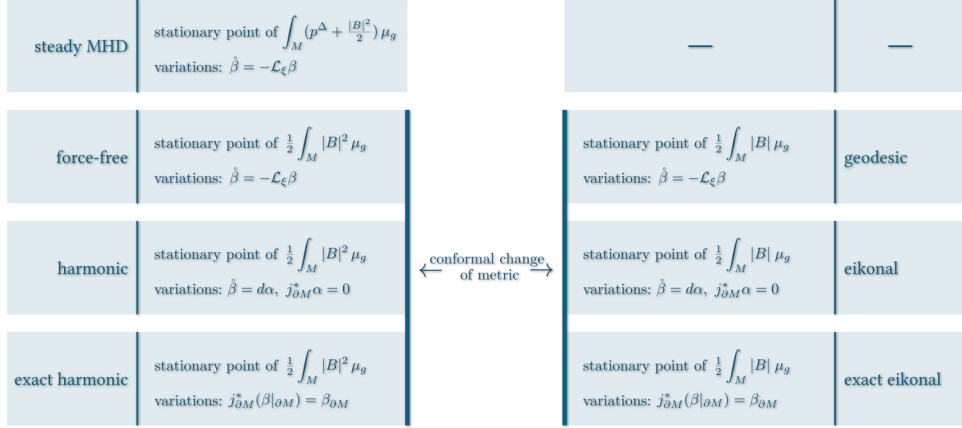


**Figure 4.2:** An overview of the variation problems that are equivalent by a conformal change of metric according to Theorem 4.12.

**Remark 4.13 (Flux-Forms with Non-Global Support)** It is well-known that stationary points of  $L^1$ -optimization problems, such as Beckmann optimal transport problems, typically exhibit sparse support ([94], Fig. 4.3). Specifically, for points  $p \in M$  where  $\beta$  vanishes it is not possible to define a non-degenerate metric using  $|\beta|^2$  as a conformal factor. However, the integrity of our theory, which focuses on the geometry of field lines, remains unaffected. The concept of a field line associated with a flux form inherently assumes that the flux form is non-vanishing. Consequently, all the theory and results presented in this thesis are only well-defined within the support of the flux form and whenever one of the integrals in Eq. (4.7) is defined.

### 4.4.3 THE SURFACE CASE

In the case that  $M$  is a surface, *i.e.*,  $n = 2$ , we find that only one implication of the equivalences in Theorem 4.12 holds. The reason for that is that the essential tool for the proof of Theorem 4.11 is the transformation of the Hodge stars under a conformal change of metric. However, with Eq. (4.6) we see that the Hodge star on 1-forms on a 2-dimensional manifold is conformally invariant. Therefore, for a 2-dimensional manifold harmonicity ( $d\beta = 0$  and  $d \star \beta = 0$ ) is a conformally invariant notion and cannot be achieved by a conformal transformation.

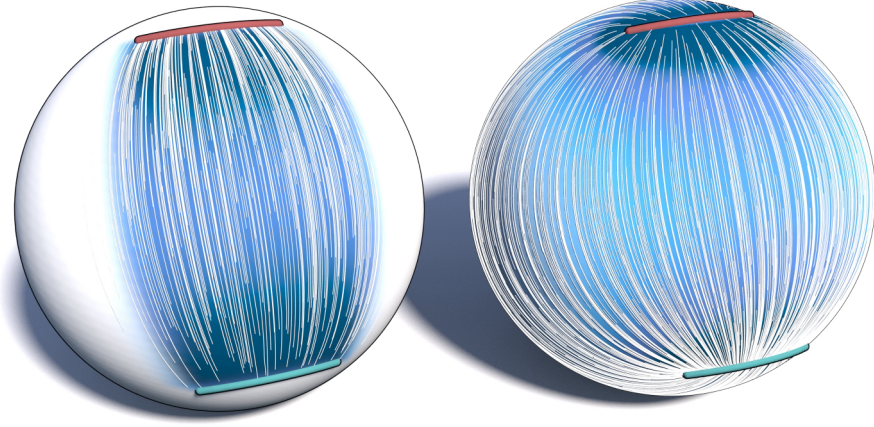


**Figure 4.3:** Vector fields  $B \in \Gamma(S^2)$  which are stationary points of the  $L^1$ -norm (left), resp.  $L^2$ -norm (right) with boundary conditions given by a source (red) and a sink (blue).

Let us discuss how this affects the situation. First we note that by Corollary 2.26 in the 2-dimensional case, force-free fields and harmonic fields are equivalent. This only leaves exact harmonic and harmonic fields for our consideration.

**Corollary 4.14** Let  $M$  be a 2-dimensional conformal manifold,  $\beta \in \Omega^1(M)$  be a closed flux form with  $j_{\partial M}^* \beta = \beta_{\partial M}$  for given boundary conditions  $\beta_{\partial M} \in \Omega^1(M)$  and  $\widehat{g}, \overline{g} \in [\widehat{g}]$  be related by  $\overline{g} = |\beta|_{\widehat{g}}^2 \widehat{g}$ . Then, if  $\beta$  is (exact) harmonic with respect to  $\widehat{g}$ ,  $\beta$  is (exact) eikonal with respect to  $\overline{g}$ .

*Proof.* The proof is analogous to the corresponding direction to proof Theorem 4.12. □

**Theorem 4.15** Let  $M$  be a 2-dimensional conformal manifold,  $\beta \in \Omega^1(M)$  be a closed and eikonal flux form with  $j_{\partial M}^* \beta = \beta_{\partial M}$  for given boundary conditions  $\beta_{\partial M} \in \Omega^1(M)$ . Then  $\beta$  is harmonic if and only if either of the two conditions holds:

- (i)  $|\beta|_g$  is constant.
- (ii)  $\text{grad } |\beta|_g$  and  $B$  are parallel.

In particular, if  $\beta$  is harmonic it is harmonic with respect to any metric in  $[g]$ .

*Proof.* By assumption  $0 = d\beta = d \star B^\flat$ . Thus, for harmonicity of  $\beta$  is equivalent to  $dB^\flat = 0$ . Since  $\beta$  is eikonal, we have  $d(\frac{B^\flat}{|B|_g}) = 0$ . Therefore,

$$dB^\flat = (d|B|_g) \wedge (\frac{B^\flat}{|B|_g}).$$

The right-hand side vanishes if and only if either (i) or (ii) hold and since  $\star$  is conformally invariant, this is true for any conformally equivalent metric.  $\square$

**Corollary 4.16** For a closed and eikonal flux form  $\beta \in \Omega^1(M)$  on a 2-dimensional conformal manifold  $M$  the 2-form  $(d|B|_g) \wedge (\frac{B^\flat}{|B|_g}) \in \Omega^2(M)$  is conformally invariant.

# CHAPTER 5

## PRESSURE CONFINED PLASMA DOMAINS

In this chapter we consider a so-called *current-sheet model* [73], *i.e.*, plasma domains which are bounded by a flux surface and confined by an ambient pressure, although their geometry is not held fixed. Such a setup is required to study relaxed states of plasma domains whose magnetic field is supported, *e.g.*, on tubular neighborhoods of a curve (Chapter 6), or to study the magnetic relaxation of knotted flux tubes in a similar setup as envisioned by Moffatt [71] (Chapter 7).

Dixon et al. [30] have employed such a model for the solar corona and pointed out that a numerical treatment of ideal plasma with free boundary conditions pose significant challenges. Lagrangian approaches to this problem were proposed in [91, 46] or for the case of the solar atmosphere [75, 76].

The main goal of this chapter is to formalize the notion of such pressure confined plasma domains with free boundaries, to which we will refer to as *plasma bubbles* (Fig. 5.1). Moreover, we derive necessary and sufficient conditions for when such a decomposition

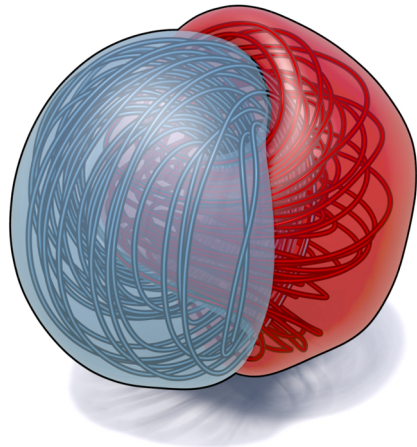


**Figure 5.1:** A plasma bubble configuration consisting of two interlinked components touching at a common boundary surface known as the current sheet.

is in a magnetohydrostatic equilibrium and the corresponding variational principles. Allowing for  $n$ -dimensional manifolds, we generalize the results presented in [75, 46, 76] which were restricted to the 3-dimensional case.

## 5.1 MAGNETOHYDROSTATIC BUBBLES

Let  $M$  be an oriented Riemannian manifold. In the absence of gravity and by Definition 2.6 (i), for a magnetohydrostatic equilibrium the pressure has to be constant away from the support of the magnetic field and is discontinuous across the bounding flux surface. It is therefore natural to decompose the manifold  $M$  into the support of the magnetic field and its complement, considering plasma configurations which restrict to smooth configurations on those regions.

**Definition 5.1** A *plasma bubble configuration* on a Riemannian manifold  $M$  consists of a decomposition of  $M$  into finitely many manifolds with corners  $M_i$ ,  $M = M_0 \cup M_B$  with  $M_B := M_1 \cup \dots \cup M_m$  and  $M_i^\circ \cap M_j^\circ = \emptyset$ , divergence-free vector fields  $B_i \in \Gamma TM_i$  tangent to non-empty interfaces  $\partial M_i \cap \partial M_j$ ,  $0 < j \neq i$  and pressure functions  $p_i \in C^\infty(M_i)$  such that  $0 \leq p_i|_{\partial M_i \cap \partial M_0} < p_0|_{\partial M_i \cap \partial M_0}$  and  $d p_i(B_i) = 0$ .

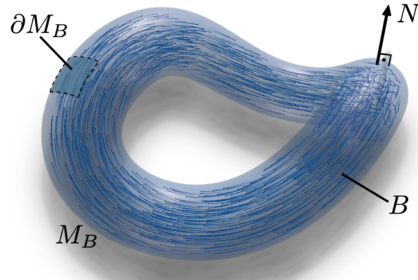


**Figure 5.2:** An isolated flux tube as an example of a plasma bubble configuration.

Examples of plasma bubble configurations are shown in Figs. 5.1 and 5.2. We define the corresponding *magnetic field*  $B \in \Gamma TM$  by

$$B(x) := \begin{cases} B_i(x) & \text{if } x \in M_i, \\ 0 & \text{if } x \in M_0^\circ, \end{cases} \quad (5.1)$$

which determines a corresponding flux-form  $\iota_B \mu_g =: \beta \in \Omega^{n-1}(M)$ . Similarly the *interior pressure*  $p^B \in C^\infty(M)$  is defined as

$$p^B(x) := \begin{cases} p_i(x) & \text{if } x \in M_i, \\ 0 & \text{if } x \in M_0^\circ. \end{cases}$$

In other words, a plasma bubble configuration  $(M_B, p^B, B)$  is a decomposition of  $M$

into two regions—a *flux domain*  $M_B$ , which supports the magnetic field  $B$  resp. flux form  $\beta \in \Omega^{n-1}(M)$  and (possibly) some gas with pressure  $p^B$ , and a *gas domain*  $M_0 = M \setminus M_B$ , which contains only gas with ambient pressure  $p_0$  but no magnetic field. Throughout this thesis we will assume that  $M_0$  is connected. For the special case of  $p^B \equiv 0$  we will refer to them as *magnetic bubble configurations*.

For now let us assume that  $\partial M = \emptyset$  and  $M_B$  is bounded by a flux surface. In Section 5.3 we will then treat the general case including boundaries. We now convince ourselves that the piecewise defined field  $B$  is divergence-free. Since we have to deal with discontinuities across the boundaries of  $M_i$ , we can only do so in a weak sense.

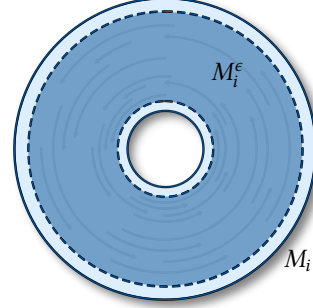
**Proposition 5.2** The field  $B$  as defined in Eq. (5.1) is weakly divergence-free.

*Proof.* Let  $M_i^\epsilon = \{x \in M_i \mid \text{dist}(x, \partial M_i) > \epsilon\}$ . Then there is a smooth function  $\varphi_i : M \rightarrow [0, 1]$  such that  $\text{supp } \varphi_i \subset M_i$  and  $\varphi_i(x) = 1$  for all  $x \in M_i^\epsilon$ .

Define

$$\tilde{B} := \sum_{i>0} \varphi_i B_i$$

and correspondingly  $\tilde{\beta} = \iota_{\tilde{B}} \mu_g$ . Moreover, let  $\phi \in C^\infty(M)$ . Since  $\varphi_i, \beta_i$  have disjoint supports from  $\varphi_j, \beta_j$  for  $i \neq j$ , using Stokes' theorem and the closedness of the  $\beta_i$  flux forms, we compute



$$\int_M \phi d\tilde{\beta} = \sum_{i>0} \int_M d(\phi \varphi_i \beta_i) - \varphi_i d\phi \wedge \beta_i \equiv \sum_{i>0} \int_{M_i} d\phi \wedge \beta_i = \sum_{i>0} \int_{\partial M_i} \phi \beta_i = 0,$$

where we use that the  $M_i$  are bounded by a flux surface, i.e.,  $\beta|_{\partial M_i} = 0$ , and  $\equiv$  denotes equality up to terms vanishing for  $\epsilon \rightarrow 0$ .  $\square$

**Definition 5.3** A plasma bubble configuration is in *magnetohydrostatic equilibrium* if it weakly satisfies the magnetohydrostatic equation.

**Theorem 5.4** A plasma bubble configuration is in magnetohydrostatic equilibrium if and only if

(i)  $p_0$  is constant.

(ii)  $\iota_B dB^b = dp^\Delta$ .

(iii)  $p^B + \frac{|B|^2}{2} = p_0$  on  $\partial M_0 \cap \partial M_B$  and  $p_i + \frac{|B_i|^2}{2} = p_j + \frac{|B_j|^2}{2}$  on non-empty  $\partial M_i \cap \partial M_j$ .

CHAPTER 5. PRESSURE CONFINED PLASMA DOMAINS

*Proof.* Let  $M_i^\epsilon = \{x \in M_i \mid \text{dist}(x, \partial M_i) > \epsilon\}$ . Then there is a smooth function  $\varphi_i : M \rightarrow [0, 1]$  such that  $\text{supp } \varphi_i \subset M_i$  and  $\varphi_i(x) = 1$  for all  $x \in M_i^\epsilon$ . As for the proof of Proposition 5.2 we define

$$\tilde{B} := \sum_{i>0} \varphi_i B_i.$$

Moreover, we define

$$\tilde{p}_0 := \varphi_0 p_0, \quad \tilde{p}^B := \sum_{i>0} \varphi_i p_i$$

and let  $Y \in \Gamma TM$ . Then, since  $\varphi_i, B_i$  have disjoint supports from  $\varphi_j, B_j$  for  $i \neq j$ , using Stokes' theorem, we compute

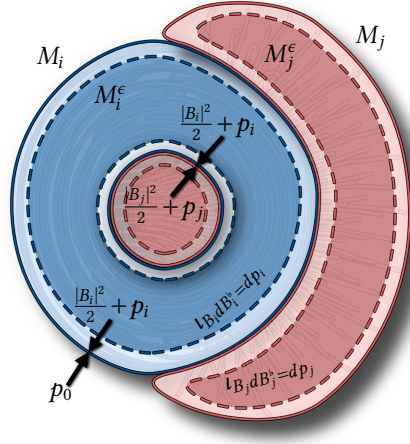
$$\begin{aligned} \int_M (\iota_{\tilde{B}} d\tilde{B}^b) \wedge \star Y^b &= \sum_{i>0} \int_M \left( \varphi_i^2 \iota_{B_i} dB_i^b + \frac{1}{2} g(\text{grad } \varphi_i^2, B_i) B_i^b - \frac{|B_i|^2}{2} d\varphi_i^2 \right) \wedge \star Y^b \\ &= \sum_{i>0} \int_M \left( \varphi_i^2 \iota_{B_i} dB_i^b \wedge \star Y^b + d\varphi_i^2 \wedge \star \left( \frac{1}{2} g(B_i, Y) B_i^b \right) - \frac{|B_i|^2}{2} d\varphi_i^2 \wedge \star Y^b \right) \\ &\equiv \sum_{i>0} \int_{M_i} \left( \iota_{B_i} dB_i^b \wedge \star Y^b + \frac{1}{2} d \left( g(B_i, Y) \star B_i^b - |B_i|^2 \star Y^b \right) \right) \\ &= \sum_{i>0} \left( \int_{M_i} \iota_{B_i} dB_i^b \wedge \star Y^b - \int_{\partial M_i} \frac{|B_i|^2}{2} \star Y^b \right) \end{aligned}$$

where  $\equiv$  denotes equality up to terms vanishing for  $\epsilon \rightarrow 0$ . Moreover, again by Stokes' theorem, we have

$$\begin{aligned} \int_M d\tilde{p}^B \wedge \star Y^b &= \sum_{i>0} \int_M (d\varphi_i \wedge (p_i \star Y^b) + \varphi_i dp_i \wedge \star Y^b) \\ &\equiv \sum_{i>0} \int_{M_i} dp_i \wedge \star Y^b - \sum_{i>0} \int_{\partial M_i} p_i \star Y^b \end{aligned}$$

and similarly

$$\int_M d\tilde{p} \wedge \star Y^b \equiv \int_{M_0} dp_0 \wedge \star Y^b - \int_{\partial M_0} p_0 \star Y^b.$$



## 5.2. VARIATIONAL PRINCIPLES FOR PLASMA BUBBLE CONFIGURATIONS

We thus obtain

$$\begin{aligned}
& \int_M (\iota_{\tilde{B}} d\tilde{B}^b - (d\tilde{p}_0 - d\tilde{p}^B)) \wedge \star Y^b \\
& \equiv \sum_{i>0} \left( \int_{M_i} (\iota_{B_i} dB_i^b - dp^\Delta) \wedge \star Y^b \right) + \int_{M_0} dp_0 \wedge \star Y^b \\
& \quad + \sum_{i,j>0} \int_{\partial M_i \cap \partial M_j} \left( \left( p_i + \frac{|B_i|^2}{2} \right) - \left( p_j + \frac{|B_j|^2}{2} \right) \right) \star Y^b \\
& \quad + \sum_{i>0} \int_{\partial M_0 \cap \partial M_i} \left( p_0 - \left( p_i + \frac{|B_i|^2}{2} \right) \right) \star Y^b
\end{aligned}$$

which vanishes for all  $Y \in \Gamma TM$  if and only if  $\iota_{B_i} dB_i^b = dp^\Delta$ ,  $\operatorname{grad} p_0 = 0$ ,  $p_i + \frac{|B_i|^2}{2} = p_0$  on  $\partial M_0 \cap \partial M_i$  for  $i > 0$  and  $p_i + \frac{|B_i|^2}{2} = p_j + \frac{|B_j|^2}{2}$  on non-empty  $\partial M_i \cap \partial M_j$ .  $\square$

## 5.2 VARIATIONAL PRINCIPLES FOR PLASMA BUBBLE CONFIGURATIONS

The work needed to create a bubble  $M_B \subseteq M$  with interior pressure  $p^B \geq 0$  in an ambient pressure  $p_0 \geq p^B$  is

$$\int_{M_B} (p_0 - p^B) \mu_g$$

and we denote the *pressure difference* between interior and ambient pressures by

$$p^\Delta := p_0 - p^B.$$

We view the constant ambient pressure  $p_0$  as an additional structure on the manifold  $M$  and therefore denote the ambient Riemannian manifold as a triple  $(M, g, p_0)$ .

**Definition 5.5** Let  $(M_B, p^B, B)$  be a plasma bubble configuration in an oriented Riemannian manifold  $(M, g, p_0)$ . Then the *magnetohydrostatic energy* is given by

$$\mathcal{E}(M_B, p^B, B) = \int_{M_B} \left( p^\Delta + \frac{|B|^2}{2} \right) \mu_g. \quad (5.2)$$

By Definition 5.1, we assume for any  $p^B$  we consider that  $dp^B(B) = 0$ , since we are interested in steady solutions to ideal MHD. Denoting  $B_t = d\chi_t(B_0)$  and  $p_t^B = p^B \circ \chi_t$  for a family of diffeomorphism  $t \mapsto \chi_t : M \rightarrow M$ , this property is

preserved when both  $B$  (*resp.*  $\beta$ ) and  $p^B$  are transported by  $\chi_t$ , since

$$dp_t^B(B_t) = \iota_{d\chi_t(B_0)}\chi_t^*dp_0^B = \chi_t^*(\iota_{B_0}dp^B) = \chi_t^*(dp^B(B_0)) = 0. \quad (5.3)$$

In order to examine the critical points of Eq. (5.2) we compute the energy variation.

**Theorem 5.6** Let  $(M_B, p^B, B)$  be a plasma bubble configuration in an  $n$ -dimensional oriented Riemannian manifold  $(M, g, p_0)$ . Then the energy variation under isotopy constraint variations, *i.e.*,  $\dot{\beta} = -\mathcal{L}_\xi \beta$  for some  $\xi \in \Gamma TM$  which is compactly supported in the interior of  $M$  is given by

$$d\mathcal{E}(\dot{\beta}) = \int_{M_B} (dp^\Delta - \iota_B dB^\flat) \wedge \iota_\xi \mu_g + \int_{\partial M_B} (p^\Delta - \frac{|B|^2}{2}) \iota_\xi \mu_g.$$

*Proof.* Let  $\chi_t$  denote the flow map of  $\xi$ . By applying the *Reynolds transport theorem* [88] to the time-dependent integrands  $p^\Delta$  and  $\frac{|B|^2}{2}$  we get

$$\begin{aligned} \frac{d}{dt} \Big|_{t=0} \int_{M_B} \chi_t^*(p^\Delta \mu_g) &= \int_{M_B} (\iota_\xi dp^\Delta) \wedge \mu_g + \int_{\partial M_B} p^\Delta \iota_\xi \mu_g \\ &= \int_{M_B} dp^\Delta \wedge \iota_\xi \mu_g + \int_{\partial M_B} p^\Delta \iota_\xi \mu_g, \end{aligned}$$

as well as

$$\frac{d}{dt} \Big|_{t=0} \int_{M_B} \frac{1}{2} \chi_t^*(\beta \wedge \star \beta) = - \int_{M_B} d\iota_\xi \beta \wedge \star \beta + \int_{\partial M_B} \frac{|B|^2}{2} \iota_\xi \mu_g.$$

Analogous to the proof of Theorem 4.4 we compute

$$\begin{aligned} - \int_M d\iota_\xi \beta \wedge \star \beta &= (-1)^n \int_M \iota_\xi \beta \wedge d \star \beta - \int_{\partial M_B} \iota_\xi \beta \wedge \star \beta \\ &= (-1)^n \int_M \xi^\flat \wedge \star (\iota_B d \star \beta) - \int_{\partial M_B} |B|^2 \iota_\xi \mu_g + \int_{\partial M_B} B^\flat(\xi) \beta \\ &= - \int_M (\iota_B dB^\flat) \wedge \star \xi^\flat - \int_{\partial M_B} |B|^2 \iota_\xi \mu_g + \int_{\partial M_B} g(\xi, B) \beta, \end{aligned}$$

which proves the claim after rearranging terms, since  $\xi|_{\partial M} = 0$  and  $\beta|_{\partial M_B} = 0$ .  $\square$

Theorem 5.6 allows us to formulate a variational characterization for a plasma bubble configuration  $(M_B, p^B, B)$  in magnetohydrostatic equilibrium.

**Theorem 5.7** A plasma bubble configuration  $(M_B, p^B, B)$  in an oriented Riemannian manifold  $(M, g, p_0)$  is a stationary point of Eq. (5.2) under isotopy constraint

variations if and only if  $B$  is in magnetohydrostatic equilibrium, *i.e.*,  $\iota_B dB^b = dp^B$  on its support and  $p^\Delta = \frac{|B|^2}{2}$  on  $\partial M_0 \cap \partial M_B$ .

**Remark 5.8** In [46, Thm. 5.3] the statement has been shown for the 3-dimensional case, where it was phrased in the vector-calculus formalism with an otherwise identical proof. For the special case of vanishing interior pressure  $p^B = 0$ , the result generalizes a version of the *minimum energy theorem for force-free fields* (Theorem 1.2) for pressure confined fields, which are bounded by a flux surface [75, 76].

### 5.3 PLASMA BUBBLES WITH FLUX BOUNDARIES

For many practical applications, the magnetic field is not bounded by a flux surface, but field lines pass through the boundary  $\partial M$ . One such example is the solar corona (Figs. 7.5 and 8.1), where the domain of interest is the exterior of the sun bounded by the sun's surface [30, 118, 75]. In solar physics, the corresponding boundary conditions which fix the isotopy class of the field in this case are commonly referred to as *line tied* [115].

Our results of Proposition 5.2 and Theorem 5.4 still hold when  $M$  is a manifold with boundary and  $\beta$  satisfies given boundary flux conditions. In that case, the only modification of the proof is to consider  $\phi \in C^\infty(M)$  resp.  $\omega \in \Omega^{n-1}(M)$  which are compactly supported away from the boundary  $\partial M$ . Similarly, the variational principle for magnetohydrostatic plasma bubbles carry over as long as we restrict to variations of the form  $\dot{\beta} = -\mathcal{L}_\xi \beta$  for some  $\xi \in \Gamma TM$  which is compactly supported in the interior of  $M$ .

**Theorem 5.9** A plasma bubble configuration  $(M_B, p^B, B)$  in an oriented Riemannian manifold  $(M, g, p_0)$  with boundary and  $j_{\partial M}^* \beta = \beta_{\partial M}$  for a given boundary condition  $\beta_{\partial M} \in \Omega^{n-1}(M)$  is a stationary point of Eq. (5.2) under isotopy constraint variations, *i.e.*,  $\dot{\beta} = -\mathcal{L}_\xi \beta$  for some  $\xi \in \Gamma TM$  which is compactly supported in the interior of  $M$  if and only if  $B$  is in magnetohydrostatic equilibrium, *i.e.*,  $\iota_B dB^b = dp^B$  on its support and  $p^\Delta = \frac{|B|^2}{2}$  on  $\partial M_0 \cap \partial M_B$ .

In addition to the flux boundary conditions many problems in physical applications require a constraint on the helicity<sup>1</sup> [104, 105, 30, 7]. Although helicity is a measure for the degree of “knottedness” of the field, constraining it does not

---

<sup>1</sup>In cases where  $M$  has a boundary only the *relative helicity* is gauge invariant and thus is the relevant quantity (see [69, 9]).

suffice to preserve the field topology. It is therefore incompatible with ideal MHD, although stationary points of the corresponding variational principle are linear force-free fields on their support [30]. For completeness we state a result from Dixon et al. [30], which generalizes the *Woltjer minimum energy principle* in three dimensions allowing for free boundaries.

**Theorem 5.10** ([30]) Let  $(M_B, B)$  be a magnetic bubble configuration in an oriented Riemannian 3-manifold  $(M, g, p_0)$  with boundary. Then, if the magnetic field  $B$  on  $M_B$  is a critical point of Eq. (5.2) under variations which respect the boundary condition  $\Phi \in C^\infty(\partial M_B \cap \partial M)$  and the relative helicity, the magnetic field is linear force-free, *i.e.*,  $\operatorname{curl} B = \lambda B$  for a constant  $\lambda$ .

An interesting observation can be made if we extend the class of admissible variations to those of the form  $\dot{\beta} = -\mathcal{L}_\xi \beta$  where  $\xi \in \Gamma TM$  no longer has a compact support in the interior of  $M$ , but merely preserves the boundary condition, *i.e.*,  $\xi$  is tangent to the boundary  $\partial M$  and  $\mathcal{L}_\xi j_{\partial M}^* \beta = \mathcal{L}_\xi \beta_{\partial M} = 0$  on  $\Sigma := \partial M \cap \partial M_B$ .

**Theorem 5.11** Let  $(M_B, B)$  be a magnetic bubble configuration in an oriented Riemannian 3-manifold  $(M, g, p_0)$  with boundary. Moreover, let  $g(B, N)(x) \neq 0$  for all  $x \in \Sigma$ , and the set  $\{x \in M_B \mid \text{the integral curve of } B \text{ through } x \text{ intersects } \partial M\}$  be dense in  $M_B$ . Then if the magnetic field  $B$  on  $M_B$  is a critical point of Eq. (5.2) under variations of the form  $\dot{\beta} = -\mathcal{L}_\xi \beta$  where  $\xi \in \Gamma TM$  is tangent to the boundary  $\partial M$  and  $\mathcal{L}_\xi j_{\partial M}^* \beta = \mathcal{L}_\xi \beta_{\partial M} = 0$  on  $\Sigma := \partial M \cap \partial M_B$ , the magnetic field is harmonic.

*Proof.* We denote all operators on  $T\partial M$  by a subscript  ${}_{\partial M}$  and omit the subscript on the volume form induced by the metric  $g$ .

With an analogous argument as for Theorem 5.9 (refering to the computation in the proof of Theorem 5.6) we note there is only one term that needs extra attention. The stationary condition states that for all  $\xi \in \Gamma TM$  which respect the boundary conditions

$$0 = \int_\Sigma g(\xi, B) \beta = \int_\Sigma g(g(B, N) \xi, B) \mu_{\partial M}. \quad (5.4)$$

Then, since the variation by  $\xi|_{\partial M} \in \Gamma TM$  respects the boundary conditions

$$\begin{aligned} 0 &= \mathcal{L}_\xi(g(B, N) \mu_{\partial M}) \\ &= (g(\operatorname{grad} g(B, N), \xi) + g(B, N) \operatorname{div}_{\partial M}(\xi)) \mu_{\partial M} \\ &= \operatorname{div}_{\partial M}(g(B, N) \xi) \mu_{\partial M}, \end{aligned}$$

### 5.3. PLASMA BUBBLES WITH FLUX BOUNDARIES

which shows that  $g(B, N)\xi \in \Gamma T\partial M$  is divergence-free (with respect to  $\mu_{\partial M}$ ). Therefore, Eq. (5.4) implies the existence of a function  $\psi \in C^\infty(\partial M)$  such that  $d\psi = j_{\partial M}^*(B^b|_{\partial M})$ . Therefore,

$$j_{\partial M}^*((dB^b)|_{\partial M}) = d(j_{\partial M}^*(B^b|_{\partial M})) = d^2\psi = 0.$$

Since  $B$  is a stationary it is necessarily force-free, *i.e.*,  $\iota_B dB^b = 0$ . Hence

$$0 = \iota_B(dB^b|_{\partial M}) = \iota_{B^T}(dB^b|_{\partial M}) + g(B, N)\iota_N(dB^b|_{\partial M}) = g(B, N)\iota_N(dB^b|_{\partial M}),$$

where  $B^T := B|_{\partial M} - g(B|_{\partial M}, N)N \in \Gamma T\partial M$ . By assumption  $g(B, N) \neq 0$ , hence  $\iota_N(dB^b|_{\partial M}) = 0$  and therefore  $dB^b|_{\partial M} = 0$  on  $\partial M$ . To conclude the proof we convince ourselves that  $dB^b$  is along the flow lines of  $B$ , *i.e.*,

$$\mathcal{L}_B dB^b = d\iota_B dB^b + \iota_B d^2 B^b = 0.$$

Therefore, since  $B$  is force-free and  $dB^b = 0$  on the boundary  $\Sigma$ , it vanishes everywhere (by continuity). Consequently  $B$  is not only co-closed by definition, but also closed, hence harmonic.  $\square$

# CHAPTER 6

## DISCRETIZATION OF IDEAL PLASMA

In this chapter we turn to the derivation of a discrete model for ideal plasma, which forms the basis for our numerical explorations in Chapter 7. For these practical considerations we restrict our attention to  $M \subseteq \mathbb{R}^3$ .

Close to the original ideas of Faraday, who envisioned electromagnetic fields as “lines of force” [35], we discretize the plasma as a collection of curves with thickness. By coupling physical quantities of the plasma to geometric properties of the curves we obtain Lagrangian modeling primitives which interact with one another. This interaction is a result of theoretical insights we obtained in the preceding sections of this thesis and allows us to describe their behavior, which is governed by electromagnetic laws, in terms of mechanical properties and processes instead.

### 6.1 PLASMA FILAMENTS

Consider a magnetic flux tube supported on a regular tubular neighborhood with circular cross-section. In this case, we have a well-defined *center curve* and we can view the flux domain  $M_B$  as a curve with thickness.

A curve with thickness is a pair  $(\gamma, A)$  consisting of a smooth, regular center curve  $\gamma : [0, L] \rightarrow M$  together with a *cross-sectional area function*  $A : [0, L] \rightarrow \mathbb{R}_{>0}$ . The flux  $h > 0$  through every cross section is constant along the center curve and does not change under deformation by orientation preserving diffeomorphisms. We refer to a curve with thickness  $(\gamma, A)$  together with a fixed flux as a *magnetic filament*.

A magnetic filament represents a bundle of field lines of  $B$  which are lumped

together. Assuming that we can neglect twisting of the associated field lines inside of the tubular neighborhood of  $\gamma$  and that the tube itself is thin—compared to the curvature of  $\gamma$  and the rate of change in its thickness—we can assume that on each cross section the magnetic field will be approximately orthogonal to the cross section and have constant magnitude  $|B| : [0, L] \rightarrow \mathbb{R}_{>0}$ . We assign a unique “magnetic field strength”  $|B|$  to the shape of a magnetic filament defined by

$$h = |B(s)|A(s),$$

where  $A = \pi r^2$  is the cross-sectional area (Fig. 6.1). Hence the radius  $r$  of the tube is determined by  $|B|$  and vice versa. Therefore we also denote plasma filaments as  $(\gamma, |B|)$ .

By allowing for interior gas pressure, we generalize the notion of magnetic filaments and define *plasma filaments* to be curves with thickness with a fixed flux  $h > 0$  and an interior pressure  $p^B \geq 0$ , which, by virtue of Eq. (1.3), is constant on the filament. The energy in Eq. (5.2) of a plasma filament is given by

$$\mathcal{E}(\gamma, p^B, |B|) = h \int_0^L \left( \frac{p^\Delta}{|B|} + \frac{|B|}{2} \right) ds. \quad (6.1)$$

**Lemma 6.1** Let  $(\gamma, |B|)$  be a plasma filament. Then for a given shape of the center curve, the energy in Eq. (6.1) is minimized for  $|B| = \sqrt{2p^\Delta}$ .

*Proof.* First we note that the integrand is convex in  $|B|$ . Taking the derivative with respect to  $|B|$  yields criticality if and only if  $-p^\Delta/|B|^2 + 1/2 = 0$ . □

From Lemma 6.1 we conclude that, accounting for interior pressure, the magnetic field strength associated to a tube geometry confined by an ambient pressure  $p_0 > 0$  is determined by

$$\frac{|B|^2}{2} = p^\Delta, \quad (6.2)$$

which is equivalent to a pressure continuity  $\frac{|B|^2}{2} + p^B = p_0$  across the boundary  $\partial M_0 \cap \partial M_B$  (Fig. 6.1). Note that this matches our results from Section 5.1.

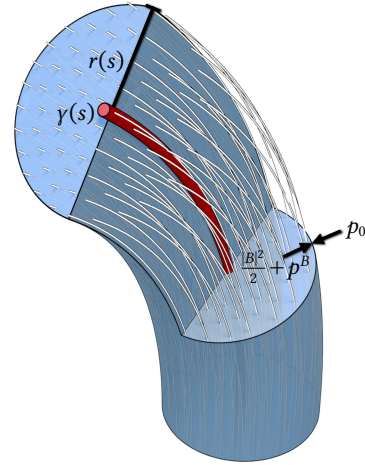


**Figure 6.1:** The geometry of a plasma filament.

### 6.1.1 CONFORMAL INTERPRETATION

We can uncover some interesting geometry from the observations in Section 6.1, even in the smooth setting. To this end we consider the energy in Eq. (5.2) to be the integrated total length of the plasma filaments with respect to the conformally changed metric with length element

$$d\tilde{s} := e^u ds := \begin{cases} \sqrt{2p^\Delta} ds & \text{in } M_0 \\ \left(\frac{p^\Delta}{|B|} + \frac{|B|}{2}\right) ds & \text{in } M_B, \end{cases} \quad (6.3)$$

which is defined on the whole of  $M$  by scaling the Euclidean length element  $ds$ . Note that the conformal factor is a continuous function as long as Eq. (6.2) holds.

**Remark 6.2** For  $M = M_B$  and in the low-beta limit ( $p^B = 0$ ) the internal energy of the system does not affect the energy and the metric in Eq. (6.3) matches the conformally changed metrics from our considerations in Chapters 3 and 4.

More precisely, in terms of the metric in Eq. (6.3) we can write

$$\mathcal{E}(M_B, p^B, |B|) = \int_{\Gamma} \mathcal{L}(\gamma) d\gamma, \quad (6.4)$$

where the integral denotes integration over the set  $\Gamma$  of all field lines with respect to the flux density measure  $d\gamma$ . In Eq. (6.3), the conformal factor in  $M_B$  accounts for the magnetic pressure exceeding the pressure  $\sqrt{2p^\Delta}$  of the same filament in an unobstructed state. This results from the factorization

$$\left(\frac{p^\Delta}{|B|} + \frac{|B|}{2}\right) = \sqrt{2p^\Delta} \left(1 + \frac{\left(\frac{|B| - \sqrt{2p^\Delta}}{2|B|\sqrt{2p^\Delta}}\right)^2}{\left(\frac{|B| - \sqrt{2p^\Delta}}{2|B|\sqrt{2p^\Delta}}\right)^2}\right). \quad (6.5)$$

As the latter summand of the second factor is non-negative, the conformal factor in  $M_B$  is bounded from below by the conformal factor in  $M_0$ . In Section 6.1.2 we show that this case represents the magnetic pressure of the filament in an unobstructed state.

### 6.1.2 UNOBSTRUCTED PLASMA FILAMENTS

A plasma filament  $(\gamma, |B|)$  is called *unobstructed* if Eq. (6.2) holds, *i.e.*, the tube around  $\gamma$  is embedded with its optimal energy minimizing fields strength  $|B| = \sqrt{2p^\Delta}$ . This uniquely determines the radius of a cross-section of an unobstructed

plasma filament by

$$r_{\text{opt}} = \sqrt{\frac{h}{\pi \sqrt{2p^\Delta}}} \circ \gamma. \quad (6.6)$$

By plugging in Eq. (6.2) into Eq. (6.1), the energy of a plasma filament

$$\mathcal{E}(\gamma, |B|) = h \sqrt{2} \int_0^L \sqrt{p^\Delta} ds$$

is only dependent on the curve shape. In particular, the energy in Eq. (6.1) is critical for geodesics.

**Theorem 6.3** Unobstructed magnetic filaments follow geodesics with respect to the conformally changed metric  $p^\Delta g$ .

At first glance, Theorem 6.3 seems trivial, since in our setting we only consider a single unobstructed filament and  $p^\Delta$  is constant. Therefore, the geodesics are straight line segments in  $\mathbb{R}^3$  [80].

However, Padilla et al. [75] showed that a reasonable choice of non-constant ambient pressure  $p_0$  admits non-trivial geodesics and the theorem statement can be interpreted as a special case of Theorem 3.41 and therefore fits our findings very well. For a very special choice of  $p_0$  one can even give explicit analytic expressions for the corresponding geodesics [75, Thm. 6]. Unfortunately, by Eq. (1.2) such non-constant choice of  $p$  is only valid when effects of gravity are taken into account and valid choices remain restrictive (see [75, App. A]). Moreover, flux boundary conditions are required to prevent plasma filaments to diverge to low pressure regions.

The situation changes drastically when we additionally account for twists of the magnetic field associated to a plasma filament (Section 6.3).

## 6.2 DISCRETE IDEAL PLASMA

A plasma domain  $M_B$  is approximated by a collection  $\Gamma$  of non-overlapping plasma filaments  $(\gamma, |B|)$ , each representing a fixed flux  $h > 0$ . We approximate the volumetric energy in Eq. (5.2) by the *discrete energy*

$$\mathcal{E}(\Gamma) = \sum_{\gamma \in \Gamma} h \int_0^{L_\gamma} \left( \frac{p_\gamma^\Delta}{|B_\gamma|} + \frac{|B_\gamma|}{2} \right) ds. \quad (6.7)$$

To ensure the non-overlapping condition is always satisfied we choose the cross-sectional radius of each  $\gamma \in \Gamma$  as

$$r_\gamma(s) = \min\{ r_{\text{opt}}(s), \frac{\text{dist}(s)}{2} \}. \quad (6.8)$$

Here,  $r_{\text{opt}}$  is given by Eq. (6.6) and  $\text{dist}$  is the minimal distance of  $\gamma(s)$  to itself (after a suitable cut-off threshold) or another curve (Fig. 6.2).

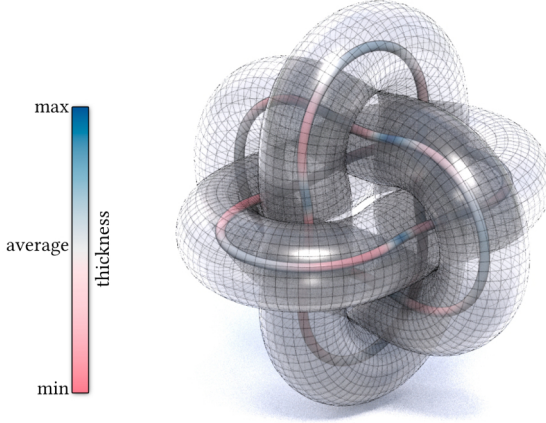


**Figure 6.2:** Relaxed state of Borromean rings discretized by a single plasma filament per link component. The center curves are colored according to the thickness of the tube indicating that a variable thickness is indeed needed to accurately represent equilibria of the energy in Eq. (5.2).

In the smooth setting, a number of properties of plasma are preserved under variations by a family of diffeomorphisms  $t \mapsto \chi_t : M \rightarrow M$ . One example is the fields helicity. Moreover, the magnetic flux form  $\beta$  and the interior pressure function are transported under diffeomorphisms by  $\beta_t = \chi_t^* \beta_0$  and  $p_t^B = p^B \circ \chi_t$ . Consequently, the property that  $p^B$  is a first integral of the flow of  $B$  is preserved (Eq. (5.3)).

In the discretized setting, diffeomorphisms are replaced by perturbations of the center curves  $\gamma$  and the corresponding tube radii. The topology of the field (hence the helicity) is preserved as long as the perturbations do not cause the curves to pass through each other<sup>1</sup>. Since, we prescribe a magnetic flux and an interior pressure per filament, these quantities are by construction constant along the field line, even when they are transported with the curves as Lagrangian

---

<sup>1</sup>In practice this can be ensured by sufficiently small step sizes for position updates.

variables. Therefore, the discretization of ideal plasma into plasma filaments is structure preserving in the sense of discrete differential geometry [26].

**Remark 6.4** The field lines of a generic magnetic field in MHS equilibrium do not have to be closed (Theorem 2.21). This problem shares similarities with the Clebsch representation of vorticity lines of fluid fields [18]. Chern et al. [18] point out that by the Poincaré recurrence theorem [81] almost every such field line will return arbitrarily closely to its initial point, making it “almost closed”, still allowing for meaningful approximations with our discretization in many cases.

### 6.3 TWISTED PLASMA FILAMENT

In the derivation of the model for plasma filaments (Section 6.1) we assume that the magnetic field lumped into a plasma filament is untwisted. In this section we explore what can be said about unobstructed plasma filaments when allowing for a twisted field.

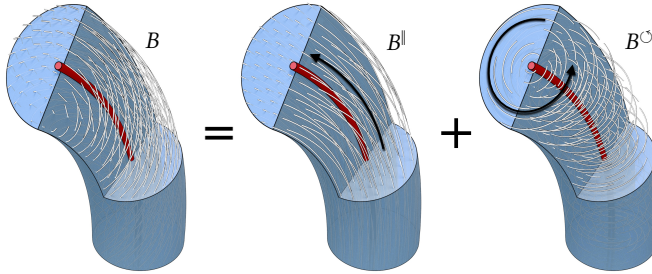


**Figure 6.3:** The magnetic field  $B$  (left) supported on the twisted plasma filaments we consider are comprised of a tangential component  $B^{\parallel}$  (middle) and a poloidal component  $B^{\circlearrowright}$  (right).

Let the center curve  $\gamma$  be parameterized by arc-length and the magnetic field inside of the tubular neighborhood of  $\gamma$  be of the form

$$B = B^{\parallel} + B^{\circlearrowright}.$$

The *tangential* component  $B^{\parallel}$  is parallel to  $\gamma'$  and has constant magnitude on each cross-section orthogonal to  $\gamma'$ , whereas the *poloidal* component  $B^{\circlearrowright}$  is tangent to each cross-section and takes the form of a velocity field of a rigid rotation around  $\gamma'(s)$  with angular velocity  $\tau(s)$  (Fig. 6.3). That is,

$$B^{\circlearrowright}(\gamma(s) + aY) = \frac{a}{A(s)}\tau(s)\gamma'(s) \times Y,$$

## CHAPTER 6. DISCRETIZATION OF IDEAL PLASMA

where  $A(s) = \pi r(s)^2$  is the cross-sectional area,  $0 \leq a \leq r(s)$  and  $Y$  is a unit normal vector to  $\gamma'(s)$ . In particular, the cross-sectional flux is given by  $h = |B^\parallel(s)|A(s)$  and since  $B^\parallel \perp B^\circlearrowright$ , the energy (Eq. (6.1)) of the twisted plasma filament is given by

$$\begin{aligned} \int_{M_B} \left( p^\Delta + \frac{|B|^2}{2} \right) \mu_g &= \int_{M_B} \left( p^\Delta + \frac{|B^\parallel|^2}{2} \right) \mu_g + \frac{1}{2} \int_{M_B} |B^\circlearrowright|^2 \mu_g \\ &= h \int_0^L \left( \frac{p^\Delta}{|B^\parallel|} + \frac{|B^\parallel|}{2} \right) ds + \frac{1}{2} \int_0^L \int_0^{2\pi} \int_0^{r(s)} \frac{|\tau(s)\rho|^2}{A(s)^2} \rho d\rho d\vartheta ds \\ &= h \int_0^L \left( \frac{p^\Delta}{|B^\parallel|} + \frac{|B^\parallel|}{2} \right) ds + \frac{\pi}{4} \int_0^L \frac{\tau(s)^2 r(s)^4}{A(s)^2} ds \\ &= h \int_0^L \left( \frac{p^\Delta}{|B^\parallel|} + \frac{|B^\parallel|}{2} \right) ds + \frac{1}{4\pi} \int_0^L \tau(s)^2 ds. \end{aligned}$$

For an unobstructed filament, with an analogous argument as in Lemma 6.1, the first summand can be written independently of the magnitude of the tangential component and the energy becomes

$$\int_{M_B} \left( p^\Delta + \frac{|B|^2}{2} \right) \mu_g = h \int_0^L \sqrt{2p^\Delta} ds + \frac{1}{4\pi} \int_0^L \tau(s)^2 ds. \quad (6.9)$$

This energy can be stated solely in terms of a framed curve  $(\gamma, N)$ , *i.e.*, a curve together with a unit normal field

$$N = \cos(\alpha) \gamma' + \sin(\alpha) \gamma' \times Z,$$

which is determined by an arbitrary parallel unit normal field  $Z$  along  $\gamma$  and

$$\alpha(s) = \int_0^s \tau(s) ds.$$

Since the integrand of the second integral in Eq. (6.9) is always non-negative, we see that having torsion only increases the energy of the plasma filament. Therefore, let us restrict our attention to variations which fix the total torsion

$$\Theta := \alpha(L) = \int_0^L \tau(s) ds$$

of the framed curve  $(\gamma, N)$ . Then, by the Cauchy-Schwartz inequality

$$L(\gamma) \int_0^L \tau(s)^2 ds = \int_0^L 1 ds \int_0^L \tau(s)^2 ds \geq \left( \int_0^L \tau(s) ds \right)^2 = \Theta^2$$

with equality if and only if  $\tau$  is constant. Therefore, with constraint total torsion, the energy in Eq. (6.9) is minimal for  $\tau = \Theta/L(\gamma)$ , so that

$$\mathcal{E}(\gamma, \Theta) = h \int_0^L \sqrt{2p^\Delta} ds + \frac{1}{4\pi} \frac{\Theta^2}{L(\gamma)} \quad (6.10)$$

has the same stationary points. We define

$$\mathcal{L}(\gamma) := \int_0^L \sqrt{2p^\Delta} ds,$$

which is the length of  $\gamma$  with respect to the conformally changed metric  $2p^\Delta g$ . Then Eq. (6.10) can be stated in a remarkably closed form by

$$\mathcal{E}(\gamma, \Theta) = h\mathcal{L}(\gamma) + \frac{1}{4\pi} \frac{\Theta^2}{L(\gamma)}, \quad (6.11)$$

only depending on the length of the curve with respect to the euclidean and the conformally changed metric as well as the total torsion. Notably, Eq. (6.11) shows that small but non-zero amounts of total torsion result in twisted flux tubes having a larger Euclidean length.

**Remark 6.5** The derivations remain unchanged for analogous setups with variable pressure function  $p_0$  as in [30, 75]. For this reason we refrain from using the constancy of  $p_0$  which we assume for our primary setup.

### 6.3.1 VARIATIONAL PRINCIPLE FOR TWISTED PLASMA FILAMENTS

Eq. (6.11) provides us with an expression for the energy in Eq. (6.1) of an unobstructed plasma filaments with total torsion  $\Theta$ , which only depends on shape of the center curve  $\gamma$ .

**Lemma 6.6** Let  $\gamma : [0, L] \rightarrow \mathbb{R}^3$  be an arc-length parameterized curve. Then for variations  $\dot{\gamma}$  with compact support in the interior we have

$$\begin{aligned} dL(\dot{\gamma}) &= - \int_0^L g(\dot{\gamma}, \gamma'') ds, \\ d\mathcal{L}(\dot{\gamma}) &= \int_0^L g(\dot{\gamma}, e^u (\text{grad } u - g(\text{grad } u, \gamma') \gamma' - \gamma'')) ds, \\ d\Theta(\dot{\gamma}) &= - \int_0^L g(\dot{\gamma}, \gamma' \times \gamma''') ds. \end{aligned}$$

*Proof.* The expressions for  $dL(\dot{\gamma})$  and  $d\Theta(\dot{\gamma})$  can be found in [80]. For the second equation we check that

$$\begin{aligned} d\mathcal{L}(\dot{\gamma}) &= \int_0^L e^u g(\text{grad } u, \dot{\gamma}) + e^u g(\gamma', \dot{\gamma}') ds \\ &= \int_0^L g(\dot{\gamma}, e^u (\text{grad } u - g(\text{grad } u, \gamma') \gamma' - \gamma'')) ds, \end{aligned}$$

which proves the claim.  $\square$

Consequently, considering variations  $\dot{\gamma}$  of  $\gamma$  we find

$$d\mathcal{E}(\dot{\gamma}) = h d\mathcal{L}(\dot{\gamma}) - \frac{\Theta^2}{4\pi L(\gamma)^2} dL(\dot{\gamma}) + \frac{\theta}{2\pi L(\gamma)} d\Theta(\dot{\gamma}).$$

Since in our setup  $p_0$  is constant and we consider a single, unobstructed plasma filament also  $p^\Delta$  is constant. Therefore, in our case  $\text{grad } u = 0$  and the variational gradient of the conformally changed length simplifies to

$$d\mathcal{L}(\dot{\gamma}) = -\sqrt{2p^\Delta} \int_0^L g(\dot{\gamma}, \gamma'') ds.$$

**Theorem 6.7** An unobstructed twisted plasma filament  $(\gamma, |B|, \tau)$  is a stationary point of Eq. (6.1) if and only if its center curve satisfies

$$0 = \left( \frac{\Theta^2}{4\pi L(\gamma)^2} - h\sqrt{2p^\Delta} \right) \gamma'' - \frac{\theta}{2\pi L(\gamma)} \gamma' \times \gamma'''. \quad (6.12)$$

**Corollary 6.8** An unobstructed twisted plasma filament  $(\gamma, |B|, \tau)$  is a stationary point of Eq. (6.1) if and only if there exists a constant  $b \in \mathbb{R}^3$  such that its center curve satisfies

$$\left( \frac{\Theta^2}{4\pi L(\gamma)^2} - h\sqrt{2p^\Delta} \right) \gamma' - \frac{\theta}{2\pi L(\gamma)} \gamma' \times \gamma'' = b.$$

*Proof.* This follows from integrating Eq. (6.12).  $\square$

**Corollary 6.9** For a curve which satisfies the conditions in Corollary 6.8 the quantities  $g(\gamma', b)$  and  $|\gamma''|^2$  are constant, *i.e.*,  $\gamma$  traces out a helix.

# CHAPTER 7

## DISCRETE IDEAL MAGNETIC RELAXATION

As with the Willmore functional or the rope length problem, precise mathematical statements about minimizers of geometric functionals are generally scarce. Consequently, the development of computational methods to approximate or visually represent such natural representatives has been an active area of research [79, 5, 101, 119, 120]. The same is true for steady solutions to the MHD equations (Eqs. (1.1)), where only for a few special cases analytic solutions are known [57, 62, 75] and in general numerical approaches are needed.

In this chapter we derive a numerical method for magnetic relaxation which is purely based on geometry optimization and describe a selection of illustrative experiments that were performed using the proposed method.

### 7.1 RELATED COMPUTATIONAL METHODS

Numerical solutions of the full MHS Eq. (1.2), incorporating hydraulic effects of the plasma and gravity, typically employ Eulerian MHD relaxation methods [22, 77, 55]. However, a Lagrangian method accounting for hydraulic effects was proposed by Smiet, Candelaresi, and Bouwmeester [100]. In the realm of force-free fields, numerical treatments employ both Eulerian [45, 66, 54, 107] and Lagrangian methods [27, 100, 75], the latter are seemingly less common. Some approaches incorporate additional image data as constraints [4], while others are grounded in Clebsch variables [114, 22, 58]. Also a variety of efficient numerical methods for computing harmonic fields from given boundary conditions exists, even on infinite domains [102, 74]. Comparisons of methods are found in [48, 118, 111, 116].

Our model is based on a domain decomposition and belongs to the so-called current-sheet models [73]. They treat the magnetic field as confined in a domain bounded by a surface—the *current sheet*—which is represented by the free-boundary in our model. Outside of this domain, in the gas domain, the magnetic field vanishes. A numerical treatment of magnetic relaxation while constraining the topology or allowing for free-boundaries involves considerable computational difficulties [30]. Lagrangian methods are generally favorable for the preservation of field topology and free boundary conditions [27, 53, 100].

The similarity of ideal magnetic relaxation and the rope length problem—both require a topology preserving tightening process [15]—led to algorithms from knot theory [79, 5] being used in the plasma context. They are used for example to approximate the energy spectra of knotted flux tubes [64, 91], although additional (geometrically more rigid) assumptions are required which neglect an elasticity of the magnetic field lines. Special cases of the problem were studied in more detail by Chui and Moffatt [23], whereas Maggioni and Ricca [64, 91] studied the problem from a geometric point of view. Ricca and Maggioni [90] found similarities between the ground-state energy spectra of magnetic knots and links and the bending energy of tight knots and links, both of which are physically motivated.

## 7.2 A GEOMETRIC RELAXATION METHOD

With a structure preserving discretization for ideal plasma in place, we now turn our attention to the energy minimization. In this section we propose a geometric approach to magnetic relaxation based on the insights of the preceding chapters and outline the implementation of our numerical experiments.

The proposed strategy for energy minimization is based on the interpretation of the energy as the length of the individual field lines measured in a conformally changed metric. The key idea is that shortening the curves decreases the energy.

However, the metric in Eq. (6.3) itself depends on the plasma state  $(M_B, p^B, B)$  approximated by the curve set of curves  $\Gamma$ . One can circumvent the coupled nature of the optimization problem by introducing a time splitting: first, given a curve configuration, the thickness of the tubular neighborhoods around the curves and hence the conformal factor in Eq. (6.5) is computed. Then, assuming the conformal factor is fixed, a *curve-shortening flow* step is performed (Eq. (6.4)). To find a fixed point, these two steps are alternated until convergence (Alg. 1).

---

**Algorithm 1** Energy Minimization
 

---

**Require:** Initial curve set  $\Gamma$ , pressures  $p^B, p_0 > 0$ .

**Ensure:**  $\Gamma$  in relaxed state.

- 1: **while** not converged **do**
  - 2:      $u, \text{grad } u \leftarrow \text{COMPUTEMETRIC}(\Gamma)$ ;
  - 3:      $\Gamma \leftarrow \text{CURVESHORTENING}(\Gamma)$ ;
  - 4: **end while**
- 

### 7.2.1 IMPLEMENTATION

For the experiments the proposed algorithm was implemented in *SideFX Houdini*, where the individual plasma filaments are represented as a *discrete curve*, i.e., a map  $\gamma : \{0, \dots, n\} \rightarrow \mathbb{R}^3$ , where the position of a vertex  $i \in \{0, \dots, n\}$  is denoted by  $\gamma_i$ . Due to the fixed flux and  $h = |B| A$ , the magnitude  $|B_i|$  of the associated magnetic field at vertex  $i$  is determined by the radius  $r$  of the plasma filament: given the collection  $\Gamma$  of discretized plasma filaments, we may compute the logarithmic conformal factors using

$$u_i = \log \left( \frac{p_i^A}{|B_i|} + \frac{|B_i|}{2} \right)$$

for every vertex  $i$  (Section 6.1). The gradient of the logarithmic conformal factor  $u_i$  is approximated employing a finite difference scheme

$$(\text{grad } u)_i \approx \sum_{\gamma_j \in \mathcal{N}(\gamma_i)} (u_j - u_i) \frac{\gamma_j - \gamma_i}{|\gamma_j - \gamma_i|^2},$$

where  $\mathcal{N}(\gamma_i)$  is a set of neighboring vertices of  $\gamma_i$  including vertices coming from virtual filaments that fill the gas domain with field strength according to Eq. (6.2). Note that for the gradient approximation we merely need to know how to evaluate the logarithmic conformal factor  $u$  on the discrete curves  $\gamma$ .

For the curve-shortening flow (with respect to the metric in Eq. (6.3)) we perform a quasi-Newton step which, denoting the  $k$ -th iterate of  $\gamma_i$  by  $\gamma_i^k$ , is given by

$$\gamma_i^{k+1} = w_+ \gamma_{i+1}^k + w_- \gamma_{i-1}^k - \frac{1}{2} (w_- \ell_-^2 + w_+ \ell_+^2) (\text{grad } u)(\gamma_i^k),$$

where  $\ell_- := |\gamma_i^k - \gamma_{i-1}^k|$ ,  $\ell_+ := |\gamma_{i+1}^k - \gamma_i^k|$  and

$$w_- := \frac{\ell_+ e^{u(\gamma_{i-1}^k)}}{\ell_+ e^{u(\gamma_{i-1}^k)} + \ell_- e^{u(\gamma_{i+1}^k)}}, \quad w_+ := \frac{\ell_- e^{u(\gamma_{i+1}^k)}}{\ell_+ e^{u(\gamma_{i-1}^k)} + \ell_- e^{u(\gamma_{i+1}^k)}}.$$

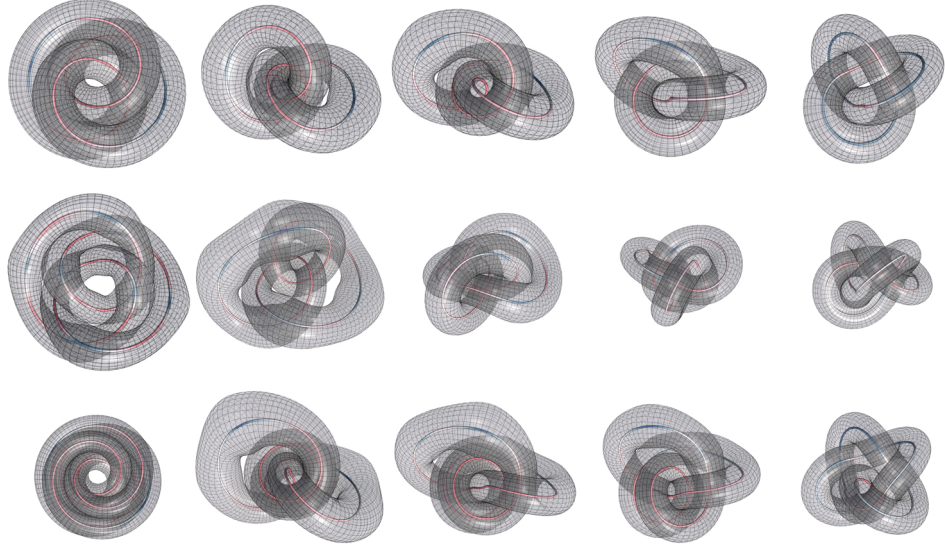


**Figure 7.1:** Consecutive stages of the evolution (left to right) of discrete ideal magnetic relaxation of a variety of knots: trefoil knot, figure eight knot, torus knot  $T_{5,2}$  (top to bottom).

For all shown experiments we choose  $p_0 = 1$  and the same constant  $p^B$  for all filaments. Moreover, in order to preserve the field topology, we bound the displacement of a vertex position in an iteration by the tube radius of the plasma filaments. A more in-depth discussion of the implementation can be found in [76].

### 7.3 STATIONARY PLASMA KNOTS AND LINKS

We were able to successfully relax a variety of knots (Fig. 7.1) and links (Fig. 7.3) using our proposed method. Pierański [79] states that “any algorithm aimed at finding the ideal conformations of prime knots should pass is the ability to bring knots  $10_{161}$  and  $10_{162}$ , the Perko pair, to a single, ideal conformation.” We successfully performed a corresponding experiment, the outcome is shown in Fig. 7.2. Another experiment considers the torus knots  $T_{2,3}$  and  $T_{3,2}$  [71], which our algorithm relaxes to the same equilibrium configuration (Figs. 1.6 and 7.1, first row).

Compared to other algorithms for relaxation from knot theory, our formulation allows for filaments with variable, time-dependent thickness—thus capturing the phenomenon of magnetic elasticity (Section 7.1). Fig. 6.2 showcases a relaxed state which exhibits a non-constant thickness along the center curves, so that this feature is indeed needed for faithful experiments.

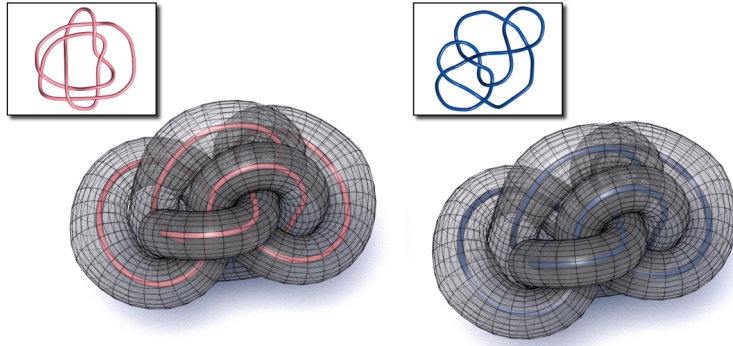


**Figure 7.2:** Relaxing the Perko pair (insets) is considered to be a benchmark for numerical algorithms aiming to find ideal conformations of prime knots. The respective configurations resulting from our method are shown side-by-side.

Including filaments with a variable thickness does not only make the presented model geometrically less rigid, but also allows our filaments to “interact” with one another. This feature is best understood from the conformal viewpoint of our model (Section 6.1.1): Eq. (6.5) states that the conformal factor relevant for the curve-shortening step in our relaxation is given by

$$e^u = \sqrt{2p^\Delta} \left( 1 + \frac{\left( |B| - \sqrt{2p^\Delta} \right)^2}{2|B|\sqrt{2p^\Delta}} \right).$$

This factorization can be understood as an *ambient pressure* factor and a *magnetic pressure* factor. For a filament which is unobstructed at  $\gamma(s)$ , i.e., its thickness is only restricted by the confining ambient pressure, the magnetic energy does not contribute to the metric, since in this case the latter summand of the magnetic pressure factor vanishes. However, whenever there is another filament close by, the thickness of the filaments is defined as half of the distance between their center curves. Consequently, the magnetic pressure factor increases the conformal factor. In a subsequent curve-shortening step, passing through regions with larger conformal factors is discouraged for the curves, causing them to separate and increase their thickness. Therefore, our model encodes the “elasticity” of magnetic flux tubes due to magnetic pressure in the conformal factor which is relevant for the relaxation process. Stationary points represent the optimal trade-off between a “detour” and “being compressed”.

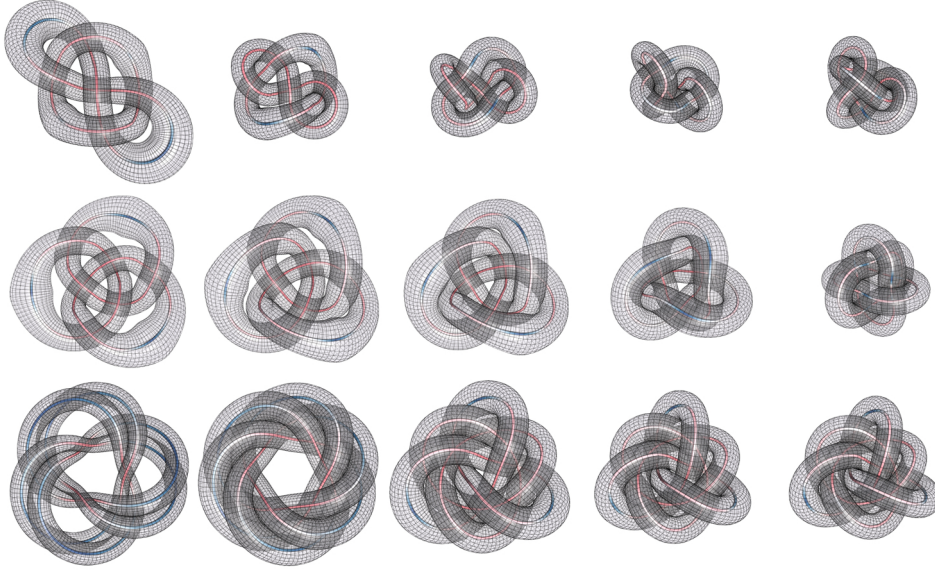


**Figure 7.3:** Consecutive stages of the evolution (left to right) of discrete ideal magnetic relaxation of a variety of links: whitehead link, Borromean rings, two linked trefoil knots (top to bottom).

### 7.3.1 APPROXIMATION OF STEADY SOLUTIONS TO IDEAL MHD

If we choose to represent a given field topology by a larger collection of field lines, the presented method could be a suitable basis for a method to approximate steady solutions for ideal MHD<sup>1</sup>. Preliminary experiments are shown in Figs. 6.2, 1.6 and 7.4. Comparing the relaxed states therein, it is clear that the approximation of the knots and links is extremely rough with only a single plasma filament per connected component. With a larger number of filaments per connected component, the results should be much closer to a “physical ground truth”, since the free boundary conditions influence the equilibrium states to a greater extent.

From Fig. 1.5 it is apparent, that the resulting equilibrium configurations share the characteristic structures that the smooth counterparts have. For example, the filaments at the outer edge are approximately of the same thickness, representing a uniform field strength matching the pressure continuity conditions (Theorem 5.4).

Our model also accounts for the formation of current sheets, which are modeled by the surfaces of the plasma filaments. Fig. 1.5 shows that the method automatically treats their formation as contact surfaces of the plasma filaments.

---

<sup>1</sup>which are equivalent to steady Euler-flows [3]



**Figure 7.4:** Initialized configurations (left column) and relaxed states (right column) of a trefoil knot discretized by 100 plasma filaments (top row) and borromean rings discretized by 50 plasma filaments per link component (bottom row).

## 7.4 THE SOLAR CORONA

The magnetic field in the solar corona is mainly known through its flux on the sun's surface, which can be measured by instruments on earth or in space. Only recently, the first ever spacecraft, the Parker solar probe, has entered the solar corona for measurements from "inside" the solar corona [112]. Therefore, a problem extensively discussed in the solar physics literature is the extrapolation of the magnetic field only from flux measurements on the solar surface [102, 111, 118]. This problem is a good example where our model of pressure confined plasma regions with flux boundary conditions can be applied (Fig. 7.5).

In general, the extrapolation problem is underdetermined. Therefore, to tie down solutions for numerical methods, additional assumptions on the field have to be made.

A common approach is to restrict sought solutions to be harmonic, or force-free. For the latter, an initial field topology has to be additionally prescribed that allows for the handling of twisted or braided fields (Fig. 8.1), which are not de-

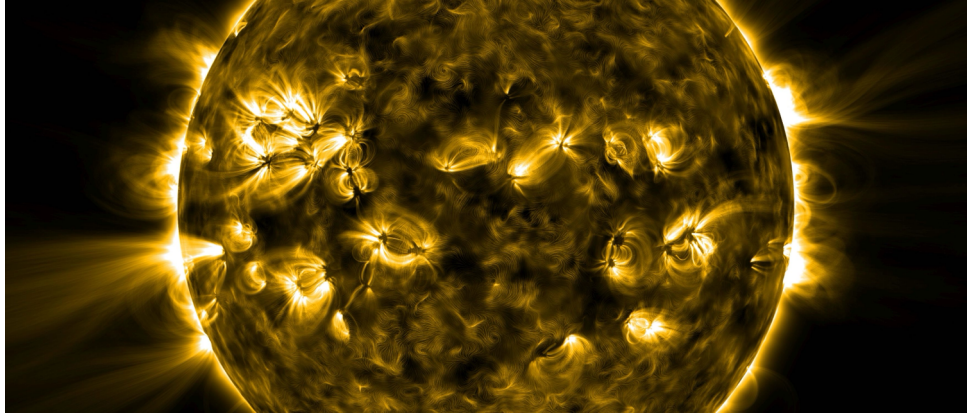


**Figure 7.5:** Rendering of a procedurally generated solar corona computed with the algorithm performing magnetic relaxation on the discretization of the ideal plasma as introduced in this thesis.

terminated by the flux boundary conditions alone. Note that both of the aforementioned cases neglect effects of gas pressure and therefore have to resort to artificial confining fields as in [86] in order to model magnetic fields without global support.

Although the details are beyond the scope of this thesis<sup>2</sup>, let us outline how an initial field topology can be determined procedurally: first we place entry and exit points of the flux on the surface with a density proportional to the prescribed magnetic flux. The flux-quantization parameter  $h > 0$  controls the total number of points placed on the surface. The initial field topology is then determined by solving a *linear assignment problem* for which the cost function is given by the length of the resulting unobstructed filament.

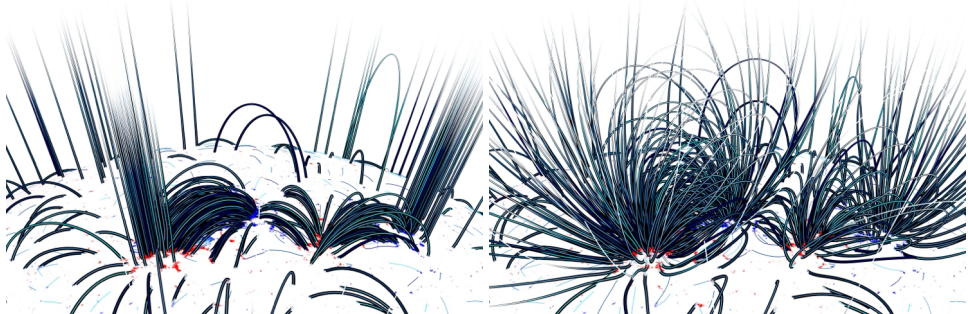


**Figure 7.6:** Left: A curve configuration initialized from a flux map. All filaments are vertical plane curves or radial straight line segments. Right: The same configuration in a relaxed state.

---

<sup>2</sup>In [75] or [76] the initialization procedure is explained in greater detail.

Based on a model of the solar atmosphere which accounts for gravity, a special (non-constant) choice of  $p_0$ , which allows for explicit expressions for geodesics, is admissible. The length of the resulting geodesics can be expressed solely in terms of the spherical distance of their base points [75, Thm. 6]. Points then receive their optimal match within a threshold of spherical distance or are matched to a virtual point at infinity. Initializing curves according to the analytic formulas at hand then fully determines the initial field topology and the relaxation can be performed according to Section 7.2 with an additional constraint on the positions of the base points of the filaments (Fig. 7.6). The insights in Chapter 4 justify the matching of the filaments base points using an optimal transport strategy with respect to an approximate cost function. Moreover, one expects the resulting field topologies to exhibit next to no twisted filaments, which was confirmed by our experimental results (Figures 1.7, 7.5 and 7.6).

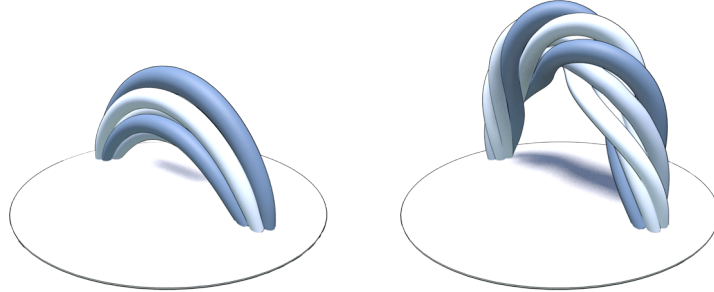


**Figure 7.7:** An untwisted (left) and a twisted coronal loop (right) obtained with the method proposed in [75]. As predicted by Eq. (6.11), the equilibrium configuration of the twisted filament (right) is longer with respect to the Euclidean metric compared to the untwisted filament (left).

Furthermore, predictions from our analytical considerations of Section 6.3 can be observed in numerical experiments. Eq. (6.11) reveals that non-zero total torsion makes it favorable to increase the euclidean length of the curve [91, 75]. Such tendencies were indeed observed in corresponding numerical experiments (Fig. 7.7). Since our model lacks the capability of representing twisted filaments, the twisted loop was modeled by a collection of intertwined plasma filaments. Ricca [89, 92] has made a similar observation and notes a tendency of twisted flux ropes in the solar corona to avoid configurations with an inflection point due to the twisting (Corollary 6.9). Depending on the strength of the twist, they either relax into braided, possibly three-dimensional equilibrium configurations, or experience so-called *kink instabilities*.

# CHAPTER 8

## CONCLUSION

This thesis studies geometric structures formed by magnetic field lines in an ideal plasma from a viewpoint of conformal geometry. The key insight is that stationary points of a hierarchy of  $L^2$  resp.  $L^1$ -optimization problems are related by a conformal change of metric, which establishes a conformal equivalence of stationary points of hierarchies of such optimization problems, distinguished by the topological constraints they impose. Most notably, we find that force-free fields are conformally geodesic and (exact) harmonic fields are (exact) eikonal. The result can be viewed as an extension of Arnold's seminal structure theorem in the sense that it finds geometric order in the cases with vanishing pressure.

Moreover, it provides novel geometric insights into physical phenomena in the realm of plasma physics. This is best illustrated by a practical example. The solar atmosphere is filled with plasma and its magnetic field forms arches connecting positive and negative surface magnetic fluxes. In more active regions of the sun's surface the magnetic fields concentrate into strong and often twisted flux ropes connecting sunspots.

In quiet regions of the solar surface the magnetic fields are relaxed to harmonic fields. In particular, one observes an absence of twisted magnetic fields in these quiet regions as the twists have been resolved through dissipative reconnection events over a longer period of relaxation time.

Theorems 1.9 and 1.10 allow precise characterizations of the distinction between active flux ropes and quite harmonic fields in terms of geodesics and optimal transports. The flux ropes consist of conformal geodesics connecting pairs of source and sink on the solar surface. The relaxed harmonic fields, on the other hand, are conformal eikonal fields which not only comprise geodesics but also

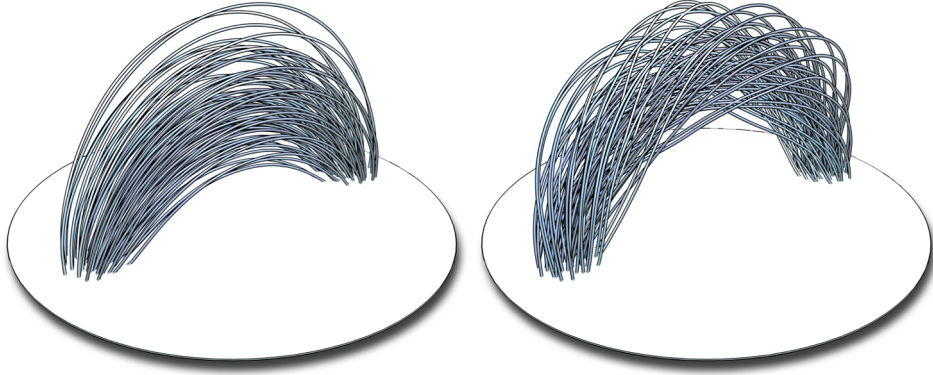


**Figure 8.1:** In a steady equilibrium and with negligible gas pressure, the magnetic field lines of coronal loops as observed in the solar corona constitute geodesic foliations. In contrast to the twisted case (right), the untwisted case (left) additionally realize the Beckmann optimal transportation plan from the source flux density to sink flux density on the solar surface.

form source–sink pairings as the Beckmann (1-Wasserstein, earth-mover) optimal transportation plan from the source flux density to sink flux density. We thus conclude a precise characterization of the observed types of structures in the solar atmosphere.

**Theorem 8.1** Potential-field models of the solar corona yield magnetic lines that are conformally Beckmann optimal transportation paths between the magnetic sources and sinks on the sun’s surface. The more general force-free magnetic fields are conformally geodesic foliations whose topological connectivity between the source and sink ends is constrained (Fig. 8.1).

Conversely, one can explore non-eikonal geodesic foliations and draw analogies from the phenomena in solar flux ropes. For example, one can connect a source and destination density by a bundle of geodesics with an overall twist. The bundle becomes untwisted when the connectivity is the optimal transport (Fig. 4.1).

Dynamics comes into play by considering the magnetic relaxation problem, which seeks to understand the self-organization of field lines in a perfectly conducting plasma. Inspired by Faraday’s idea of magnetic fields, we propose a novel interpretation of such a relaxation process in terms of conformal geometry. From a discrete model for pressure confined regions of ideal plasma with free bound-

## CHAPTER 8. CONCLUSION

ary conditions, we develop a novel approach for numerically performing a discrete analogue of magnetic relaxation. The presented computational method is geometrically less rigid than previous approaches as it allows for a gas pressure inside of the modeled plasma filaments, plasma filaments of variable thickness and it models the “elasticity” which is experienced by interacting magnetic field lines. Our plasma filaments indeed interact with each other and allow for an energy minimization without having to impose additional constraints. Thus, the proposed model gives a novel geometric interpretation and insights into the relaxation problem.

Beyond the scope of this thesis, there are still many open questions. Although basic numerical experiments have been successful, especially for cases such as the solar atmosphere or for parametric initializations of knots and links when the initialization was already close to the equilibrium state, one cannot yet expect to find true global minima based on generic initial configurations with the local nature of the current algorithmic framework. The strictly local nature of the quasi-Newton method for energy minimization is prone to getting stuck in local minima. For a more efficient energy minimization which is likely to attain global minima, a more elaborate optimization (as performed in, e.g., [120]) is needed.

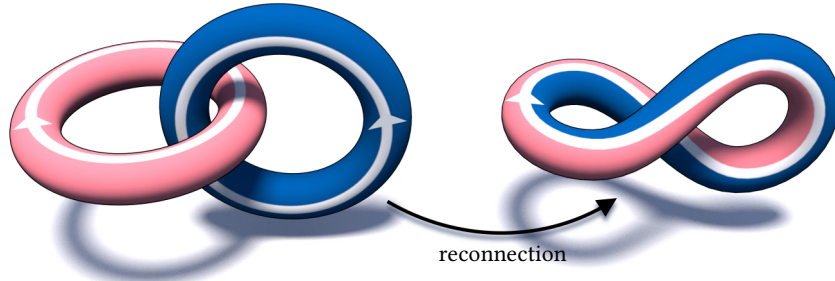


**Figure 8.2:** Accounting for weak resistivity, helicity preserving relaxation of a Hopf link consisting of two unknotted, linked components each carrying an untwisted field with flux  $h > 0$  leads to a reconnection in such a way that the two tubes become a single, twisted tube carrying flux  $h$ .

Other than computational performance, the applicability of our model is limited to ideal plasma. However, many physical scenarios including simulations of superfluids [95, 21, 83], the solar corona [30] or plasma in controlled fusion reactors [14, 52, 7, 6] are often modeled by seeking for minimal energy states under a constraint on the total helicity (Theorem 1.5). It is therefore desirable to extend the model to include reconnection mechanisms.

Though this could be approached by, *e.g.*, smoothing Clebsch variables [21, 18] representing the plasma filaments, it is unclear how to capture the helicity preservation that is sought for in many applications. For our discrete model of ideal plasma we inherently assume our plasma filaments to represent untwisted magnetic fields. Therefore, our model cannot yet account for the twist resulting from helicity preserving reconnection of, *e.g.*, a Hopf link as shown in Fig. 8.2 [67, 95, 83].

For now, however, it remains unclear whether and how questions relating to helicity or reconnection can be understood or addressed with the help of conformal geometry.

## REFERENCES

- [1] V. I. Arnold. *Mathematical Methods of Classical Mechanics*. Vol. 60. Graduate Texts in Mathematics. Springer, 1989. doi: [10.1007/978-1-4757-2063-1](https://doi.org/10.1007/978-1-4757-2063-1).
- [2] V. I. Arnold. “Sur la topologie des écoulements stationnaires des fluides parfaits.” In: *Vladimir I. Arnold - Collected Works: Hydrodynamics, Bifurcation Theory, and Algebraic Geometry 1965-1972*. Ed. by A. B. Givental, B. A. Khesin, A. N. Varchenko, V. A. Vassiliev, and O. Y. Viro. Springer, 2014, pp. 15–18. doi: [10.1007/978-3-642-31031-7\\_3](https://doi.org/10.1007/978-3-642-31031-7_3).
- [3] V. I. Arnold and B. A. Khesin. *Topological methods in hydrodynamics*. Vol. 125. Applied Mathematical Sciences. Springer, 2008. doi: [10.1007/978-3-030-74278-2](https://doi.org/10.1007/978-3-030-74278-2).
- [4] M. J. Aschwanden, K. Reardon, and D. B. Jess. “Tracing the Chromospheric and Coronal Magnetic Field with AIA, IRIS, IBIS, and ROSA Data.” In: *Astrophys. J.* 826.1 (2016), p. 61. doi: <https://doi.org/10.3847/0004-637X/826/1/61>.
- [5] T. Ashton, J. Cantarella, M. Piatek, and E. J. Rawdon. “Knot tightening by constrained gradient descent.” In: *Experiment. Math.* 20.1 (2011), pp. 57–90. doi: [10.1080/10586458.2011.544581](https://doi.org/10.1080/10586458.2011.544581).
- [6] P. M. Bellan. “Caltech Lab Experiments and the Insights They Provide Into Solar Corona Phenomena.” In: *J. Geophys. Res.* 125.8 (2020), e2020JA028139. doi: [10.1029/2020JA028139](https://doi.org/10.1029/2020JA028139).
- [7] P. M. Bellan. *Magnetic Helicity, Spheromaks, Solar Corona Loops, And Astrophysical Jets*. World Scientific Publishing Company, 2018. doi: [10.1142/q0151](https://doi.org/10.1142/q0151).
- [8] V. N. Berestovskii and Y. G. Nikonorov. “Killing vector fields of constant length on Riemannian manifolds.” In: *Sib. Math. J.* 49.3 (2008), pp. 395–407. doi: [10.1007/s11202-008-0039-3](https://doi.org/10.1007/s11202-008-0039-3).
- [9] M. A. Berger. “Introduction to magnetic helicity.” In: *Plasma Phys. Control. Fusion* 41.12B (Dec. 1999), B167. doi: [10.1088/0741-3335/41/12B/312](https://doi.org/10.1088/0741-3335/41/12B/312).
- [10] P. Berger, A. Florio, and D. Peralta-Salas. “Steady Euler Flows on  $\mathbb{R}^3$  with Wild and Universal Dynamics.” In: *Comm. Math. Phys.* (2023), pp. 1–47. doi: [10.1007/s00220-023-04660-6](https://doi.org/10.1007/s00220-023-04660-6).
- [11] A. L. Besse. *Einstein manifolds*. Springer, 2007. doi: [10.1007/978-3-540-74311-8](https://doi.org/10.1007/978-3-540-74311-8).
- [12] M. L. Boas. *Mathematical methods in the physical sciences*. 3rd ed. Wiley, 2006. ISBN: 0471365807.
- [13] H. Brezis and P. Mironescu. “The Plateau problem from the perspective of optimal transport.” In: *C. R. Math.* 357.7 (2019), pp. 597–612. doi: [10.1016/j.crma.2019.07.007](https://doi.org/10.1016/j.crma.2019.07.007).
- [14] J. Cantarella. “Topological structure of stable plasma flows.” PhD thesis. University of Pennsylvania, 1999. URL: <https://www.proquest.com/openview/cca4694a6599437817bf4613163e7fbe/1?pq-origsite=gscholar&cbl=18750&diss=y>.
- [15] J. Cantarella, R. B. Kusner, and J. M. Sullivan. “On the minimum ropelength of knots and links.” In: *Invent. Math.* 150 (2002), pp. 257–286. doi: [10.1007/s00222-002-0234-y](https://doi.org/10.1007/s00222-002-0234-y).
- [16] R. Cardona. “Steady Euler flows and Beltrami fields in high dimensions.” In: *Ergod. Theory Dyn. Syst.* 41.12 (2021), pp. 3610–3633. doi: [10.1017/etds.2020.124](https://doi.org/10.1017/etds.2020.124).

## REFERENCES

- [17] R. Cardona Aguilar. “[The geometry and topology of steady euler flows, integrability and singular geometric structures.](#)” PhD thesis. Universitat Politècnica de Catalunya, 2021. doi: [10.5821/dissertation-2117-349573](https://doi.org/10.5821/dissertation-2117-349573).
- [18] A. Chern, F. Knöppel, U. Pinkall, and P. Schröder. “[Inside Fluids: Clebsch Maps for Visualization and Processing.](#)” In: *ACM Trans. Graph.* 36.4 (2017). doi: [10.1145/3072959.3073591](https://doi.org/10.1145/3072959.3073591).
- [19] A. Chern. “[Fluid Dynamics with Incompressible Schrödinger Flow.](#)” PhD thesis. California Institute of Technology, 2017. url: <https://resolver.caltech.edu/CaltechTHESIS:06052017-102338732>.
- [20] A. Chern and O. Gross. [Force-Free Fields are Conformally Geodesic.](#) 2023. doi: [10.48550/arXiv.2312.05252](https://doi.org/10.48550/arXiv.2312.05252). arXiv: [2312.05252](https://arxiv.org/abs/2312.05252).
- [21] A. Chern, F. Knöppel, U. Pinkall, P. Schröder, and S. Weißmann. “[Schrödinger’s Smoke.](#)” In: *ACM Trans. Graph.* 35.4 (2016). doi: [10.1145/2897824.2925868](https://doi.org/10.1145/2897824.2925868).
- [22] R. Chodura and A. Schlüter. “[A 3D code for MHD Equilibrium and Stability.](#)” In: *J. Comput. Phys.* 41.1 (1981), pp. 68–88. doi: [10.1016/0021-9991\(81\)90080-2](https://doi.org/10.1016/0021-9991(81)90080-2).
- [23] A. Y. K. Chui and H. K. Moffatt. “[Minimum energy magnetic fields with toroidal topology.](#)” In: *Topological Aspects of the Dynamics of Fluids and Plasmas*. Ed. by H. K. Moffatt, G. M. Zaslavsky, P. Comte, and M. Tabor. Springer, 1992, pp. 195–218. doi: [10.1007/978-94-017-3550-6\\_9](https://doi.org/10.1007/978-94-017-3550-6_9).
- [24] K. Cieliebak and E. Volkov. “[First steps in stable Hamiltonian topology.](#)” In: *J. Eur. Math. Soc.* 017.2 (2015), pp. 321–404. doi: [10.4171/JEMS/505](https://doi.org/10.4171/JEMS/505).
- [25] J. N. Clelland and T. Klotz. “[Beltrami fields with nonconstant proportionality factor.](#)” In: *Arch. Ration. Mech. Anal.* 236.2 (2020), pp. 767–800. doi: [10.1007/s00205-019-01481-7](https://doi.org/10.1007/s00205-019-01481-7).
- [26] K. Crane, ed. *An Excursion Through Discrete Differential Geometry*. Vol. 76. American Mathematical Society, 2020. isbn: 978-1-4704-4662-8.
- [27] C. E. DeForest and C. C. Kankelborg. “[Fluxon Modeling of Low-Beta Plasmas.](#)” In: *J. Atmos. Sol.-Terr. Phys.* 69.1 (2007), pp. 116–128. doi: [10.1016/j.jastp.2006.06.011](https://doi.org/10.1016/j.jastp.2006.06.011).
- [28] S. Deshmukh and V. A. Khan. “[Geodesic vector fields and Eikonal equation on a Riemannian manifold.](#)” In: *Indag. Math.* 30.4 (2019), pp. 542–552. doi: [10.1016/j.indag.2019.02.001](https://doi.org/10.1016/j.indag.2019.02.001).
- [29] S. Deshmukh, P. Peska, and N. Bin Turki. “[Geodesic vector fields on a Riemannian manifold.](#)” In: *Mathematics* 8.1 (2020), p. 137. doi: [10.3390/math8010137](https://doi.org/10.3390/math8010137).
- [30] A. M. Dixon, M. A. Berger, E. R. Priest, and P. K. Browning. “[A generalization of the Woltjer minimum-energy principle.](#)” In: *Astron. Astrophys.* 225 (1989), p. 156. url: <https://ui.adsabs.harvard.edu/abs/1989A&A...225..156D>.
- [31] T. Dombre, U. Frisch, J. M. Greene, M. Hénon, A. Mehr, and A. M. Soward. “[Chaotic streamlines in the ABC flows.](#)” In: *J. Fl. Mech.* 167 (1986), pp. 353–391. doi: [10.1017/S0022112086002859](https://doi.org/10.1017/S0022112086002859).
- [32] M. Dunajski and W. Kryński. “[Variational principles for conformal geodesics.](#)” In: *Lett. Math. Phys.* 111 (2021), pp. 1–18. doi: [10.1007/s11005-021-01469-z](https://doi.org/10.1007/s11005-021-01469-z).
- [33] A. Enciso and D. Peralta-Salas. “[Beltrami fields with a nonconstant proportionality factor are rare.](#)” In: *Arch. Ration. Mech. Anal.* 220 (2016), pp. 243–260. doi: [10.1007/s00205-015-0931-5](https://doi.org/10.1007/s00205-015-0931-5).
- [34] J. Etnyre and R. Ghrist. “[Contact topology and hydrodynamics: I. Beltrami fields and the Seifert conjecture.](#)” In: *Nonlinearity* 13.2 (Mar. 2000), p. 441. doi: [10.1088/0951-7715/13/2/306](https://doi.org/10.1088/0951-7715/13/2/306).
- [35] M. Faraday. “[V. Experimental researches in electricity.](#)” In: *Phil. Tr. R. Soc. Lond. A* 122 (1832), pp. 125–162. doi: [10.1098/rstl.1832.0006](https://doi.org/10.1098/rstl.1832.0006).
- [36] A. Fialkow. “[Conformal geodesics.](#)” In: *Trans. Amer. Math. Soc.* 45.3 (1939), pp. 443–473. doi: [10.2307/1990011](https://doi.org/10.2307/1990011).

## REFERENCES

- [37] A. Fialkow. “The conformal theory of curves.” In: *Trans. Amer. Math. Soc.* 51 (1942), pp. 435–501. doi: [10.2307/1990075](https://doi.org/10.2307/1990075).
- [38] T. Frankel. *The Geometry of Physics: An Introduction*. 3rd ed. Cambridge University Press, 2011. doi: [10.1017/CBO9781139061377](https://doi.org/10.1017/CBO9781139061377).
- [39] M. H. Freedman, Z.-X. He, and Z. Wang. “Möbius Energy of Knots and Unknots.” In: *Ann. of Math.* 139.1 (1994), pp. 1–50. doi: [10.2307/2946626](https://doi.org/10.2307/2946626).
- [40] M. H. Freedman. “A note on topology and magnetic energy in incompressible perfectly conducting fluids.” In: *J. Fl. Mech.* 194 (1988), pp. 549–551. doi: [10.1017/S002211208800309X](https://doi.org/10.1017/S002211208800309X).
- [41] V. L. Ginzburg and B. Khesin. “Steady fluid flows and symplectic geometry.” In: *J. Geom. and Phys.* 14.2 (1994), pp. 195–210. doi: [10.1016/0393-0440\(94\)90006-X](https://doi.org/10.1016/0393-0440(94)90006-X).
- [42] H. Gluck. *Can space be filled by geodesics, and if so, how?* (Open letter on geodesible flows). 1979.
- [43] H. Gluck. “Dynamical behavior of geodesic fields.” In: *Global Theory of Dynamical Systems*. Ed. by Z. Nitecki and C. Robinson. Vol. 819. Lecture Notes in Mathematics. Springer, 2006, pp. 190–215. doi: [10.1007/BFb0086988](https://doi.org/10.1007/BFb0086988).
- [44] O. Gonzalez and J. H. Maddocks. “Global curvature, thickness, and the ideal shapes of knots.” In: *Proc. Nat. Acad. Sci.* 96.9 (1999), pp. 4769–4773. doi: [10.1073/pnas.96.9.4769](https://doi.org/10.1073/pnas.96.9.4769).
- [45] H. Grad and H. Rubin. “Hydromagnetic Equilibria and Force-Free Fields.” In: *J. nucl. Energy* 7.3-4 (1958), pp. 284–285. doi: [10.1016/0891-3919\(58\)90139-6](https://doi.org/10.1016/0891-3919(58)90139-6).
- [46] O. Gross, U. Pinkall, and P. Schröder. “Plasma Knots.” In: *Phys. Lett. A* 480 (2023), p. 128986. doi: [10.1016/j.physleta.2023.128986](https://doi.org/10.1016/j.physleta.2023.128986).
- [47] B. Guilfoyle. “A structure theorem for stationary perfect fluids.” In: *Class. Quantum Gravity* 22.9 (2005), p. 1599. doi: [10.1088/0264-9381/22/9/008](https://doi.org/10.1088/0264-9381/22/9/008).
- [48] Y. Guo, C. Xia, R. Keppens, and G. Valori. “Magneto-frictional modeling of coronal nonlinear force-free fields. I. Testing with analytic solutions.” In: *Astrophys. J.* 828.2 (2016), p. 82. doi: [10.3847/0004-637X/828/2/82](https://doi.org/10.3847/0004-637X/828/2/82).
- [49] W. R. Hamilton. “Theory of Systems of Rays.” In: *Trans. Roy. Irish Acad.* 15 (1828), pp. 69–174. URL: <http://www.jstor.org/stable/30078906>.
- [50] R. Harvey and H. B. Lawson. “Calibrated geometries.” In: *Acta Math.* 148 (1982), pp. 47–157. doi: [10.1007/BF02392726](https://doi.org/10.1007/BF02392726).
- [51] H. Hopf. “Über die Abbildungen der dreidimensionalen Sphäre auf die Kugelfläche.” In: *Math. Ann.* 104.1 (1931), pp. 637–665. doi: [10.1007/BF01457962](https://doi.org/10.1007/BF01457962).
- [52] S. R. Hudson, E. Startsev, and E. Feibusch. “A new class of magnetic confinement device in the shape of a knot.” In: *Phys. Plasmas*. 21.1 (2014), p. 010705. doi: [10.1063/1.4863844](https://doi.org/10.1063/1.4863844).
- [53] S. R. Hudson et al. “Computation of multi-region relaxed magnetohydrodynamic equilibria.” In: *Phys. Plasmas*. 19.11 (2012), p. 112502. doi: [10.1063/1.4765691](https://doi.org/10.1063/1.4765691).
- [54] B. Inhester and T. Wiegmann. “Nonlinear Force-Free Magnetic Field Extrapolations: Comparison of the Grad Rubin and Wheatland Sturrock Roumeliotis Algorithm.” In: *Sol. Phys.* 235.1 (2006), pp. 201–221. doi: [10.1007/s11207-006-0065-x](https://doi.org/10.1007/s11207-006-0065-x).
- [55] Å. M. Janse, B. C. Low, and E. N. Parker. “Topological Complexity and Tangential Discontinuity in Magnetic Fields.” In: *Phys. Plasmas*. 17.9 (2010), p. 092901. doi: [10.1063/1.3474943](https://doi.org/10.1063/1.3474943).
- [56] L. H. Kauffman. *Knots and Applications*. K. & E. series on knots and everything. World Scientific, 1995. doi: [10.1142/2515](https://doi.org/10.1142/2515).
- [57] R. Kippenhahn and A. Schlüter. “Eine Theorie der Solaren Filamente. Mit 7 Textabbildungen.” In: *Z. Astrophys.* 43 (1957), pp. 36–62. URL: <https://ui.adsabs.harvard.edu/abs/1957ZA.....43...36K/abstract>.

## REFERENCES

- [58] J. A. Klimchuk and P. A. Sturrock. “Three-dimensional force-free magnetic fields and flare energy buildup.” In: *Astrophys. J.* 385 (1992), pp. 344–353. doi: [10.1086/170943](https://doi.org/10.1086/170943).
- [59] W. Kühnel. *Differentialgeometrie: Kurven - Flächen - Mannigfaltigkeiten*. Aufbaukurs Mathematik. Springer, 2012. doi: [10.1007/978-3-658-00615-0](https://doi.org/10.1007/978-3-658-00615-0).
- [60] K. Kuperberg. “A Smooth Counterexample to the Seifert Conjecture.” In: *Ann. of Math.* 140.3 (1994), pp. 723–732. doi: [10.2307/2118623](https://doi.org/10.2307/2118623).
- [61] R. B. Kusner and J. M. Sullivan. “Möbius-invariant knot energies.” In: *Ideal knots*. Ed. by A. Stasiak, V. Katritch, and L. H. Kauffman. Vol. 19. World Scientific, 1998, pp. 315–352. doi: [10.1142/9789812796073\\_0017](https://doi.org/10.1142/9789812796073_0017).
- [62] B. C. Low. “Magnetostatic atmospheres with variations in three dimensions.” In: *Astrophys. J.* 263 (1982), pp. 952–969. doi: [10.1086/160563](https://doi.org/10.1086/160563).
- [63] R. S. MacKay. “Differential forms for plasma physics.” In: *J. Plasma Phys.* 86.1 (2020), p. 925860101. doi: [10.1017/S0022377819000928](https://doi.org/10.1017/S0022377819000928).
- [64] F. Maggioni and R. L. Ricca. “On the groundstate energy of tight knots.” In: *Proc. R. Soc. Lond. A* 465 (2009), pp. 2761–2783. doi: [10.1098/rspa.2008.0536](https://doi.org/10.1098/rspa.2008.0536).
- [65] J. C. Maxwell. “On physical lines of force. Part 1. The theory of molecular vortices applied to magnetic phenomena.” In: *Philos. Mag.* 21.139 (1861), pp. 161–175. doi: [10.1080/14786446108643033](https://doi.org/10.1080/14786446108643033).
- [66] A. N. McClymont, L. Jiao, and Z. Mikić. “Problems and progress in computing three-dimensional coronal active region magnetic fields from boundary data.” In: *Sol. Phys.* 174 (1997), pp. 191–218. doi: [10.1023/A:1004976720919](https://doi.org/10.1023/A:1004976720919).
- [67] H. K. Moffatt. “Some remarks on topological fluid mechanics.” In: *An introduction to the geometry and topology of fluid flows*. Ed. by R. L. Ricca. Springer, 2001, pp. 3–10. doi: [10.1007/978-94-010-0446-6\\_1](https://doi.org/10.1007/978-94-010-0446-6_1).
- [68] H. K. Moffatt. “Some topological aspects of fluid dynamics.” In: *J. Fl. Mech.* 914 (2021), P1. doi: [10.1017/jfm.2020.230](https://doi.org/10.1017/jfm.2020.230).
- [69] H. K. Moffatt. “The degree of knottedness of tangled vortex lines.” In: *J. Fl. Mech.* 35.1 (1969), pp. 117–129. doi: [10.1017/S0022112069000991](https://doi.org/10.1017/S0022112069000991).
- [70] H. K. Moffatt. “Magnetostatic equilibria and analogous Euler flows of arbitrarily complex topology. Part 1. Fundamentals.” In: *J. Fl. Mech.* 159 (1985), pp. 359–378. doi: [10.1017/S0022112085003251](https://doi.org/10.1017/S0022112085003251).
- [71] H. K. Moffatt. “The energy spectrum of knots and links.” In: *Nature* 347.6291 (1990), pp. 367–369. doi: [10.1038/347367a0](https://doi.org/10.1038/347367a0).
- [72] H. K. Moffatt. “Helicity and singular structures in fluid dynamics.” In: *Proc. Nat. Acad. Sci.* 111.10 (2014), pp. 3663–3670. doi: [10.1073/pnas.1400277111](https://doi.org/10.1073/pnas.1400277111).
- [73] H. Moradi et al. “Modeling the Subsurface Structure of Sunspots.” In: *Sol. Phys.* 267.1 (2010), pp. 1–62. doi: [10.1007/s11207-010-9630-4](https://doi.org/10.1007/s11207-010-9630-4).
- [74] M. S. Nabizadeh, R. Ramamoorthi, and A. Chern. “Kelvin transformations for simulations on infinite domains.” In: *ACM Trans. Graph.* 40.4 (2021), 97:1–97:15. doi: [10.1145/3450626.3459809](https://doi.org/10.1145/3450626.3459809).
- [75] M. Padilla, O. Gross, F. Knöppel, A. Chern, U. Pinkall, and P. Schröder. “Filament Based Plasma.” In: *ACM Trans. Graph.* 41.4 (2022), 153:1–153:14. doi: [10.1145/3528223.3530102](https://doi.org/10.1145/3528223.3530102).
- [76] M. Padilla. “The solar corona: modeled, discretized, visualized.” PhD thesis. Technische Universität Berlin, 2023. doi: [10.14279/depositonce-18889](https://doi.org/10.14279/depositonce-18889).
- [77] E. N. Parker. *Spontaneous Current Sheets in Magnetic Fields: With Applications to Stellar X-Rays*. Vol. 1. Ox. U. P., 1994. doi: [10.1093/oso/9780195073713.001.0001](https://doi.org/10.1093/oso/9780195073713.001.0001).
- [78] D. Peralta-Salas. “Selected topics on the topology of ideal fluid flows.” In: *Int. J. Geom. Methods Mod. Phys.* 13.Supp. 1 (2016), p. 1630012. doi: [10.1142/S0219887816300129](https://doi.org/10.1142/S0219887816300129).

## REFERENCES

- [79] P. Pierański. “In search of ideal knots.” In: *Ideal knots*. Ed. by A. Stasiak, V. Katritch, and L. H. Kauffman. Vol. 19. World Scientific, 1998, pp. 20–41. doi: [10.1142/9789812796073\\_0002](https://doi.org/10.1142/9789812796073_0002).
- [80] U. Pinkall and O. Gross. *Differential Geometry: From Elastic Curves to Willmore Surfaces*. Compact Textbooks in Mathematics. Birkhäuser, 2024. doi: [10.1007/978-3-031-39838-4](https://doi.org/10.1007/978-3-031-39838-4).
- [81] H. Poincaré. “Sur les équations de la dynamique et le problème des trois corps.” In: *Acta Math.* 13.1 (1890), p. 270.
- [82] E. R. Priest. *Magnetohydrodynamics of the Sun*. Cam. U. P., 2014. doi: [10.1017/CBO9781139020732](https://doi.org/10.1017/CBO9781139020732).
- [83] E. R. Priest and D. W. Longcope. “The creation of twist by reconnection of flux tubes.” In: *Sol. Phys.* 295.3 (2020), p. 48. doi: [10.1007/s11207-020-01608-0](https://doi.org/10.1007/s11207-020-01608-0).
- [84] C. Prior and A. R. Yeates. “Twisted Versus Braided Magnetic Flux Ropes in Coronal Geometry – I. Construction and Relaxation.” In: *Astron. Astrophys.* 587 (2016), p. 15. doi: [10.1051/0004-6361/201527231](https://doi.org/10.1051/0004-6361/201527231).
- [85] C. Prior and A. R. Yeates. “Twisted Versus Braided Magnetic Flux Ropes in Coronal Geometry – II. Comparative Behaviour.” In: *Astron. Astrophys.* 591 (2016), p. 20. doi: [10.1051/0004-6361/201528053](https://doi.org/10.1051/0004-6361/201528053).
- [86] L. A. Rachmeler, C. E. DeForest, and C. C. Kankelborg. “Reconnectionless CME eruption: Putting the Aly-Sturrock conjecture to rest.” In: *Astrophys. J.* 693.2 (2009), pp. 1431–1436. doi: [10.1088/0004-637x/693/2/1431](https://doi.org/10.1088/0004-637x/693/2/1431).
- [87] A. Rechtman. “Pièges dans la théorie des feuilletages: exemples et contre-exemples.” PhD thesis. Ecole normale supérieure de Lyon, 2009. url: <https://theses.hal.science/tel-00361633>.
- [88] M. Reddiger and B. Poirier. *On the Differentiation Lemma and the Reynolds Transport Theorem for Manifolds with Corners*. 2020. doi: [10.48550/arXiv.1906.03330](https://doi.org/10.48550/arXiv.1906.03330). arXiv: [1906.03330](https://arxiv.org/abs/1906.03330).
- [89] R. L. Ricca. “Evolution and inflectional instability of twisted magnetic flux tubes.” In: *Sol. Phys.* 172 (1997), pp. 241–248. doi: [10.1023/A:1004942121307](https://doi.org/10.1023/A:1004942121307).
- [90] R. L. Ricca and F. Maggioni. “Groundstate energy spectra of knots and links: magnetic versus bending energy.” In: *New Directions in Geometric and Applied Knot Theory*. Ed. by P. Reiter, S. Blatt, and A. Schikorra. De Gruyter, 2022, pp. 276–288. doi: [10.1515/9783110571493-013](https://doi.org/10.1515/9783110571493-013).
- [91] R. L. Ricca and F. Maggioni. “On the groundstate energy spectrum of magnetic knots and links.” In: *J. Phys. A: Math. Theor.* 47.20 (2014), p. 205501. doi: [10.1088/1751-8113/47/20/205501](https://doi.org/10.1088/1751-8113/47/20/205501).
- [92] R. L. Ricca. “Inflectional disequilibrium of magnetic flux-tubes.” In: *Fluid Dyn. Res.* 36.4-6 (2005), p. 319. doi: [10.1016/j.fluiddyn.2004.09.004](https://doi.org/10.1016/j.fluiddyn.2004.09.004).
- [93] D. Rowe and A. Chern. “Sparse Stress Structures from Optimal Geometric Measures.” In: *SIGGRAPH Asia 2023 Conference Papers*. 60. 2023. doi: [10.1145/3610548.3618193](https://doi.org/10.1145/3610548.3618193).
- [94] F. Santambrogio. *Optimal transport for applied mathematicians*. Birkhäuser, 2015. doi: [10.1007/978-3-319-20828-2](https://doi.org/10.1007/978-3-319-20828-2).
- [95] M. W. Scheeler, D. Kleckner, D. Proment, G. L. Kindlmann, and W. T. Irvine. *Helicity conservation in topology-changing reconnections: the flow of linking and coiling across scales*. 2014. doi: <https://doi.org/10.48550/arXiv.1404.6513>. arXiv: [1404.6513](https://arxiv.org/abs/1404.6513).
- [96] W. K. Schief. “Nested toroidal flux surfaces in magnetohydrostatics. Generation via soliton theory.” In: *J. Plasma Phys.* 69.6 (2003), pp. 465–484. doi: [10.1017/S0022377803002472](https://doi.org/10.1017/S0022377803002472).
- [97] W. K. Schief. “Hidden integrability in ideal magnetohydrodynamics: The Pohlmeier–Lund–Regge model.” In: *Phys. Plasmas*. 10.7 (2003), pp. 2677–2685. doi: [10.1063/1.1577347](https://doi.org/10.1063/1.1577347).
- [98] Y. Schwartzburg, R. Testuz, A. Tagliasacchi, and M. Pauly. “High-contrast computational caustic design.” In: *ACM Trans. Graph.* 33.4 (2014), pp. 1–11. doi: [10.1145/2601097.2601200](https://doi.org/10.1145/2601097.2601200).
- [99] G. Schwarz. *Hodge Decomposition – A method for solving boundary value problems*. Springer, 2006. doi: [10.1007/BFb0095978](https://doi.org/10.1007/BFb0095978).

## REFERENCES

- [100] C. B. Smiet, S. Candelaresi, and D. Bouwmeester. “Ideal relaxation of the Hopf fibration.” In: *Phys. Plasmas*. 24.7 (2017), p. 072110. doi: [10.1063/1.4990076](https://doi.org/10.1063/1.4990076).
- [101] Y. Soliman, A. Chern, O. Diamanti, F. Knöppel, U. Pinkall, and P. Schröder. “Constrained Willmore Surfaces.” In: *ACM Trans. Graph.* 40.4 (2021). doi: [10.1145/3450626.3459759](https://doi.org/10.1145/3450626.3459759).
- [102] D. Stansby, A. R. Yeates, and S. T. Badman. “`pfsppy`: A Python Package for Potential Field Source Surface Modelling.” In: *J. Open Source Softw.* 5.54 (2020), p. 2732. doi: [10.21105/joss.02732](https://doi.org/10.21105/joss.02732).
- [103] D. Sullivan. “A foliation of geodesics is characterized by having no ‘tangent homologies’.” In: *J. Pure Appl. Algebra* 13.1 (1978), pp. 101–104. doi: [10.1016/0022-4049\(78\)90046-4](https://doi.org/10.1016/0022-4049(78)90046-4).
- [104] J. B. Taylor. “Relaxation of Toroidal Plasma and Generation of Reverse Magnetic Fields.” In: *Phys. Rev. Lett.* 33 (1974), pp. 1139–1141. doi: [10.1103/PhysRevLett.33.1139](https://doi.org/10.1103/PhysRevLett.33.1139).
- [105] J. B. Taylor. “Relaxation and magnetic reconnection in plasmas.” In: *Rev. Mod. Phys.* 58 (1986), pp. 741–763. doi: [10.1103/RevModPhys.58.741](https://doi.org/10.1103/RevModPhys.58.741).
- [106] D. Tischler. “On fiberings certain foliated manifolds over  $S^1$ .” In: *Topology* 9.2 (1970), pp. 153–154. doi: [10.1016/0040-9383\(70\)90037-6](https://doi.org/10.1016/0040-9383(70)90037-6).
- [107] V. S. Titov, C. Downs, Z. Mikić, T. Török, J. A. Linker, and R. M. Caplan. “Regularized Biot–Savart Laws for Modeling Magnetic Flux Ropes.” In: *Astrophys. J. Lett.* 852.2 (2018), p. L21. doi: [10.3847/2041-8213/aaa3da](https://doi.org/10.3847/2041-8213/aaa3da).
- [108] A. W. Wadsley. “Geodesic foliations by circles.” In: *J. Diff. Geom.* 10.4 (1975), pp. 541–549. doi: [10.4310/jdg/1214433160](https://doi.org/10.4310/jdg/1214433160).
- [109] S. Wang and A. Chern. “Computing Minimal Surfaces with Differential Forms.” In: *ACM Trans. Graph.* 40.4 (2021), 113:1–113:14. doi: [10.1145/3450626.3459781](https://doi.org/10.1145/3450626.3459781).
- [110] S. Wang, M. S. Nabizadeh, and A. Chern. “Exterior Calculus in Graphics.” In: SIGGRAPH Course (2023). URL: <https://stephaniwang.page/ExteriorCalculusInGraphics/>.
- [111] H. P. Warren, N. A. Crump, I. Ugarte-Urra, X. Sun, M. J. Aschwanden, and T. Wiegmann. “Toward a Quantitative Comparison of Magnetic Field Extrapolations and Observed Coronal Loops.” In: *Astrophys. J.* 860.1 (2018), p. 46. doi: [10.3847/1538-4357/aac20b](https://doi.org/10.3847/1538-4357/aac20b).
- [112] A. Witze. “NASA spacecraft ‘touches’ the Sun for the first time ever.” In: *Nature* (2021). doi: [10.1038/d41586-021-03751-5](https://doi.org/10.1038/d41586-021-03751-5).
- [113] L. Wolter. “A theorem on force-free magnetic fields.” In: *Proc. Nat. Acad. Sci.* 44.6 (1958), pp. 489–491. doi: [10.1073/pnas.44.6.489](https://doi.org/10.1073/pnas.44.6.489).
- [114] W. H. Yang, P. A. Sturrock, and S. K. Antiochos. “Force-free magnetic fields-The magneto-frictional method.” In: *Astrophys. J.* 309 (1986), pp. 383–391. doi: [10.1086/164610](https://doi.org/10.1086/164610).
- [115] A. R. Yeates. “Magnetohydrodynamic Relaxation Theory.” In: *Topics in Magnetohydrodynamic Topology, Reconnection and Stability Theory*. Ed. by D. MacTaggart and A. Hillier. Springer, 2020, pp. 117–143. doi: [10.1007/978-3-030-16343-3\\_4](https://doi.org/10.1007/978-3-030-16343-3_4).
- [116] A. R. Yeates. “On the limitations of magneto-frictional relaxation.” In: *Geophys. Astrophys. Fluid Dyn.* 116.4 (2022), pp. 305–320. doi: [10.1080/03091929.2021.2021197](https://doi.org/10.1080/03091929.2021.2021197).
- [117] A. R. Yeates and G. Hornig. “A complete topological invariant for braided magnetic fields.” In: *J. Phys. Conf. Ser.* 544.1 (2014), p. 012002. doi: [10.1088/1742-6596/544/1/012002](https://doi.org/10.1088/1742-6596/544/1/012002).
- [118] A. R. Yeates et al. “Global Non-Potential Magnetic Models of the Solar Corona During the March 2015 Eclipse.” In: *Space Sci. Rev.* 214.5 (2018), p. 99. doi: [10.1007/s11214-018-0534-1](https://doi.org/10.1007/s11214-018-0534-1).
- [119] C. Yu, C. Brakensiek, H. Schumacher, and K. Crane. “Repulsive Surfaces.” In: *ACM Trans. Graph.* 40.6 (2021), 268:1–268:19. doi: [10.1145/3478513.3480521](https://doi.org/10.1145/3478513.3480521).

## REFERENCES

- [120] C. Yu, H. Schumacher, and K. Crane. “[Repulsive Curves](#).” In: *ACM Trans. Graph.* 40.2 (2021), 10:1–10:21.  
DOI: [10.1145/3439429](https://doi.org/10.1145/3439429).
- [121] Y. Zhang. “[Gluing Techniques in Calibrated Geometry](#).” PhD thesis. Stony Brook University, 2013. URL:  
<http://hdl.handle.net/11401/76417>.